REMARKS

The Present Invention

The present invention pertains to a method for the therapeutic treatment of cancer due to a genetic defect in the p53 gene, a method for the prophylactic or therapeutic treatment of cancer due to ataxia telangiectasia, and a method for the prophylactic treatment of cancer.

The Pending Claims

Claims 1, 4-21, 28, and 30-49 are currently pending of which claims 1 and 4-21 are directed to a method for the therapeutic treatment of cancer due to a genetic defect in the p53 gene, claim 28 is directed to a method for the prophylactic or therapeutic treatment of cancer due to ataxia telangiectasia or Li Fraumeni's syndrome, and claims 30-49 are directed to a method for the prophylactic treatment of cancer. Claims 4-21 and 31-48 have been withdrawn from consideration by the Office as being directed to a non-elected species.

Request to Return Claims 4-21 and 31-48 to Consideration

The Office Action indicates that claims 4-21 and 31-48 are withdrawn from consideration. The Office Action issued November 15, 2000, set forth a restriction requirement that required only an election of a species. The Office Action states, "Applicant is required, in reply to this action, to elect a single species ... to which the claims shall be restricted if no generic claim is finally held to be allowable ... Upon the allowance of a generic claim, applicant will be entitled to consideration of claims to additional species which are written in dependent form or otherwise include all the limitations of an allowed generic claim as provided by 37 CFR 1.141" (see pages 2-3 of Office Action). In the response filed December 15, 2002, applicants elected the species 4-hydroxy-2,2,6,6-tetramethylpiperidine-1-oxyl (i.e., Tempol). This species was elected *for search purposes only.* Accordingly, applicants request claims 4-21 and 31-48 be returned to consideration.

Summary of the Office Action

The Office has rejected claims 1, 28, 30, and 49 under Section 112, first paragraph, as allegedly lacking enablement. Claims 28, 30, and 49 have been rejected under the judicially created doctrine of obviousness-type double patenting as being unpatentable over claim 22 of U.S. Patent No 5,462,946 (hereinafter "the '946 patent") and/or claim 2 of U.S. Patent No. 6,605,619 (hereinafter "the '619 patent"). Reconsideration of the rejections is hereby requested.

Discussion of the Enablement Rejection

The Office Action rejects claims 1, 28, 30, and 49 under Section 112, first paragraph, for allegedly failing to enable the skilled artisan to practice the full scope of the claimed invention without undue experimentation. The Office Action acknowledges that the specification is enabling for treating ataxia telangiectasia or Li Fraumeni's syndrome with Tempol, but alleges it is *not* enabling for (a) a method for the therapeutic treatment of cancer due to a genetic defect of the p53 gene with a compound of Formula I or II (claim 1), (b) a method for prophylactic or therapeutic treatment of cancer due to ataxia telangiectasia or Li Fraumeni's syndrome with a compound of Formula I or II other than Tempol (claim 28), or (c) a method for the prophylactic treatment of cancer with a compound of Formula I or II (claims 30 and 49). More specifically, the Office alleges the specification is not enabled for treatment of all cancers, all cancers due to a genetic defect in the p53 gene, or for using the vast number of possible compounds in the genus described by Formulas I and II.

To meet the burden of proof for an enablement rejection, the Office must advance acceptable reasoning that is inconsistent with enablement. *In re Wright*, 999 F.2d 1557, 1562, 27 U.S.P.Q.2d 1510, 1513 (Fed. Cir. 1993), *In re Strahilevitz*, 668 F.2d 1229, 1232, 212 U.S.P.Q. 561, 563 (C.C.P.A. 1982). In other words, the burden is on the Office to provide sufficient reasons for doubting any assertions in the specification as to the scope of enablement. In the present application, the Office has not provided a reasonable basis to conclude that one of ordinary skill in the art would not have been able to practice the claimed invention. No specific reasons or evidence are set forth to support the allegation as to why one of ordinary skill in the art could not practice the methods of claims 1, 28, 30, and 49 without undue experimentation. For example, the Office did not provide evidence to support why compounds of Formula I and II other than Tempol are not considered enabled.

Even if it were shown that the Office has met its burden of proof (which applicants contend is not the case), the burden of proof shifts to the applicant to prove enablement. To this end, applicants have provided ample support both in the specification and literature that one of ordinary skill in the art would be able to make and use the invention of claims 1, 28, 30, and 49 without undue experimentation.

In the case at hand, numerous examples of the efficacy of a compound of Formula I (i.e., a specie of the claimed genus) are provided. As discussed below, the specification and

literature support that compounds of Formulas I and II have similar properties (e.g., acting as SOD-mimetics). Thus, based on the numerous *in vivo* examples of a compound of the claimed genus and the known similarities in the compounds' activities, one of ordinary skill in the art would have a reasonable expectation of success in practicing the methods of claims 1, 28, 30, and 49. Moreover, MPEP Section 2164.02 states:

> The presence of only one working example should never be the sole reason for rejecting claims as being broader than the enabling disclosure ... one must evaluate all the facts and evidence and state why one would not be able to extrapolate that one example across the entire scope of the claims.

Furthermore, the specification provides ample guidance to the ordinary skilled artisan to practice the full scope of the claimed invention, as defined by claims 1, 28, 30, and 49, without undue experimentation. Applicants teach those of ordinary skill in the art how to make and use the present invention of claims 1, 28, 30, and 49. Examples I and II of the instant specification describe the *in vivo* efficacy of compounds of Formulas I and II to treat or prevent cancers susceptible to prevention or treatment by nitroxides. Other exemplary cancers that are susceptible to prevention or treatment by the compounds, or prodrugs thereof, encompassed within the scope of the present invention, are described in the specification at, for example, page 6, lines 12-29. Compounds of Formula I and II are described in the specification at, for example, page 7, line 24, to page 10, line 14. Chemical synthesis of nitroxides is described in the specification at, for example, page 11, lines 12-26. Suitable doses are described in the specification at, for example, page 10, line 27, to page 11, line 11. Formulations of nitroxides of Formula I and II are described in the specification at, for example, page 12, line 8, to page 15, line 12, and includes modes of administration, carriers, and concentrations.

With respect to claims 1 and 49, the Office Action alleges that applicants have not named any specific cancers caused by a genetic defect in the p53 gene. However, the specification need not disclose, and preferably omits, that which is well-known in the art. *In re Buchner*, 929 F.2d 660, 661, 18 U.S.P.Q.2d 1331, 1332 (Fed. Cir. 1991). As of the priority date of May 27, 1997, specific cancers caused by a genetic defect in the p53 gene were known in the art. For example, Hollstein et al., *Science* 253: 49-53 (1991) (of record) teaches that p53 mutations are common to human cancers, including cancers of the colon,

lung, esophagus, breast, liver, brain, reticuloendothelial tissue, and hematopoietic tissues. See also, Harris, C. C., *J. Nat'l Cancer Inst.* 88: 1442-1455 (1996) (of record).

Claim 28 is directed to a method for the prophylactic or therapeutic treatment of cancer, wherein the cancer is due to ataxia telangiectasia or Li Fraumeni's syndrome. According to the Office, "the state of the art does not recognize the administration of any compounds or compositions to prevent or completely eliminate (cure) the cancers of [sic] ataxia telangiectasia or Li Fraumeni's syndrome as required in the instant claims" (Office Action, page 4, first full paragraph). To support this statement, the Office cites two recent publications about ataxia telangiectasia and Li Fraumeni's syndrome. The first reference, "NINDS Ataxia Telangiectasia Information Page" (The National Institute of Neurological Disorders and Stroke, NIH, 2003), discloses information about ataxia telangiectasia and related treatments, prognoses, and research. The second reference, "Genetic Testing on Embryos Hits New Milestone" (Matloff, E., Reuters News, 2001), reports on the genetic testing of an embryo to screen for Li Fraumeni syndrome. The report further states that "[t]here is no cure for Li Fraumeni syndrome, and to date, no effective surveillance of risk reduction plan for these individuals and their family members" (page 2, first full paragraph). These references do not suggest that treatment and prophylaxis are impossible, nor that the rate of occurrence and the attendant effects of these diseases cannot be lessened. Moreover, these references do not address the inventive methods and compositions of the present invention. Accordingly, these references do not support a *prima facie* finding that the claimed invention is not enabled by the specification.

Moreover, the Office mischaracterizes claim 28. In contrast to the Office's allegation, claim 28 does not aim to cure ataxia telangiectasia or Li Fraumeni's syndrome *per se*, but rather is directed to a method of treating or preventing a cancer associated with these two disorders. The term "prophylactic" means any degree in inhibition of the onset of the cancer, and "therapeutic" means any degree in inhibition of the progression of the cancer, including delay of onset, and/or slowing the progression of the cancer (see, for example, page 10, lines 18-20 of the specification). Applicants previously demonstrated the prophylactic treatment with Tempol of *Atm*-deficient mice, which are good models of ataxia telangiectasia, (see the Declaration under 37 C.F.R. § 1.132 of Dr. James B. Mitchell attached to response to Office Action filed September 16, 2003).

Claim 30 is directed to a method for the prophylactic treatment of cancer. Claim 49 is directed to a method for the prophylactic treatment of cancer, wherein the cancer is due to a genetic defect in the p53 gene. The Office contends that these claims are not enabled for a method for the prophylactic treatment of any cancer (claim 30) or any cancer with a defect in the p53 gene (claim 49) with a compound of Formula I or II. Compounds of Formula I and II have been shown to protect cells and animals against the untoward acute effects of short-term exposure to lethal doses of free radicals and oxidative species, such as superoxide, hydrogen peroxide, hydroxyl radicals, and hydroperoxides, by functioning as antioxidants (see, U.S. Patent 5,462,946, incorporated by reference and page 2, lines 24-28, of the instant specification). In other words, any cancer that generates free radicals and oxidative species are cancers susceptible to prophylactic treatment with a compound of Formula I or II (or a prodrug thereof) in claims 30 and 49. The specific type of cancer that is prophylactically treated does not matter as long as free radicals and/or oxidative species are produced; the mechanism of action should be the same. One of ordinary skill in the art, therefore, is enabled to practice the present inventive method. This is supported by Example 2 and Mitchell et al., *Free Radical Biology & Medicine* 34: 93-102 (2003) (made of record in applicants' response to Office Action submitted September 16, 2003), which show that spontaneous tumor incidence in mice decreases upon treatment with Tempol. These data accordingly demonstrate that the spontaneous incidence of *any* cancer can be prophylactically treated with a compound of Formulas I and II, such as Tempol, or a prodrug thereof because administration of Tempol resulted in a delay of progression from the G1 to S phase of the cell cycle, which subsequently led to a slowing of cellular proliferation and prolonged latency to tumor formation (see Mitchell et al., *Free Radical Biology & Medicine* 34: 93-102 (2003), page 10, second paragraph).

In regards to the Office's contention that the specification is not enabled for compounds other than Tempol, applicants submit that the compounds of Formulas I and II (and prodrugs thereof) all have a common characteristic in that all the compounds have superoxide dismustase (SOD)-like activity. Because cancer development can be mediated through a free radical process, the skilled artisan would reasonably believe that the nitroxides of Formulas I and II, would be active for the therapeutic and prophylactic treatment of those cancers.

More specifically, nitroxides of Formulas I and II having SOD-mimetic activity typically belong to two different classes based on the ring size: 1) six-membered piperidine-

based nitroxides (e.g., Tempo, Tempol, and Oxo Tempo) (i.e., compounds of Formula I); and 2) five-membered doxyl derivatives (e.g., Cyclo hexane Doxyl (CHDO) and Oxano) (i.e., compounds of Formula II). SOD mimetic activity in both of these classes has been reported in the literature (see, for example, Samuni et al., *J. Biol. Chem.*, 263(34): 17921-1724 (1988); Mitchell et al., *Biochemistry*, 29(11): 2802 (1990); Krishna et al., *Proc. Natl. Acad. Sci. U.S.A.*, 89(12): 5537-5541 (1992); Krishna et al., *J. Biol. Chem.*, 271(42): 26026-26031 (1996); and Krishna et al., *J. Med. Chem.*, 41(18): 3477-3492 (1998) (copies enclosed). Thus the SOD-mimetic activity of nitroxides is not restricted to Tempol only, but also to other nitroxides, such as those of Formulas I and II.

In the present application, an exemplary compound, Tempol, has been shown to have activity for the prophylactic and therapeutic treatment of cancer due to a p53 defect, cancer due to ataxia telangiectasia, cancer due to Li Fraumeni's syndrome, and cancer in general. As stated above, Tempol and the other compounds of Formulas I and II have SOD-mimetic activity, and thus will have similar prophylactic and therapeutic activities for cancer. The examples provided in the specification and Dr. Mitchell's Rule 132 Declaration illustrate that cancers other than cancer due to ataxia telangiectasia or Li Fraumeni's syndrome are enabled (e.g., with the use of p53 knock-out mice). As such, in view of the teachings in the specification and scientific literature and data provided in the specification and Rule 132 Declaration, it is respectfully submitted that the scope of the subject matter defined by claims 1, 28, 30, and 49 is reasonably correlated to the enablement provided by the specification.

In view of the foregoing arguments, it is submitted that claims 1, 28, 30, and 49 are enabled. Applicants request that the rejection of these claims be withdrawn.

Discussion of the Obviousness-Type Double Patenting Rejection

Claims 28, 30, and 49 have been rejected for obviousness-type double patenting as being not patentably distinct over claim 22 of the '946 patent and/or claim 2 of the '619 patent. Claim 22 of the '946 patent recites a method for treating the effects of oxidative stress due to the production of harmful free radical species comprising administering a composition comprising an anti-oxidative stress effective amount of Tempol to an organism or biological material susceptible to oxidative stress. Claim 2 of the '619 patent recites a method for treating or preventing damage to normal cells, tissues, or organs in a mammal that has been exposed to ionizing radiation comprising administering to said mammal, after exposure to ionizing radiation, a composition comprising an anti-radiation damage effective

amount of Tempol. According to the Office, since the mammal or organism recited in claims 22 or 2 would also be at risk for developing cancer, thus these claims render pending claims 28, 30, and 49 obvious. However, practice of claim 22 of the '946 patent and claim 2 of the '619 patent does not necessarily lead to the method of claims 28, 30, and 49 because prevention of cancer is not the only possible result of exposure to ionizing radiation or oxidative stress.

For inherency to apply in an anticipation situation, the later-claimed product or method must always (i.e., inevitably or necessarily) be the result of the practice of the prior art. Treating the effects of oxidative stress and/or treating or preventing damage caused by ionizing radiation does not *always* yield prevention of cancer because of the nature of the patient being treated. More specifically, a patient that is to be treated for the effects of oxidative stress is *not* necessarily at risk of cancer at the time Tempol is administered. Therefore, at the time of administration, there is no cancer for Tempol to prevent in the patient. Similarly, oxidative stress and/or ionizing radiation can have deleterious effects, including mucositis and cataracts (see, for example, col. 2, lines 61-62 and col. 3, lines 4-6 of the '619 patent). Thus, treating the disorders of claim 22 of the '946 patent and claim 2 of the '619 patent does not *always* result in preventing cancer. As such, it cannot be said that pending claims 28, 30, and 49 are not patentably distinct from claim 22 of the '946 patent and claim 2 of the '619 patent, and the obviousness-type double patenting rejection should be withdrawn.

Conclusion

The application is considered in good and proper form for allowance, and the Examiner is respectfully requested to pass this application to issue. If, in the opinion of the Examiner, a telephone conference would expedite the prosecution of the subject application, the Examiner is invited to call the undersigned attorney.

Respectfully submitted,

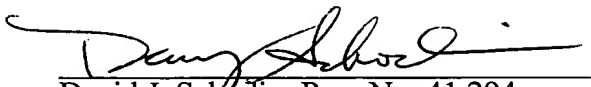

David J. Schodin, Reg. No. 41,294
LEYDIG, VOIT & MAYER, LTD.
Two Prudential Plaza, Suite 4900
180 North Stetson Avenue
Chicago, Illinois 60601-6780
(312) 616-5600 (telephone)
(312) 616-5700 (facsimile)

Date: August 19, 2004

Communication

THE JOURNAL OF BIOLOGICAL CHEMISTRY
Vol. 263, No. 34, Issue of December 5, pp. 17921-17924, 1988
Printed in U.S.A.

A Novel Metal-free Low Molecular Weight Superoxide Dismutase Mimic*

(Received for publication, August 5, 1988)

Amram Samuni‡, C. Murali Krishna, Peter Riesz, Eli Finkelstein, and Angelo Russo

From the Radiation Oncology Branch, Clinical Oncology Program, Division of Cancer Treatment, National Cancer Institute, National Institutes of Health, Bethesda, Maryland 20892 and the ‡Department of Molecular Biology, School of Medicine, Hebrew University, Jerusalem, 91010, Israel

2-Ethyl-1-hydroxy-2,5,5-trimethyl-3-oxazolidine (OXANOH), the one-electron reduction product of the stable nitroxide radical, 2-ethyl-2,5,5-trimethyl-3-oxazolidinoxyl (OXANO), is reportedly oxidized by superoxide, and its oxidation has been proposed as a method for assaying superoxide. We find that superoxide can both reduce OXANO and oxidize OXANOH. The respective rate constants, k_1 and k_2, were determined using two superoxide-generating systems (xanthine oxidase/xanthine as well as ionizing radiation). OXANOH oxidation and OXANO reduction are both inhibitable by superoxide dismutase, pH-dependent (4.5–9.3), and result in a steady state distribution of [OXANO] and [OXANOH], independent of their initial concentrations, *i.e.* the OXANO/OXANOH couple exhibits a metal-independent superoxide dismutase-like function. Thus it provides a prototype for future development of improved low molecular weight superoxide dismutase mimics which will also function in cellular hydrophobic (aprotic) compartments such as membranes.

Although most prokaryotes and eukaryotes are sustained by molecular oxygen, O_2 metabolism results in the production of several potentially harmful species such as superoxide and its secondary radicals. The key role of constitutive levels of superoxide dismutase in protection against oxygen-mediated biological damage is extensively documented (1–4). Elevating intracellular superoxide dismutase levels was found to further lessen damage inflicted by oxygen-derived radicals (5, 6), and administering exogenous superoxide dismutase was reported to result in an anti-inflammatory effect and to reduce damage induced under ischemia/reperfusion (7–9). These promising findings prompted the use of exogenous superoxide dismutase for various pathologic conditions (7–9). However, the inability of superoxide dismutase to penetrate into the cell where superoxide is formed has led to a search for membrane-permeable low molecular weight compounds possessing superoxide dismutase like activity (10–14).

The catalytic dismutation of $O_2^{\cdot-}$ by superoxide dismutase involves alternate reduction and oxidation of the transition metal ion in the metalloenzyme in a "ping-pong"-like mechanism (15, 16). Various chelates of iron, manganese, and particularly copper readily undergo similar redox reactions and are reportedly effective treatment in animal models of inflammation, ulcers, cancer, diabetes, and radiation-induced lethality (17). These findings stimulated interest in the screening and synthesizing of transition metal chelates possessing superoxide dismutase activity. To substitute effectively for superoxide dismutase in biological systems, a superoxide dismutase mimic should have a reduction potential of $-0.16\ V < E_o < 0.89\ V$, low reactivity toward oxygen, and be nontoxic, water-soluble, cell-permeable, nonimmunogenic, active within the physiological pH range, and relatively stable to cell metabolism. The search for superoxide dismutase mimics yielded a variety of chelates which were efficient catalysts for $O_2^{\cdot-}$ dismutation (10–14). Unfortunately, the metal chelates easily dissociate, can catalyze other undesirable redox processes in the cell, exhibit high affinity toward proteins and amino acids, and may lose their activity upon binding to cellular components (18).

Results from studies of $O_2^{\cdot-}$ radical and nitroxide spin adducts (19, 20) indicated that superoxide can react with nitroxides in a metal-free fashion. Stable nitroxide radicals have been used as biophysical tools for ESR spectroscopic studies, particularly of membranes and proteins (21), and more recently as contrast agents for *in vivo* NMR imaging and spin label oximetry (22, 23). Not surprisingly, the distribution and metabolism of such nitroxides are currently being extensively investigated (23, 24). The major pathway by which nitroxide spin labels decay within cells is through a one-electron reduction to diamagnetic ("ESR-silent") hydroxylamines (22, 24), which can be reversibly oxidized in a transition metal-dependent reaction (25). One particular hydroxylamine, 2-ethyl-1-hydroxy-2,5,5-trimethyl-3-oxazolidine (OXANOH),[1] is readily oxidized at pH 7.8 by superoxide to a stable radical, 2-ethyl-2,5,5-trimethyl-3-oxazolidinoxyl (OXANO), with a rate constant of $6.7 \times 10^3\ M^{-1}\ s^{-1}$. OXANOH oxidation by $O_2^{\cdot-}$ is metal-independent and has been employed to detect and assay superoxide (25). In the current study we confirm that superoxide can oxidize OXANOH to OXANO and find that superoxide is *also* capable of reducing OXANO to OXANOH. This cyclic reduction and oxidation of superoxide indicates that OXANO can function as a superoxide dismutase mimic.

EXPERIMENTAL PROCEDURES

Chemicals—Hypoxanthine (HX) was obtained from Calbiochem; 3-carbamoyl-2,2,5,5-tetramethyl-3-pyrrolidin-1-yloxy and 4-hydroxypyrazolo[3,4-*d*]pyrimidine (allopurinol) were purchased from Aldrich; xanthine oxidase (EC 1.2.3.2, xanthine:oxygen oxidoreductase), grade III from buttermilk, xanthine, Cu,Zn-superoxide dismutase, diethylenetriaminepentaacetic acid (DTPA), and ferricytochrome c ($cyt\text{-}c^{III}$) were obtained from Sigma. All chemicals were prepared and used without further purification. Distilled-deionized water was used throughout all experiments. Unless otherwise stated the experiments were conducted at room temperature. The stable nitroxide OXANO

* This work was supported in part by a grant from the Israel-USA Binational Science Foundation. The costs of publication of this article were defrayed in part by the payment of page charges. This article must therefore be hereby marked "*advertisement*" in accordance with 18 U.S.C. Section 1734 solely to indicate this fact.

[1] The abbreviations and trivial name used are: OXANOH, 2-ethyl-1-hydroxy-2,5,5-trimethyl-3-oxazolidine; OXANO, 2-ethyl-2,5,5-trimethyl-3-oxazolidinoxyl; DTPA, diethylenetriaminepentaacetic acid; HX, hypoxanthine; allopurinol, 4-hydroxypyrazolo[3,4-*d*]pyrimidine; S.S., steady state; $cyt\text{-}c^{III}$, ferricytochrome c.

was synthesized as previously described (26), and its hydroxylamine OXANOH was prepared by bubbling an OXANO solution with H_2 in the presence of a platinum catalyst for 45 min (27).

Electron Spin Resonance—Samples were drawn into a gas-permeable Teflon capillary (Zeus Industries, Raritan, NJ) of 0.81-mm inner diameter, 0.38-mm wall thickness, and 15 cm long. Each capillary was folded twice, inserted into an open 2.5-mm, inner diameter, quartz tube, and then placed into the ESR cavity. During the experiments, gases of desired compositions were blown through the quartz tube and around the sample within the ESR cavity. ESR spectra were recorded on a Varian E4 (or E9) X-band spectrometer, with the field set at 3357 G, modulation frequency of 100 KHz, modulation amplitude of 1 G, 10^3–10^4 gain, and a nonsaturating microwave power. Radical concentrations were calibrated using 3-carbamoyl-2,2,5,5-tetramethyl-3-pyrrolidin-1-yloxy.

RESULTS AND DISCUSSION

Upon exposure of OXANO to HX/xanthine oxidase, a superoxide-generating system, OXANO was reduced. The OXANO spin loss required the simultaneous presence of both xanthine oxidase enzyme and either xanthine or HX, as neither the enzyme nor the substrate alone had any effect on the nitroxide signal. The metal chelating agent DTPA did not affect the nitroxide decay, indicating metal independence, but adding superoxide dismutase to the reaction system prevented the spin loss. The major, though not sole, process by which nitroxides decay in biological systems was shown to be a one-electron reduction (24). It is possible, therefore, that superoxide reacts with OXANO to yield hydroxylamine.

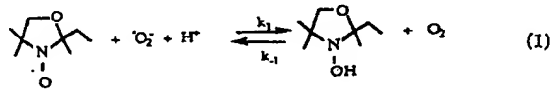

(1)

To test this hypothesis, OXANO was added to the xanthine/xanthine oxidase superoxide-generating system. After decay of the nitroxide ESR signal, 10 mM allopurinol (a selective inhibitor of xanthine oxidase) and 10 units/ml superoxide dismutase were added to block further $O_2^{\cdot-}$ formation and effect, followed by the addition of 5 mM ferricyanide. The original signal was fully restored, indicating that the spin loss caused by superoxide results from a one-electron reduction of OXANO to OXANOH.

Complete reduction of OXANO in the presence of HX/xanthine oxidase was never observed. Instead, a steady state residual concentration of the nitroxide is achieved and maintained as long as the $O_2^{\cdot-}$ flux persists. The failure of superoxide to reduce completely all the nitroxide agrees with previous reports that OXANOH and $O_2^{\cdot-}$ react to yield OXANO (25).

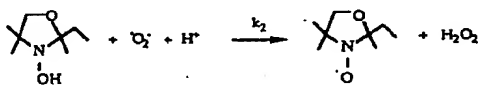

(2)

Adding Equations 1 and 2 together yields the following dismutation reaction.

$$2H^+ + 2O_2^{\cdot-} \rightarrow H_2O_2 + O_2 \quad (3)$$

In the presence of O_2 and $O_2^{\cdot-}$, Reactions 1 and 2 result in a steady-state distribution of OXANO and OXANOH concentrations. Since the superoxide-driven depletion and generation reactions of OXANO appear to be coupled, the overall rate equation for OXANO is as follows.

$$d[OXANO]/dt = k_2 \cdot [OXANOH] \cdot [O_2^{\cdot-}] + k_{-1} \cdot [O_2] \cdot [OXANOH] - k_1 \cdot [OXANO] \cdot [O_2^{\cdot-}] \quad (4)$$

At steady state, $d[OXANO]/dt = 0$, and the following is expected.

$$[OXANO]/[OXANOH] = k_2/k_1 + k_{-1} \cdot [O_2]/k_1 \cdot [O_2^{\cdot-}] \quad (5)$$

To verify the steady-state assumption, [OXANO] was varied between 2 and 500 μM, exposed to HX/xanthine oxidase at pH 7.3, and the residual ESR signal intensities monitored. The oxygen concentration was kept constant by the use of a gas-permeable Teflon capillary. The OXANO was partly reduced, but the relative unreduced fraction remained the same indicating that the steady-state concentration ($[OXANO]_{s.s.}$) depends on $[OXANO]/[OXANOH]$, not on $[OXANO]_{initial}$. Similarly, various concentrations of OXANOH were exposed to the HX/xanthine oxidase superoxide-generating system and scanned for the ESR signal to determine the final $[OXANO]_{s.s.}$. The relative $[OXANO]_{s.s.}$ was found to be the same as that observed when OXANO was the starting reagent. With increasing fluxes of $O_2^{\cdot-}$ generated by a 10-fold increase of [XO] at constant pH, $[OXANO]_{s.s.}$ slightly decreased (~30%) as anticipated by Equation 5.

Since HO_2 and $O_2^{\cdot-}$ generally differ in their reactivities, the ratio k_2/k_1 was anticipated to vary with pH, and proof was obtained when either OXANO or OXANOH was incubated with HX/xanthine oxidase at different pH values, and the final ESR signal of $[OXANO]_{s.s.}$ was measured. The results show, as illustrated in Fig. 1, an increase of $[OXANO]_{s.s.}/([OXANO]_{s.s.} + [OXANOH]_{s.s.})$ with pH which suggests the respective increase of k_2/k_1 with pH.

The kinetics of OXANO reduction were examined using the competition reaction for $O_2^{\cdot-}$ against cyt-c^{III}. The superoxide radicals, for which both OXANO and cyt-c^{III} compete, were generated enzymatically by HX/xanthine oxidase when [cyt-c^{III}] was held constant while [OXANO] was varied. The rates of cyt-c^{III} production in the absence (V) and the presence (v) of OXANO were determined and the data analyzed as shown in Fig. 2*A*. The kinetics of OXANOH oxidation were studied using a ^{137}Cs γ-source to produce superoxide radicals

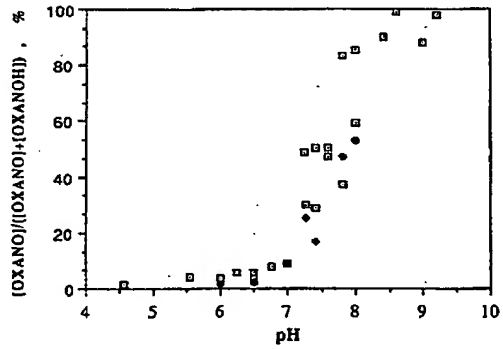

FIG. 1. The pH dependence of the steady-state concentration distribution of [OXANO]/([OXANO] + [OXANOH]) under superoxide flux. The steady-state residual ESR signal following exposure of 10 μM OXANO (*open symbols*) or OXANOH (*closed symbols*) in 50 mM phosphate and 25 μM DTPA to a constant $O_2^{\cdot-}$ flux under various pH values is shown. The residual fraction of OXANO is displayed *versus* pH as a percentage of initial total concentration ([OXANO] + [OXANOH]). Superoxide was generated enzymatically with 4 mM hypoxanthine and 0.033 unit/ml xanthine oxidase under air at room temperature.

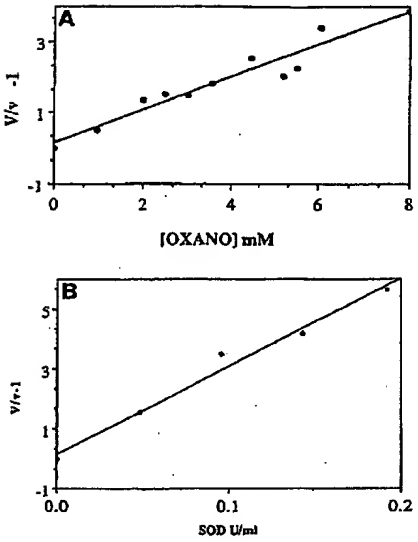

FIG. 2. **The determination of $k_{1(OXANO+O_2^{\cdot-})}$ and $k_{2(OXANOH+O_2^{\cdot-})}$ by competition reactions.** *a*, inhibition of superoxide-mediated reduction of cyt-c^{III} by OXANO. 0.1 mM ferricytochrome *c* (cyt-c^{III}) in 10 mM phosphate buffer, pH 6.5, 25 μM DTPA was incubated with 1 mM hypoxanthine and 0.001 unit/ml xanthine oxidase. Formation rates of cyt-c^{III} were monitored spectrophotometrically at 550 nm in the absence (V) and in the presence (v) of various OXANO concentrations. Data were analyzed by plotting $V/v - 1$ *versus* [OXANO], and k_1 was calculated, knowing $k_{cyt\text{-}c^{III}+superoxide}$, according to $V/v = 1 + k_1 \cdot [OXANO]/k_{cyt\text{-}c^{III}+superoxide} \cdot [cyt\text{-}c^{III}]$. *b*, inhibition of OXANOH oxidation by superoxide dismutase (*SOD*). 100 μM OXANOH in 10 mM phosphate buffer, pH 8.15, 5 mM formate, and 25 μM DTPA were γ-irradiated at room temperature under air for 5 min at a dose rate of 1.05 gray $\cdot$ min^{-1}. Under these conditions all primary radicals were converted into $O_2^{\cdot-}$ and the rates of OXANOH oxidation in the absence (V) and in the presence (v) of various superoxide dismutase concentrations were determined by measuring the formation of OXANO ESR signal (units of superoxide dismutase are defined by the assay method of McCord and Fridovich (1)). The results were analyzed by plotting $V/v - 1$ *versus* [SOD], and k_2 was evaluated according to: $V/v = 1 + k_{superoxide\ dismutase} \cdot [superoxide\ dismutase]/k_2 \cdot [OXANOH]$.

radiolytically in aerated phosphate buffer containing 5 mM formate, 25 μM DTPA, and OXANOH. Under such conditions all primary radicals generated from water radiolysis are converted into $O_2^{\cdot-}$. Superoxide dismutase was used to compete for the $O_2^{\cdot-}$ radicals (25) while [OXANOH] was held constant. The amount of OXANO formed was assayed by measuring its ESR signal, and the results were analyzed as illustrated in Fig. 2*B*. To study the pH dependences of k_1 and k_2, the experiments described in Fig. 2 were repeated over a wide pH range. For the calculation of k_1 the pH-dependent values for $k_{cyt\text{-}c^{III}+superoxide}$ were used (28), while for the calculation of k_2 the activity of superoxide dismutase was standardized against cyt-c^{III} (1). As presented in Fig. 3 the results show that both k_1 and k_2 increase with $[H^+]$. Yet, the marked increase in k_1 causes the pH dependence plots of k_1 and k_2 to cross each other. As seen in Fig. 1 the relative ratio of k_1 and k_2 at various pH values reasonably agrees with the pH dependence of $[OXANO]_{s.s.}$. In the presence of $O_2^{\cdot-}$ at pH > 8 where $k_1 \ll k_2$ OXANO predominates, whereas at pH < 7 where $k_1 \gg k_2$ most of the nitroxide persists in the reduced form.

Since no acid-base equilibrium is envisaged for OXANO (29), the strong pH dependence of k_1 is attributable to different reactivities of $O_2^{\cdot-}$ and $HO_2^{\cdot}$. In such a case the effective rate constant k_1 would depend on the relative distribution of

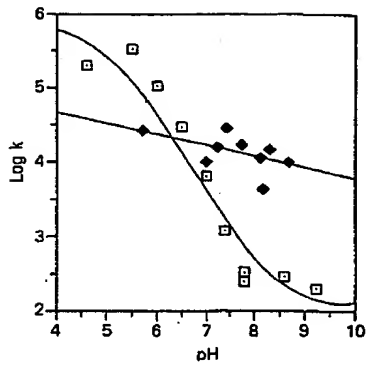

FIG. 3. **The pH dependences of $k_{1(OXANO+O_2^{\cdot-})}$ and $k_{2(OXANOH+O_2^{\cdot-})}$.** The kinetics of superoxide reactions with OXANO (Equation 1) and OXANOH (Equation 2) were studied over a wide pH range, the rate constants were evaluated as shown in Fig. 2, and the pH dependences of k_1 (*open symbols*) and k_2 (*closed symbols*) are displayed. The marked effect of pH on k_1 was analyzed by fitting a "single pK" equation to the observed data, $k_1 = k_{1(O_2^{\cdot-})} + (k_{1(HO_2^{\cdot})} - k_{1(O_2^{\cdot-})}) \cdot K_{eq} \cdot [H^+]/(1 + K_{eq} \cdot [H^+])$, assuming different rate constants for OXANO reactions with $O_2^{\cdot-}$ and with its protonated form ($HO_2^{\cdot}$). Curve fitting was performed, using the MLAB computer program, assuming pK = 4.78 for $O_2^{\cdot-}/HO_2^{\cdot}$.

the two superoxide forms and consequently on the pH and the characteristic pK = 4.78 for $O_2^{\cdot-}/HO_2^{\cdot}$. The pH dependence of k_1 was analyzed by fitting a "single pK" equation to the experimental points to yield k_1 values of 7.1×10^5 M^{-1} s^{-1} and 1.3×10^2 M^{-1} s^{-1} for $HO_2^{\cdot}$ and $O_2^{\cdot-}$, respectively, from which the *solid line* shown in Fig. 3 was traced. The rate constant k_{-1} was determined directly by placing 1 mM OXANOH in phosphate buffer (pH 6, 8, and 9) containing 50 μM DTPA within the ESR spectrometer in a gas-permeable capillary, while oxygen was flowed around the sample. The gradual appearance of OXANO signal followed pseudo-zero order kinetics. OXANOH was oxidized at a rate of 0.25 μM $\cdot$ min^{-1}, with a second order rate constant k_{-1} estimated as 0.004 M^{-1} s^{-1}.

As was previously discussed (30), for other superoxide dismutase mimics, the actual observed value (k_{app}) of the catalytic rate constant differs from its limiting value (k_{cat}).

$$k_{app} = 2k_1k_2/(k_1 + k_2 + k_{-1}[O_2]/[O_2^{\cdot-}] \quad (6)$$

$$k_{cat} = 2k_1k_2/(k_1 + k_2) \quad (7)$$

k_{app} is always less than k_{cat}, due to the oxidation of the reduced catalyst by oxygen, with a rate constant of k_{-1}. However, a comparison of k_2, k_1, and k_{-1} values suggests that under high $O_2^{\cdot-}$ flux, while $k_{-1}[O_2]/[O_2^{\cdot-}] \ll (k_1 + k_2)$, k_{app} approaches k_{cat}. Previous attempts to develop superoxide dismutase mimics resulted in metal chelates such as $(phenanthroline)_2Cu$ or $(histidine)_2Cu$ having high reactivity toward oxygen (large k_{-1}) which resulted in apparent catalytic constants, k_{app}, much lower than k_{cat} (16). In contrast, the slow reaction with oxygen is a tremendous advantage of OXANO having $k_{-1} \ll k_1$, thus "enabling" $k_{app(OXANO)}$ to approach $k_{cat(OXANO)}$ with a consequent improved superoxide dismutase mimic activity. Moreover, cell permeability, low toxicity, relative stability, and solubility in both lipophilic and hydrophilic compartments make OXANO/OXANOH a promising superoxide dismutase mimic. $k_{cat(OXANO)}$ is 5 orders of magnitude lower than $k_{cat(superoxide\ dismutase)}$; however, in view of the potentially high concentrations achievable of OXANO/OXANOH the redox

pair may well be effective, particularly in places where superoxide dismutase is excluded such as cell membranes.

The biological implications of the present observations of this metal-free superoxide dismutase mimic might be far reaching. The OXANO spin label, which is soluble both in polar and nonpolar solvents and is relatively stable within cells, certainly exhibits a superoxide dismutase mimic activity. As this compound, in the millimolar range, is nontoxic[2] it might substitute for and augment superoxide dismutase-protective functions both inside and outside the cells. Results from preliminary studies indicate that other oxazolidine nitroxides also show superoxide dismutase-like activity. We are currently investigating the generality of this reaction of nitroxides, its specific requirements, and the degree of divergence within the oxazolidine system that will still serve as superoxide dismutase mimic. It is likely that a chemical modification will yield other superior nitroxides with improved catalytic efficiency and more selective biological activity.

Acknowledgments—We thank Dr. I. Fridovich and Dr. H. M. Swartz for helpful discussions and suggestions, and Dr. G. M. Rosen for providing the initial OXANO sample.

REFERENCES

1. McCord, J. M., and Fridovich, I. (1969) *J. Biol. Chem.* **244**, 6049–6055
2. Fridovich, I. (1972) *Accts. Chem. Res.* **5**, 321–326
3. Fridovich, I. (1974) *Adv. Enzymol. Relat. Areas Mol. Biol.* **41**, 35–97
4. Fridovich, I. (1975) *Annu. Rev. Biochem.* **44**, 147–159
5. Gregory, E. M., and Fridovich, I. (1973) *J. Bacteriol.* **114**, 543–548
6. Hassan, H. M., and Fridovich, I. (1977) *J. Biol. Chem.* **252**, 7667–7672
7. Werns, S. W., Shea, M. J., and Lucchesi, B. R. (1985) *J. Free Rad. Biol. Med.* **1**, 103–110
8. McCord, J. M., Stokes, S. J., and Wong, K. (1979) *Adv. Inflammation Res.* **1**, 273–278
9. McCord, J. M. (1985) *N. Engl. J. Med.* **132**, 159–163
10. Brigelius, R., Spottl, R., Bors, W., Lengfelder, E., Saran M., and Weser, U. (1974) *FEBS Lett.* **47**, 72–75
11. De Alvare, L. R., Goda, K., and Kimura, T. (1976) *Biochem. Biophys. Res. Commun.* **69**, 687–694
12. Lengfelder, E., Fuchs, C., Younes, M., and Weser, U. (1979) *Biochim. Biophys. Acta* **567**, 492–502
13. Weinstein, J., and Bielski, B. H. J. (1980) *J. Am. Chem. Soc.* **102**, 4916–4919
14. Koppenol, W. H., Levine, F., Hatmaker, T. L., Epp, J., and Rush, J. D. (1986) *Arch. Biochem. Biophys.* **251**, 594–599
15. Klug, D., Rabani, J., and Fridovich, I. (1972) *J. Biol. Chem.* **247**, 4839–4842
16. Goldstein, S., Michel, C., Bors, W., Saran, M., and Czapski, G. (1987) *Free Rad. Biol. Med.* **4**, 295–303
17. Sorenson, J. R. C. (1982) in *Metals in Biological Systems* (Sigel, H., ed) Vol. 14, p. 77, Marcel Dekker, Inc., New York
18. Darr, D., Zarilla, K. A., and Fridovich, I. (1987) *Arch. Biochem. Biophys.* **258**, 351–355
19. Samuni, A., Krishna, C. M., Riesz, P., Finkelstein, E., and Russo, A. (1989) *Free Rad. Biol. Med.* **6**, in press
20. Samuni, A., Black, C. D. V., Krishna, C. M., Malech, H. L., Bernstein, E. F., and Russo, A. (1988) *J. Biol. Chem.* **263**, 13797–13801
21. McConnell, H. M. (1976) in *Spin Labeling: Theory and Applications* (Berliner, L. J., ed) p. 525, Academic Press, New York
22. Magin, R. L., Wright, S. M., Niesman, M. R., Chan, H. C., and Swartz, H. M. (1986) *Magn. Reson. Med.* **3**, 440–447
23. Swartz, H. M., Chen, K., Pals, M., Sentjurc, M., and Morse, P. D., II (1986) *J. Magn. Reson.* **3**, 169–174
24. Swartz, H. M., Sentjurc, M., and Morse, P. D., II (1986) *Biochim. Biophys. Acta* **888**, 82–90
25. Rosen, G. M., Finkelstein, E., and Rauckman, E. J. (1982) *Arch. Biochem. Biophys.* **215**, 367–378
26. Rosen, G. M., Rauckman, E. J., and Hanck, K. W. (1977) *Toxicol. Lett. (Amst.)* **1**, 71–74
27. Rozantsev, E. G. (1970) *Free Nitroxyl Radicals*, pp. 93–94, Plenum Publishing Corp., New York
28. Butler, J., Jayson, G. G., and Swallow, A. J. (1975) *Biochim. Biophys. Acta* **408**, 215–222
29. Aurich, H. G. (1982) in *The Chemistry of Amino, Nitroso and Nitro Compounds and Their Derivatives* (Patai, S., ed) Part 1, p. 565, John Wiley and Sons, New York
30. Czapski, G., and Goldstein, S. (1988) *Free Rad. Res. Commun.* **4**, 225–232

[2] J. B. Mitchell, unpublished results.

Biochemistry 1990, *29*, 2802–2807

Biologically Active Metal-Independent Superoxide Dismutase Mimics

James B. Mitchell,*,‡ Amram Samuni,§ Murali C. Krishna,‡ William G. DeGraff,‡ Min S. Ahn,‡ Uri Samuni,‡ and Angelo Russo‡

Radiation Oncology Branch, Clinical Oncology Program, Division of Cancer Treatment, National Cancer Institute, National Institutes of Health, Bethesda, Maryland 20892, and Molecular Biology, School of Medicine, Hebrew University, Jerusalem 91010, Israel

Received August 21, 1989; Revised Manuscript Received October 27, 1989

ABSTRACT: Superoxide dismutase (SOD) is an enzyme that detoxifies superoxide ($O_2^{\cdot -}$), a potentially toxic oxygen-derived species. Attempts to increase intracellular concentrations of SOD by direct application are complicated because SOD, being a relatively large molecule, does not readily cross cell membranes. We have identified a set of stable nitroxides that possess SOD-like activity, have the advantage of being low molecular weight, membrane permeable, and metal independent, and at pH 7.0 have reaction rate constants with $O_2^{\cdot -}$ ranging from 1.1×10^3 to 1.3×10^6 M^{-1} s^{-1}. These SOD mimics protect mammalian cells from damage induced by hypoxanthine/xanthine oxidase and H_2O_2, although they exhibit no catalase-like activity. In addition, the nitroxide SOD mimics rapidly oxidize DNA–Fe^{II} and thus may interrupt the Fenton reaction and prevent formation of deleterious OH radicals and/or higher oxidation states of metal ions. Whether by SOD-like activity and/or interception of an electron from redox-active metal ions they protect cells from oxidative stress and may have use in basic and applied biological studies.

In an oxygen-containing environment, cellular metabolism results in the production of several potentially harmful oxygen-derived species. The first in this cascade of active oxygen metabolites is the one-electron reduction product, superoxide ($O_2^{\cdot -}$). The function of the superoxide-detoxifying metalloenzyme superoxide dismutase (SOD)[1] in protecting against oxygen-mediated biological damage is well documented (McCord & Fridovich, 1969; Fridovich, 1972, 1974, 1975; Gregory & Fridovich, 1973; Hassan & Fridovich, 1977). Increasing intracellular levels of SOD or administering exogenous SOD, among other salutary effects, reportedly lessens inflammation, decreases ischemia-induced reperfusion injury, decreases damage from tumor necrosis factor, and mitigates the damage caused by rheumatoid arthritis (Menander & Huber, 1977; McCord et al., 1979; McCord, 1985; Clark et al., 1988). Such reports have prompted further research to explore the clinical utility of administered SOD. Because $O_2^{\cdot -}$ can potentially be produced both inside and outside cells and because exogenously applied SOD has limited membrane permeabililty, detoxification of intracellularly produced $O_2^{\cdot -}$ by extracellular SOD would be limited. Hence, compounds with SOD-like activity having low molecular weight, biological stability, and membrane permeability have been sought. A number of metal chelates having SOD-like activity have been synthesized (Weinstein & Bielski, 1980; Koppenol et al., 1986; Darr et al., 1987; Nagano et al., 1988). These metal-dependent agents, however, might become ineffective in cells because of metal–ligand dissociation with subsequent random and potentially deleterious binding of the dissociated metal ions to critical cellular constituents (Darr et al., 1987). Thus, metal independence would be a desirable added criterion for a potential biologically useful SOD mimic. We have identified a family of stable cyclic nitroxide free radicals that possess these characteristics. Our initial observation was that a persistent nitroxide spin adduct resulting from the reaction between $^{\cdot}OH$ and DMPO, a commonly used electron spin-trapping agent, reacts with superoxide (Samuni et al., 1989). We extended the initial observation to show that a related stable free radical, 2-ethyl-2,5,5-trimethyl-3-oxazolidine-1-oxyl (OXANO; compound I, Table I), and its hydroxylamine react with $O_2^{\cdot -}$ independent of metal ions (Samuni et al., 1988).

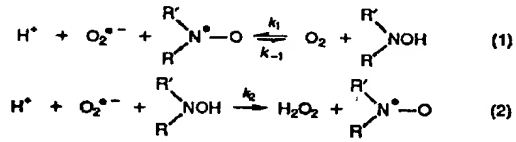

(1)

(2)

Summing reaction 1 and 2 results in

$$2O_2^{\cdot -} + 2H^+ \rightarrow O_2 + H_2O_2 \qquad (3)$$

and therefore, OXANO act as a low molecular weight, metal-free, SOD mimic. We have synthesized a series of chemically related stable nitroxide radicals with varying pendent groups and physical characteristics and have determined their SOD-like activity. To explore the potential usefulness of these agents, we examined their mechanism of action and effects on mammalian cells exposed to oxidative stress resulting from either HX/XO or direct H_2O_2 exposure.

Experimental Procedures

Chemicals. Desferrioxamine (DF) was a gift from Ciba Geigy; hypoxanthine (HX) was purchased from Calbiochem-Boehringer Co.; 2,2,6,6-tetramethylpiperidine-1-oxyl (TEMPO), 4-hydroxy-2,2,6,6-tetramethylpiperidine-1-oxyl (TEMPOL), 4-hydroxypyrazolo[3,4,-*d*]pyrimidine (allopurinol), *p*-toluenesulfonic acid, 2-amino-2-methyl-1-propanol, 2-butanone, and cyclohexanone were purchased from Aldrich Chemical Co.; tris(oxalato)chromate(III) [$K_3[Cr(C_2O_4)_3]$·

* Address correspondence to this author at the Radiation Oncology Branch, NCI, Building 10, Room B3-B69, Bethesda, MD 20892.
‡ NCI, National Institutes of Health.
§ Hebrew University.

[1] Abbreviations: EPR, electron paramagnetic resonance; CHD, spiro[cyclohexane-1,2′-doxyl] [spiro[cyclohexane-1,2′-(4′,4′-dimethyloxazolidine-3′-oxyl)]]; DTPA, diethylenetriaminepentaacetate; OXANO, 2-ethyl-2,4,4-trimethyloxazolidine-3-oxyl; TEMPOL, 4-hydroxy-2,2,6,6-tetramethylpiperidine-1-oxyl; TEMPO, 2,2,6,6-tetramethylpiperidine-1-oxyl; SOD, superoxide dismutase; DF, desferrioxamine; XO, xanthine oxidase; HX, hypoxanthine.

$3H_2O$] (CrOx) was prepared and recrystallized as previously described (Bailar & Young, 1939); xanthine oxidase (EC 1.2.3.2; xanthine:oxygen oxidoreductase), grade III, from buttermilk, superoxide dismutase (SOD), and grade V ferricytochrome *c* were obtained from Sigma. H_2O_2 was bought from Fisher Scientific Co. XO was further purified on a G-25 Sephadex column. All other chemicals were prepared and used without further purification. Distilled–deionized water was used throughout all experiments.

Synthesis of Oxazolidine Derivatives. Spiro[cyclohexane-1,2′-doxyl] [CHD; spiro[cyclohexane-1,2′-(4′,4′-dimethyl-oxazolidine-3′-oxyl)]] and 2-ethyl-2,4,4-trimethyl-oxazolidine-3-oxyl (OXANO) as well as other nitroxides were synthesized as previously described (Keana et al., 1967). For the general synthesis of the cyclic amines, the appropriate starting ketone was reacted with 2-amino-2-methyl-1-propanol in benzene in the presence of catalytic amounts of *p*-toluenesulfonic acid. As the cyclic structure formed, water was eliminated. The volume of water collected in a Dean–Stark apparatus was monitored and used to gauge the reaction progress. The amines thus produced were purified through fractional distillation under reduced pressure, characterized by 220-MHz ^1H NMR, IR, UV, either EI or CI mass spectroscopy, and subsequently oxidized to the corresponding nitroxides by using *m*-chloroperbenzoic acid. The nitroxides were purified by silica flash chromatography (Still et al., 1978). Water/octanol ratios were determined by placing a quantity of nitroxide in water + octanol within a separatory funnel. The mixture was shaken thoroughly and allowed to separate for 15 min, whereupon aliquots were taken from both fractions and the ratio of nitroxide distribution was determined according to electron paramagnetic resonance (EPR) spectroscopy by comparing the intensities of signal obtained under N_2.

Ferricytochrome c Reduction Assay. The SOD-inhibitable ferricytochrome *c* reduction assay (Fridovich, 1985) was used to determine rate constants of reaction with $O_2^{\cdot -}$. Superoxide radicals were generated at 25 °C in aerated phosphate buffer (50 mM) containing 50 μM DTPA, 5 mM HX, and 10–50 μM ferricytochrome *c* (with or without 65 units/mL catalase). The reaction was started by adding 0.01 unit/mL XO, and the rate of ferricytochrome *c* reduction, in the absence (V) and in the presence (v) of various nitroxides, was spectrophotometrically followed at 550 nm. Both reference and sample cuvettes contained all the agents, with the reference containing 100 units/mL SOD, thereby eliminating spurious reactions from interfering with the determination of rate constants. Data were analyzed by plotting V/v as a function of [nitroxide], and k_1 was calculated, knowing $k_{CytC+superoxide}$, according to $(V/v) - 1 = k_1[\text{nitroxide}]/k_{CytC+superoxide}[\text{Cyt-c}^{III}]$.

Cell Culture. Chinese hamster V79 cells were grown in F12 medium supplemented with 10% fetal calf serum, penicillin, and streptomycin. Survival was assessed in all studies by the clonogenic assay. The control plating efficiency ranged between 80 and 90%. Stock cultures of exponentially growing cells were trypsinized, rinsed, plated (5×10^5 cells/dish) into a number of 100-mm Petri dishes, and incubated 16 h at 37 °C prior to experimental protocols. Cells were exposed for 1 h at 37 °C to either 0.5 mM hypoxanthine (HX) + 0.05 unit/mL xanthine oxidase (XO) for varying lengths of time or H_2O_2 at different concentrations. To assess possible modulation in cytotoxicity, catalase, 100 units/mL; SOD, 100 μg/mL; DF, 500 μM; and 5 mM of each of the nitroxides from Tables I and II were added to parallel cultures. CHD was prepared in a stock solution in ethanol and diluted into medium such that the final concentration was 5 mM. This resulted in a final concentration of 1% ethanol in the medium which was not cytotoxic and did not influence the cellular response to HX/XO or H_2O_2. TEMPOL is water soluble and was prepared directly in tissue culture medium. Neither catalase, SOD, DF, CHD, or TEMPOL was cytotoxic alone at the concentrations used. DF was added either 2 h prior to or immediately before and then left on during treatment while the other agents were present only during HX/XO or H_2O_2 treatment. Following treatment, cells were rinsed, trypsinized, counted, and plated for macroscopic colony formation. For each dose determination cells were plated in triplicate and the experiments were repeated a minimum of two times. Plates were incubated 7 days, after which colonies were fixed with methanol/acetic acid, stained with crystal violet, and counted. Colonies containing >50 cells were scored. Error bars represent SD of the mean and are shown when larger than the symbol.

Some studies required exposure to H_2O_2 under hypoxic conditions. For these studies cells dispersed in 1.8 mL of medium were plated into specially designed glass flasks (Russo et al., 1985). The flasks were sealed with soft rubber stoppers, and 19-gauge needles were pushed through to act as entrance and exit ports for a humidified gas mixture of 95% nitrogen/5% CO_2 (Matheson Gas Products). Each flask was also equipped with a ground-glass side-arm vessel which when rotated and inverted could deliver 0.2 mL of medium containing H_2O_2 at a concentration that when added to the cell monolayer resulted in a final concentration of H_2O_2 of 600 μM. Stoppered flasks were connected in series, mounted on a reciprocating platform, and gassed at 37 °C for 45 min. This gassing procedure results in an equilibrium between the gas and liquid phase (in both the medium over the cell monolayer and the solution in the side arm) and yielded oxygen concentrations in the effluent gas phase of <10 ppm as measured by a Thermox probe (Russo et al., 1985). After 45 min of gassing, the hypoxic H_2O_2 solution was added to the cell monolayer culture. The cells were exposed to H_2O_2 for 1 h under hypoxic conditions. N_2 gas flow was maintained during the H_2O_2 exposure. In parallel flasks, DF and CHD were added as described above and were present during the entire gassing procedure. Following treatment cell survival was assessed as described above.

Electron Paramagnetic Resonance. For EPR experiments samples (0.05–0.1 mL) of either solutions of chemicals or cell suspensions were drawn by a syringe into a gas-permeable teflon capillary of 0.8 mm inner diameter and 0.05 mm wall thickness (Zeus Industrial Products, Inc., Raritan, NJ). Each capillary was folded twice, inserted into a narrow quartz tube which was open at both ends (2.5 mm i.d.), and then placed horizontally into the EPR cavity. During the experiments, gases of desired compositions were blown around the sample without having to disturb the alignment of the tube within the EPR cavity. EPR spectra were recorded on a Varian E4 (or E9) X-band spectrometer, with field set at 3357 G, modulation frequency of 100 KHz, modulation amplitude of 1 G, and nonsaturating microwave power. The EPR spectrometer was interfaced to an IBM-PC through an analog-to-digital converter and a data translation hardware (DT2801), and the spectra were digitized by using commercial acquisition software, enabling subtraction of background signals. To study the kinetics of the spin loss, the spectra were deliberately overmodulated, and the magnetic field was kept constant while the intensity of the EPR signal was followed.

H_2O_2 Assay. Hydrogen peroxide was assayed by using a YSI Model 27 industrial analyzer (Yellow Springs Instru-

Table I: Five-Membered Oxazolidine-3-oxyl (Doxyl)

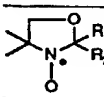

nitroxide notation	ring substituents R_1	ring substituents R_2	yield (%)	partition coefficient[a]
I	OXANO	CH_3	C_2H_5	42	10
II		CH_3	C_5H_{11}	52	145
III		CH_3	C_4H_9	49	58
IV	CHD	spirocyclohexyl		77	80
V		CH_3	C_6H_5	22	720

[a] Octanol/water.

Table II: Kinetic Data: SOD-like Activity of Five- and Six-Membered Cyclic Nitroxides

chemical structure:	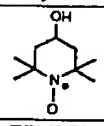		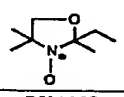	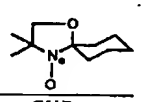
nitroxide notation	TEMPOL	TEMPO	OXANO	CHD
steady-state EPR signal (%)[a]	100	100	50	30
$k_{R'RNO+O_2^{\cdot-}}$ (M^{-1} s^{-1})[b]	3.4×10^5	1.3×10^6	1.1×10^3	3.5×10^3

[a] Steady-state EPR signal of nitroxides (% from total R'RNO + R'RNOH) after exposure to 5 mM HX + 0.03 unit/mL XO in air-saturated PBS, pH 7.2. [b] Rate constants were determined at low ionic strength (10 mM HEPES), pH 7.0, and 22 °C.

ments) equipped with a selective electrode for H_2O_2. For analysis of cellular preparations, the cells, except during the brief time required for removal of aliquots for analysis, were kept in T25 culture flasks maintained at 37 °C in complete medium (pH 7.2). Aliquots of 25 μL were sampled from the reaction or cell preparation system at varying time points and injected into the analyzer. $[H_2O_2]$ was determined after calibrating the instrument with known concentrations of H_2O_2. The concentrations of standard H_2O_2 solutions were calibrated according to the iodometric assay (Hochanadel, 1952).

Results

Nitroxide Synthesis and Characterization. To check whether oxazolidineoxyl derivatives other than OXANO manifest SOD-like activity, we synthesized several nitroxides having different ring substituents. Table I shows representative synthesized nitroxides with accompanying physical characteristics. Exposure of these five-membered cyclic nitroxides to $O_2^{\cdot-}$ flux formed by HX/XO resulted in a decrease in their EPR signal, as previously found for OXANO (Samuni et al., 1989). After terminating the HX/XO reaction by allopurinol, the nitroxide spin loss was reversed by adding 0.5 mM ferricyanide, indicating that $O_2^{\cdot-}$ reduces the nitroxide to its respective hydroxylamine (Samuni et al., 1989). On the other hand, no effect of $O_2^{\cdot-}$ on the EPR signal of six-membered ring nitroxides such as TEMPO and TEMPOL was detectable (see Table II). The failure of superoxide to affect TEMPO and TEMPOL apparently suggested that six-membered cyclic nitroxides lack SOD-like activity. As a further check, the reaction of representatives of both five- and six-membered cyclic nitroxides with $O_2^{\cdot-}$ was studied. Superoxide flux was generated by HX/XO reaction system, and the nitroxide effect on the SOD-inhibitable reduction of ferricytochrome *c* was followed spectrophotometrically (Fridovich, 1985). All of the

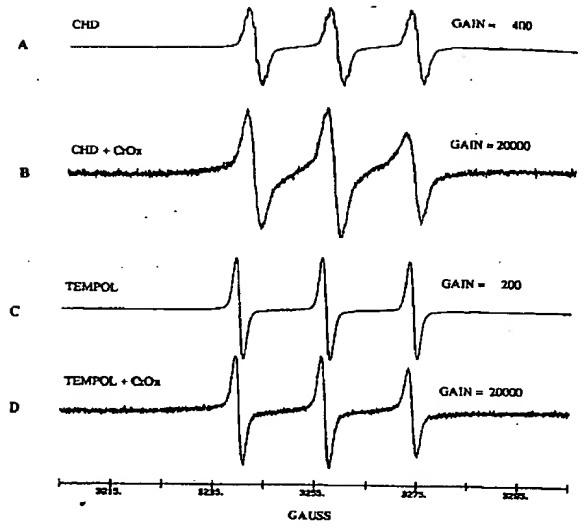

FIGURE 1: EPR spectra of CHD and TEMPOL demonstrating the partitioning of each nitroxide (1 mM) in both the intra- and extracellular space of V79 cells. The EPR signal intensity of the total concentration of CHD or TEMPOL (intra- and extracellular) in 6.4×10^7 V79 cells/mL (traces A and C) and in the presence of 110 mM tris(oxalato)chromiate (CrOx) (traces B and D). The gains for individual spectra are as cited in the individual traces.

stable nitroxide radicals studied demonstrated reaction with $O_2^{\cdot-}$. The rate constants of the synthetic nitroxides' reaction with $O_2^{\cdot-}$ at low ionic strength (10 mM HEPES) and pH 7.0 ranged from 1.1×10^3 to 1.3×10^6 M^{-1} s^{-1} (see Table II), as compared with 2.3×10^9 M^{-1} s^{-1} for k_{cat} of native SOD.

None of the nitroxides shown in Tables I and II exhibited cytotoxicity (determined by clonogenic assay) in V79 cells exposed for 1 h at 5 mM. For subsequent studies the most lipophilic nitroxide, CHD, and the most hydrophilic one, TEMPOL, were chosen.

Nitroxide Intracellular Localization. Traces A and C of Figure 1 illustrate the EPR signal from 1 mM CHD and TEMPOL, respectively, suspended with 6.4×10^7 V79 cells/mL. This EPR signal represents the total concentration of intra- and extracellular CHD or TEMPOL. Tris(oxalato)chromate is a paramagnetic broadening agent which remains excluded from the intracellular volume space and causes the EPR signal from extracellular species to become nondetectable (Lai, 1988). When cells were added to CHD or TEMPOL in the presence of 110 mM tris(oxalato)chromiate, a much smaller yet observable intracellular signal was detected, as shown in Figure 1B,D. The observable line broadening and loss of the hyperfine structure of the intracellular signal indicate that CHD, though not TEMPOL, has decreased freedom of motion (anisotropy) within the intracellular environment and is located primarily in a membranous compartment as can be anticipated on the basis of the difference between their lipophilicities.

Protection from Oxidative Damage. To expose the cells to oxidative stress, they were incubated with HX/XO. Figure 2 shows a survival curve for cells exposed to HX/XO. Cell survival was not altered when SOD was present during the HX/XO exposure. In contrast, 5 mM CHD or TEMPOL fully protected the cells. The other nitroxides, presented in Tables I and II, afforded similar protection (data not shown). Figure 2 also shows that either catalase or DF provides complete protection from HX/XO-derived damage. Complete

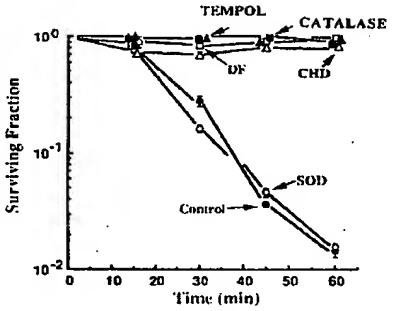

FIGURE 2: Protection from HX/XO-induced cell killing. Chinese hamster V79 cells in full medium at 37 °C were exposed to 0.05 unit/mL XO + 0.5 mM HX for various time periods in the presence of various additives: (●) control, no additives; (■) 100 units/mL catalase; (○) 100 units/mL SOD; (□) 500 μM DF, preincubated for 2 h with the cells prior to addition of XO; (△) 5 mM CHD; (▲) 5 mM TEMPOL.

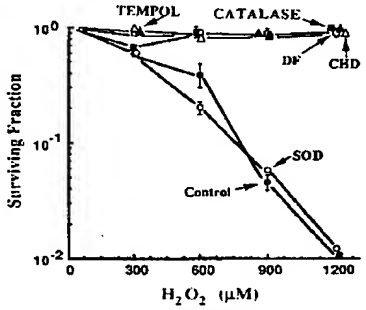

FIGURE 3: Protection from H_2O_2-induced cell killing. The effect of various agents on cell survival was measured by clonogenic assay of Chinese hamster V79 cells exposed in full medium at 37 °C to various concentrations of H_2O_2 for 1 h: (●) control, no additives; (■) 100 units/mL catalase; (○) 100 μg/mL SOD; (□) 500 μM DF, preincubated for 2 h with the cells prior to H_2O_2 addition; (△) 5 mM CHD; (▲) 5 mM TEMPOL.

protection by DF required a 2-h preincubation with DF before cells were exposed to HX/XO, whereas DF addition simultaneously with HX/XO offered only partial protection (data not shown).

One interpretation of the data shown in Figure 2 was that H_2O_2 is the principal cytotoxic species produced by the HX/XO system (Link & Riley, 1988). This assumption is based on the fact that extracellular catalase provided complete protection from HX/XO (Figure 2). To test if cell protection by the SOD mimic resulted by preventing the effect of H_2O_2, cells were exposed to H_2O_2 as shown in Figure 3. The results of these experiments were identical with those shown in Figure 2, in that SOD did not protect, but catalase, DF, TEMPOL, and CHD provided complete protection against H_2O_2 cytotoxicity. At this point it was questioned if CHD might have other features apart from acting as a SOD mimic, namely, whether CHD affects H_2O_2 concentration. Figure 4 shows the concentration of H_2O_2 in tissue culture exposed to HX/XO. With time there was a buildup followed by a slow decline in $[H_2O_2]$. The presence of CHD did not significantly alter the pattern of H_2O_2 accumulation by HX/XO. Thus, the cellular protection afforded by CHD to HX/XO and H_2O_2 could not be attributed to a direct reaction of CHD with H_2O_2.

Even with direct exposure of cells to H_2O_2 there is the possibility that superoxide could be produced intracellularly as a result of the H_2O_2 treatment. If superoxide were produced intracellularly, CHD protection of cells from HX/XO and

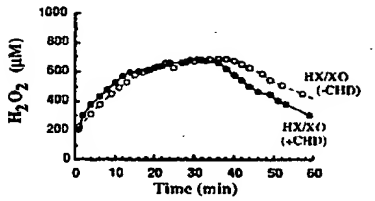

FIGURE 4: Nitroxide effect on accumulation and decay of H_2O_2 upon exposure of cells to HX/XO. Chinese hamster V79 cells were plated in full medium and incubated at 37 °C with 5 mM HX + 0.04 unit/mL XO, sampled at various time points, and assayed for H_2O_2 by using a hydrogen peroxide selective electrode.

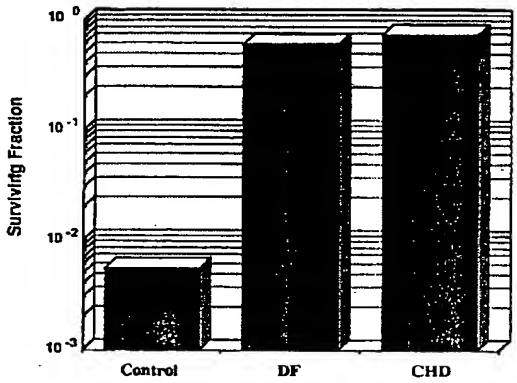

FIGURE 5: Survival of Chinese hamster V79 cells exposed to 600 μM H_2O_2 ± DF or CHD in full medium at 37 °C for 1 h under hypoxic conditions.

H_2O_2 might be expected, given the findings that CHD can penetrate intracellular spaces as shown in Figure 1. To test if the cytoprotection provided by CHD was solely a result of its reaction with superoxide, CHD effectiveness was examined when H_2O_2 was applied to cells incubated in an hypoxic environment, conditions in which the chance for superoxide formation would be significantly limited. As is seen in Figure 5, CHD protects against H_2O_2 cytotoxicity even under hypoxic conditions.

Figure 5 also shows that DF provides complete protection to H_2O_2 cytotoxicity under hypoxic conditions. The pattern of DF protection shown in Figures 2, 3, and 5 suggested that the cytotoxicity of HX/XO and H_2O_2 may directly involve intracellular reduction of H_2O_2 by ferrous ion to produce the highly toxic $^{\bullet}OH$. It was also questioned whether the aerobic and hypoxic protection by CHD to H_2O_2 exposure was a result of CHD directly accepting electrons from ferrous ions, thereby preventing generation of $^{\bullet}OH$. Because cellular iron is chelated, the possible reaction of nitroxide with chelated iron(II) was examined by repeating the experiment in the presence of DNA. To study the possibility of nitroxide-induced oxidation of transition metals, CHD was hypoxically mixed with iron(II) in the presence of 0.1 mg/mL salmon DNA. Consequently, DNA–Fe^{III} was formed and the nitroxide EPR signal disappeared. The reaction kinetics were investigated by maintaining either CHD or Fe(II) in excess while the absorbance due to DNA–Fe^{III} and the nitroxide spin loss were monitored respectively (Figure 6). Both the decay of the EPR signal and the appearance of the OD_{353nm} obeyed pseudo-first-order kinetics from which the second-order reaction rate constant was calculated as 44 M^{-1} s^{-1} or 33 M^{-1} s^{-1} by using the data from EPR or optical absorption, respectively. When TEMPOL was hypoxically mixed with DNA–Fe^{II}, a similar reaction took

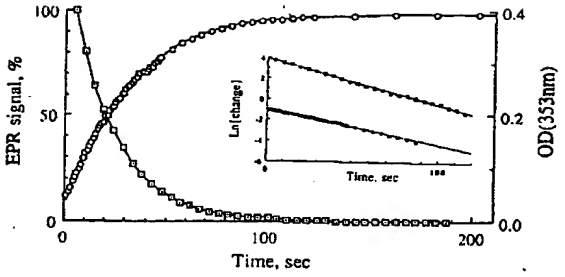

FIGURE 6: Reaction between CHD and DNA–Fe^{II}. CHD in 50 mM MOPS buffer, pH 7.0, was anoxically mixed at 22 °C with DNA–Fe^{II}. All solutions always contained 0.1 mg/mL salmon DNA. The appearance of DNA–Fe^{III} was spectrophotometrically monitored at 353 nm, whereas the spin loss of CHD was monitored by following its EPR signal. To study the time dependence of ΔOD_{353nm} (○), 1 mM CHD was mixed with 0.1 mM Fe(II). To follow the spin loss of CHD (□), 1 mM Fe(II) was mixed with 0.1 mM CHD. Inset: Time dependence of ln (EPR signal) (□) and of ln ($OD_\infty - OD_t$) (○).

place having a second-order reaction rate constant of 40 M^{-1} s^{-1}. The spin loss was completely reversed by adding 2 mM ferricyanide, thus indicating that DNA–Fe^{II} reduced the respective nitroxide to its hydroxylamine.

Discussion

The recent finding that OXANO can function as a metal-independent SOD mimic (Samuni et al., 1988) opened the possibility that nitroxides, which have already found considerable utility in both EPR and NMR spectroscopy (McConnell, 1976; Magin et al., 1986; Swartz et al., 1986), might also exhibit unique biological characteristics. The data presented here evaluating representative five- and six-membered ring nitroxides clearly demonstrate their utility in protecting mammalian cells against oxidative stress. In our experiments using two different means of inducing cytotoxicity, all nitroxides tested afforded protection. Initially, when considering the large difference in catalytic capabilities between native SOD and the nitroxide SOD mimics, it would appear that the mimics would be less than ideal for biological applications. However, since nitroxide SOD mimics can be used at relatively high concentrations without cytotoxicity and are capable of penetrating through membranes into the cellular compartments, the effective detoxification of intracellular superoxide seems plausible.

In both systems used to access cytotoxicity (HX/XO and direct H_2O_2 exposure), extracellular application of SOD did not offer protection. There are several conclusions that can be drawn from this finding. Possibly extracellular superoxide does not have any inherent toxicity, and therefore applying an agent like SOD extracellularly would afford little benefit. Another possibility is that the HX/XO-derived superoxide is only toxic after it crosses the cell membrane. However, the amount of SOD applied (Figure 2) is sufficient to have converted all of the extracellularly generated superoxide to H_2O_2. Therefore, we conclude that exogenously produced superoxide is not in and of itself responsible for cytotoxicity. If exogenous $O_2^{\cdot -}$ is not responsible for the toxicity, what is? Since the HX/XO system produces both H_2O_2 and $O_2^{\cdot -}$ (which yields H_2O_2), the former appears to be the major initial cytotoxic species produced by HX/XO (Link & Riley, 1988). The present results support this conclusion. Both catalase and DF (see Figure 2) protected from both HX/XO and H_2O_2 by inhibiting the Fenton reaction (Rush & Koppenol, 1986):

$$\text{DNA–Fe}^{II} + H_2O_2 \rightarrow \text{DNA–Fe}^{II}\text{–}H_2O_2 \qquad (4)$$

The peroxo complex can generate $^{\cdot}OH$ radicals and/or higher oxidation states of the metal (Masarwa et al., 1988):

$$\text{DNA–Fe}^{II}\text{–}H_2O_2 \rightarrow \text{DNA–Fe}^{III} + OH^- + {}^{\cdot}OH \qquad (4a)$$

$$\text{DNA–Fe}^{II}\text{–}H_2O_2 \rightarrow \text{DNA–Fe}^{IV} + 2OH^- \qquad (4b)$$

By catalyzing H_2O_2 production through reactions 1 and 2, CHD and TEMPOL might be expected to increase cytotoxicity; however, reactions 4, 4a, and 4b constitute only the second half of the Haber–Weiss reaction (Fenton reaction), the first half being a superoxide-driven reduction of ferric ion to the oxidized metal, i.e.

$$\text{Fe}^{III} + O_2^{\cdot -} \rightarrow \text{Fe}^{II} + O_2 \qquad (5)$$

Removal of either the labile intracellular ferric ion (by chelators such as DF) or removal of intracellular superoxide (by SOD mimics such as CHD or TEMPOL) could result in cessation of $^{\cdot}OH$ production and a decrease in toxicity as is demonstrated in Figures 2, 3, and 5.

Further, we have demonstrated that nitroxides are reduced by Fe(II) chelated to DNA. The reaction rate of CHD with DNA–Fe^{II} (see Figure 6) is comparable with that of H_2O_2 plus Fe(II) (68 M^{-1} s^{-1}) (Kozlov et al., 1974). This comparison, however, might be inconsequential because the exact nature, concentrations, and sites of redox-active iron within the cell are not known, nor is the rate of reaction of DNA–Fe^{II} with H_2O_2; hence, direct comparison to the CHD reaction with DNA–Fe^{II} is not possible. Yet, it is possible that where [nitroxide] $\gg$ [H_2O_2], redox-active iron would react with nitroxide in preference to H_2O_2

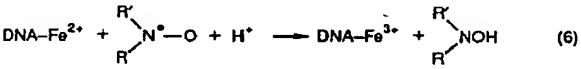

(6)

therefore preempting the intracellular generation of $^{\cdot}OH$ through reactions 4 and 4a.

Nitroxide also protected (Figure 5) when H_2O_2 treatment was conducted under hypoxic conditions, where the availability of oxygen for the formation of intracellular $O_2^{\cdot -}$ generation is greatly if not completely eliminated. It should be noted that, even in the absence of oxygen, intracellular catalase could convert H_2O_2 to oxygen which might then become available to form superoxide. Thus, it cannot be stated categorically that nitroxides protect independent of reactions with intracellular superoxide. Yet, taken together, our data suggest that (a) the major intracellular toxicity of superoxide may be an indirect contribution to $^{\cdot}OH$ production rather than direct reactions with biological molecules like DNA and (b) the beneficial function of intracellular SOD might be in decreasing metal-catalyzed $^{\cdot}OH$ production. Such a function for SOD is consistent with the seemingly incongruous relatively low direct reactivity of superoxide (Sawyer & Valentine, 1981). An alternative explanation for the nitroxide protective effect can be found by assuming that they react with and detoxify secondarily produced organic free radicals. Although nitroxide free radicals are relatively stable, they rapidly couple with carbon-centered and oxygen-centered free radicals and exhibit diffusion-controlled reaction rate constants. Such a detoxification was recently found to decrease lipid peroxidation in cell-free systems (Takahashi et al., 1989; Nilsson et al., 1989).

In addition to ameliorating cytotoxicity as shown in Figures 2, 3, and 5, the penetration of the nitroxides into intracellular spaces could possibly allow for a better understanding of intracellular damage sites of superoxide and/or H_2O_2. The design and synthesis of other nitroxide SOD mimics that can be used to probe specifically the effects of $O_2^{\cdot -}$ within different cellular compartments and organelles may, in part, be based

on simple lipid/water partitioning coefficients. Since the partitioning ratio between membranous and intracellular or extracellular aqueous compartments can be approximated by the octanol/water partition coefficient, then in addition to the design of specific site-directed stable nitroxide radicals one may be able to produce a first generation of mimics with more aqueous or lipid activity (Table I). We are just beginning to explore these possibilities.

The nitroxide based SOD mimics described here are tolerated by mammalian cells and act to protect against oxidative damage, whereas extracellular application of SOD does not offer such protection. It is anticipated that these SOD mimics or similar derivatives may find use as basic biologic probes to study the effects of superoxide acting in specific cellular compartments. Additionally, they might be used to probe the intracellular mechanisms of "redox-active" drugs that ostensibly mediate damage through specific oxygen metabolites. Our finding may ultimately have application in protection from biologic damage caused by postischemic reperfusion injury associated with reopening of arteries after heart attacks or strokes, as well as lessening the life-threatening toxic effects of exposure to elevated oxygen concentration as is sometimes necessary while providing life support during acute care.

References

Bailar, J. C., Jr., & Young, E. M. (1939) *Inorg. Synth. 1*, 35–38.

Clark, I. A., Chaudhri, G., & Cowden, W. B. (1988) in *Oxyradicals in Molecular Biology and Pathology* (Cerutti, P. A., Fridovich, I., & McCord, J. M., Eds.) pp 53–60, Alan R. Liss, New York.

Darr, D., Zarilla, K. A., & Fridovich, I. (1987) *Arch. Biochem. Biophys. 258*, 351–355.

Fridovich, I. (1972) *Acc. Chem. Res. 5*, 321–326.

Fridovich, I. (1974) *Adv. Enzymol. 41*, 35–97.

Fridovich, I. (1975) *Annu. Rev. Biochem. 44*, 147–159.

Fridovich, I. (1985) in *Handbook of Methods for Oxygen Radical Research* (Greenwald, R. A., Ed.) pp 213–215, CRC Press, Roca Raton, FL.

Gregory, E. M., & Fridovich, I. (1973) *J. Bacteriol. 114*, 543–548.

Hassan, H. M., & Fridovich, I. (1977) *J. Biol. Chem. 252*, 7667–7672.

Hochanadel, C. J. (1952) *J. Phys. Chem. 56*, 587–594.

Keana, J. F. W., Keana, S. B., & Beetham, D. (1967) *J. Am. Chem. Soc. 89*, 3055–3056.

Koppenol, W. H., Levine, F., Hatmaker, T. L., Epp, J., & Rush, J. D. (1986) *Arch. Biochem. Biophys. 251*, 594–599.

Kozlov, Y. N., Nadezhdin, A. D., & Pourmal, A. P. (1974) *Int. J. Chem. Kinet. 6*, 383–394.

Lai, C.-S., Froncisz, W., & Hopwood, L. E. (1988) *Biophys. J. 52*, 625–628.

Link, E. M., & Riley, P. A. (1988) *Biochem. J. 249*, 391–399.

Magin, R. L., Wright, S. M., Niesman, M. R., Chan, H. C., & Swartz, H. M. (1986) *Magn. Reson. Med. 3*, 440–447.

Masarwa, M., Cohen, H., Meyerstein, D., Hickman, D. L., Bakac, A., & Espenson, J. H. (1988) *J. Am. Chem. Soc. 110*, 4293–4297.

McConnell, H. M. (1976) in *Spin Labelling: Theory and Applications* (Berliner, L. J., Ed.) pp 525–560, Academic Press, New York.

McCord, J. M. (1985) *N. Engl. J. Med. 312*, 159–163.

McCord, J. M., & Fridovich, I. (1969) *J. Biol. Chem. 244*, 6049–6055.

McCord, J. M., Stokes, S. H., & Wong, K. (1979) *Adv. Inflammation Res. 1*, 273–280.

Menander-Huber, K. B., & Huber, W. (1977) in *Superoxide and Superoxide Dismutases* (Michelson, A. M., McCord, J. M., & Fridovich, I., Eds.) pp 537–549, Academic Press, London.

Nagano, T., Hirano, T., & Hirobe, M. (1988) in *Medical, Biochemical and Chemical Aspects of Free Radicals* (Hayaishi, O., Niki, E., Kondo, M., & Yoshikawa, T., Eds.) pp 125–132, Elsevier Science Publishers, Amsterdam.

Nilsson, U. A., Olsson, L.-I., Carlin, G., & Bylund-Fellenius, A.-C. (1989) *J. Biol. Chem. 264*, 11131–11135.

Rush, J. D., & Koppenol, W. H. (1986) *J. Biol. Chem. 261*, 6730–6733.

Russo, A., Mitchell, J. B., Finkelstein, E., DeGraff, W. G., Spiro, I. J., & Gamson, J. (1985) *Radiat. Res. 103*, 232–239.

Samuni, A., Krishna, C. M., Riesz, P., Finkelstein, E., & Russo, A. (1988) *J. Biol. Chem. 263*, 17921–17924.

Samuni, A., Krishna, C. M., Riesz, P., Finkelstein, E., & Russo, A. (1989) *Free Radical Biol. Med. 6*, 141–148.

Sawyer, D. T., & Valentine, J. S. (1981) *Acc. Chem. Res. 14*, 393–400.

Still, W. C., Kahn, M., & Mitra, A. (1978) *J. Org. Chem. 43*, 2923–2925.

Swartz, H. M. (1986) *Bull. Magn. Reson. 8*, 172–175.

Takahashi, M. Tsuchiya, J., & Niki, E. (1989) *J. Am. Chem. Soc. 111*, 6350–6353.

Weinstein, J., & Bielski, B. H. J. (1980) *J. Am. Chem. Soc. 102*, 4916–4919.

Proc. Natl. Acad. Sci. USA
Vol. 89, pp. 5537–5541, June 1992
Biochemistry

Oxoammonium cation intermediate in the nitroxide-catalyzed dismutation of superoxide

(electron paramagnetic resonance/hydrogen peroxide/superoxide radical/superoxide dismutase/oxoammonium cation)

MURALI C. KRISHNA*, DAVID A. GRAHAME†, AMRAM SAMUNI‡, JAMES B. MITCHELL*, AND ANGELO RUSSO*§

*Radiation Oncology Branch, Clinical Oncology Program, Division of Cancer Treatment, National Cancer Institute, and †Laboratory of Biochemistry, National Heart Lung and Blood Institute, National Institutes of Health, Bethesda, MD 20892; and ‡Molecular Biology, School of Medicine, Hebrew University, Jerusalem, 91010, Israel

Communicated by Thressa C. Stadtman, March 24, 1992

ABSTRACT **Dismutation of superoxide has been shown previously to be catalyzed by stable nitroxide compounds. In the present study, the mechanism of superoxide ($\cdot O_2^-$) dismutation by various five-membered ring and six-membered ring nitroxides was studied by electron paramagnetic resonance spectrometry, UV-visible spectrophotometry, cyclic voltammetry, and bulk electrolysis. Electron paramagnetic resonance signals from the carbocyclic nitroxide derivatives (piperidinyl, pyrrolidinyl, and pyrrolinyl) were unchanged when exposed to enzymatically generated $\cdot O_2^-$, whereas, in the presence of $\cdot O_2^-$ and reducing agents such as NADH and NADPH, the nitroxides underwent reduction to their respective hydroxylamines. The reaction of 4-hydroxy-2,2,6,6-tetramethyl-1-hydroxypiperidine (Tempol-H) with $\cdot O_2^-$ was measured and, in agreement with earlier reports on related compounds, the rate was found to be too slow to be consistent with a mechanism of $\cdot O_2^-$ dismutation involving the hydroxylamine as an intermediate. Voltammetric analyses of the carbocyclic nitroxide derivatives revealed a reversible one-electron redox couple at positive potentials. In contrast, oxazolidine derivatives were irreversibly oxidized. At negative potentials, all of the nitroxides studied exhibited a broad, irreversible reductive wave. The rate of $\cdot O_2^-$ dismutation correlated with the reversible midpoint redox potential. Bulk electrolysis at positive potentials was found to generate a metastable oxidized form of the nitroxide. The results indicate that the dismutation of $\cdot O_2^-$ is catalyzed by the oxoammonium/nitroxide redox couple for carbocyclic nitroxide derivatives. In addition to the one-electron mitochondrial reduction pathway, the present results suggest the possibility that cellular bioreduction by a two-electron pathway may occur subsequent to oxidation of stable nitroxides. Furthermore, the cellular destruction of persistent spin adduct nitroxides might also be facilitated by a primary univalent oxidation.**

Stable nitroxide free radicals have found a wide range of applications in biology and medicine. These compounds have been used to monitor intracellular redox reactions (1), oxygen concentration (2), and pH (3), as well as electron paramagnetic resonance (EPR) microscopy of spheroids (4), as contrast agents in magnetic resonance imaging (5), and as probes in EPR imaging (6). Persistent nitroxide adducts resulting from reaction of a precursor nitrone (spin trap) with transient free radical species have been used to detect, characterize, and quantitate the production of free radicals in various *in vitro* and *in vivo* model systems (7). The cellular and *in vivo* pharmacology of stable nitroxides and persistent spin adduct nitroxides has been investigated in detail (8–10). One-electron reduction of stable nitroxides to the corresponding hydroxylamine is the primary metabolic pathway (11–15). Whereas the metabolic fate of spin adduct nitroxides is not clearly understood, oxidative degradation has been suggested (16, 17).

Previous studies have identified a stable five-membered nitroxide, 2-ethyl-2,5,5-trimethyl-3-oxazolidine-1-oxyl (OXANO), as a cell-permeable, nontoxic, catalyst of superoxide ($\cdot O_2^-$) dismutation (18). Subsequent cellular studies established this and other stable nitroxides to be protective agents for cells subjected to oxidative stress induced by agents such as $\cdot O_2^-$, H_2O_2, organic hydroperoxides, and ionizing radiation (19, 20). These initial studies prompted synthesis and screening of various five- and six-membered nitroxides to explore their range as superoxide dismutase (SOD) mimics and the degree of protection they can provide against oxidative damage in mammalian cells (21). The lipophilic piperidinyl nitroxide 2,2,6,6-tetramethylpiperidine-1-oxyl (Tempo) ameliorates post-ischemic reperfusion injury (22), and stable nitroxides have been identified as a new class of non-thiol radioprotectors *in vitro* (20). A number of mechanisms for cytoprotection have been advanced; they include oxidation of reduced transition metal ions, detoxification of intracellular radicals such as alkyl, alkoxyl, and alkylperoxyl radicals (19, 20, 23, 24), and direct catalytic removal of $\cdot O_2^-$ by dismutation.

Dismutation of $\cdot O_2^-$ was originally observed by exposing a five-membered cyclic nitroxide to a flux of $\cdot O_2^-$; a lower, yet time-invariant, level of the nitroxide radical EPR signal resulted (18). In the presence of an enzymatic or radiolytic source of $\cdot O_2^-$, either OXANO or its respective hydroxylamine, 2-ethyl-1-hydroxy-2,5,5-trimethyl-3-oxazolidine (OXANOH), gave rise to equivalent levels of residual, steady-state EPR signal. The calculated steady-state ratio ([nitroxide]/[hydroxylamine]) was independent of time, of $\cdot O_2^-$ flux, and of the total concentration of the nitroxide (OXANO· + OXANOH). The proposed mechanism of catalysis entailed initial reduction of nitroxide by $\cdot O_2^-$ to form the corresponding hydroxylamine and subsequent reoxidation of the hydroxylamine by $\cdot O_2^-$. However, when piperidinyl nitroxide derivatives were allowed to react with $\cdot O_2^-$, no decrease in EPR signal levels was detected (25). To account

The publication costs of this article were defrayed in part by page charge payment. This article must therefore be hereby marked "*advertisement*" in accordance with 18 U.S.C. §1734 solely to indicate this fact.

Abbreviations: EPR, electron paramagnetic resonance; Tempo, 2,2,6,6-tetramethylpiperidine-1-oxyl; Tempol, 4-hydroxy-2,2,6,6-tetramethylpiperidine-1-oxyl; Tempol-H, 4-hydroxy-2,2,6,6-tetramethyl-1-hydroxypiperidine; Tempamine, 4-amino-2,2,6,6-tetramethylpiperidine-1-oxyl; Tempone, 4-oxo-2,2,6,6-tetramethylpiperidine-1-oxyl; OXANO, 2-ethyl-2,5,5-trimethyl-3-oxazolidine-1-oxyl; OXANOH, 2-ethyl-1-hydroxy-2,5,5-trimethyl-3-oxazolidine; CHDO, 2-spirocyclohexane-5,5-dimethyl-3-oxazolidine-1-oxyl; DTPA, diethylenetriaminopentaacetic acid; SOD, superoxide dismutase; CAT, catalase; CV, cyclic voltammetry; $\cdot O_2^-$, superoxide; HX, hypoxanthine; XO, xanthine oxidase; NHE, normal hydrogen electrode.

§To whom reprint requests should be addressed at: Radiation Oncology Branch, National Cancer Institute, Building 10, Room B3 B69, National Institutes of Health, Bethesda, MD 20892.

for the persistence of the EPR signal, rapid reoxidation of the hydroxylamine was postulated (25).

In the present study, the mechanism of $\cdot O_2^-$ reactions with nitroxides and hydroxylamines has been investigated using EPR spectrometry, cyclic voltammetry (CV), and bulk electrolysis. Rapid reoxidation of the hydroxylamine form of Tempol by $\cdot O_2^-$ was not observed, and, in contrast to the previously proposed mechanism, evidence is presented herein that demonstrates that dismutation of $\cdot O_2^-$ can proceed by a mechanism involving an intermediate oxoammonium cation.

MATERIALS AND METHODS

Chemicals. Xanthine oxidase (XO), nicotinamide adenine dinucleotide reduced (NADH) and oxidized (NAD^+), and catalase (CAT) were purchased from Boehringer Mannheim. Diethylenetriaminopentaacetic acid (DTPA), 3-carbamoyl-2,2,5,5-tetramethyl-3-pyrroline-1-oxyl, 3-carbamoyl-2,2,5,5-tetramethylpyrrolidine-1-oxyl, 3-carboxy-2,2,5,5-tetramethylpyrrolidine-1-oxyl, 3-cyano-2,2,5,5-tetramethylpyrrolidine-1-oxyl, 3-aminomethyl-2,2,5,5-tetramethylpyrrolidine-1-oxyl, Tempo, 4-hydroxy-2,2,6,6-tetramethylpiperidine-1-oxyl (Tempol), and 4-amino-2,2,6,6-tetramethylpiperidine-1-oxyl (Tempamine) were purchased from Aldrich. 4-Oxo-2,2,6,6-tetramethylpiperidine-1-oxyl (Tempone) was from Molecular Probes. The hydroxylamine form of Tempol [4-hydroxy-2,2,6,6-tetramethyl-1-hydroxypiperidine (Tempol-H)] and OXANO were prepared as described earlier (18, 20). EPR analyses were conducted as described (18).

Electrochemical Analysis. Redox properties of nitroxides were investigated at 23°C by CV and square wave voltammetry techniques using a BAS 100A electrochemical analyzer (Bioanalytical Systems, West Lafayette, IN). Aqueous solutions of the nitroxides were analyzed using a vitreous carbon working electrode and a platinum auxiliary electrode. The reference was a Ag/AgCl electrode, calibrated against a primary saturated calomel electrode (SCE). Data from CV were collected over several sweep cycles, each from −1000 mV to +1000 mV and back to −1000 mV versus the reference Ag/AgCl. Square wave voltammetry was performed according to the method of Osteryoung and Osteryoung (26) at a frequency of 15 Hz and amplitude of 25 mV stepped at 4-mV increments, with potential sweeps in negative and positive directions between +1000 mV and −1000 mV versus the reference electrode. All potentials are reported versus the normal hydrogen electrode (NHE) using a value of +0.2415 V as the standard reduction potential of SCE versus NHE. In bulk electrolysis experiments, an electrochemical reactor similar to that described by Miner and Kissinger (27) was used. The cell consisted of a working electrode of graphite packed inside a porous Vycor glass tube (5-mm i.d.), through which the test solutions were pumped (≈2 ml/min). An outer glass cylinder, with separate electrolyte, contained the platinum auxiliary electrode and a Ag/AgCl reference electrode. Controlled potential electrolysis was performed with a CV-27 Potentiostat (Bioanalytical Systems). The reactor effluent was analyzed directly by EPR.

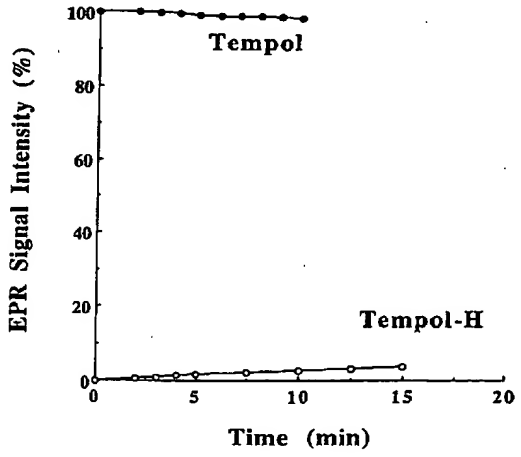

FIG. 1. EPR signal intensity of Tempol followed as a function of time of exposure of Tempol, 100 μM (closed symbols), and Tempol-H (open symbols) to $\cdot O_2^-$ generated by HX (2.5 mM)/XO (0.02 unit/ml) in air-saturated phosphate buffer (50 mM, pH 7.8) in the presence of CAT (100 units/ml) and DTPA (50 μM). The Tempol-H oxidation to Tempol was completely inhibited by SOD (100 units/ml).

RESULTS

EPR Analysis of Nitroxide Reaction with $\cdot O_2^-$. The reaction of $\cdot O_2^-$ with the nitroxide Tempol and its hydroxylamine form (Tempol-H) was studied by exposure to $\cdot O_2^-$ generated by the aerobic reaction of hypoxanthine (HX) and XO. The EPR signal of Tempol was monitored as a function of reaction time, and the results are shown in Fig. 1. No significant decrease in the EPR signal was observed. Higher fluxes of $\cdot O_2^-$, generated in reactions with higher XO levels, also failed to decrease the EPR signal. Similar results were found with other pyrrolidinyl, pyrrolinyl, and piperidinyl nitroxides. These findings stand in contrast with the observed decrease

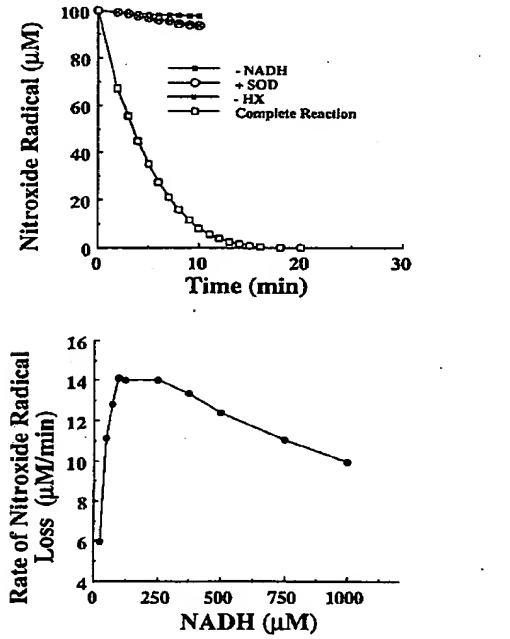

FIG. 2. (*Upper*) Time dependence of EPR signal (open squares) of Tempol following the addition of 0.02 unit of XO per ml to 50 mM phosphate buffer (pH 7.8) containing 50 μM DTPA, 2.5 mM HX, 100 units of CAT per ml, and 100 μM Tempol in air at room temperature in the presence of 250 μM NADH. Control experiments are as follows: complete reaction plus 300 units of SOD per ml (open circles); without hypoxanthine (×); without NADH (closed squares). (*Lower*) Initial rates of loss of Tempol EPR signal as a function of [NADH] following the addition of 0.02 unit of XO per ml to 50 mM phosphate buffer (pH 7.8) containing 50 μM DTPA, 2.5 mM HX, 100 units of CAT per ml, and 100 μM Tempol in air at room temperature.

of the EPR signal when oxazolidine nitroxide derivatives are allowed to react with $\cdot O_2^-$ (18, 25).

To test for oxidation of the hydroxylamine by $\cdot O_2^-$, Tempol-H was allowed to react under similar conditions. As shown in Fig. 1, the nitroxide radical formation was exceedingly slow. The slow rate of reaction of Tempol-H with $\cdot O_2^-$ was independently determined by the ferricytochrome *c* reduction assay and found to be $4 \times 10^2\ M^{-1} \cdot s^{-1}$. This value is two orders of magnitude below that estimated for the reaction of $\cdot O_2^-$ with Tempol (25) and in the same order of magnitude estimated for Tempo-H (28). Thus the previously proposed mechanism of $\cdot O_2^-$ dismutation involving an intermediate hydroxylamine is not consistent with these observed rates.

Although a clear demonstration of the hydroxylamine formation from the piperidinyl nitroxides has been shown in $\cdot O_2^-$-dependent reactions, sulfhydryl compounds were required as reducing agents (29). Since thiols can function as either one- or two-electron donors, we have chosen to test the reaction using a reducing agent such as NADH, which is an obligate two-electron donor. Shown in Fig. 2 are the results of the reaction of Tempol with $\cdot O_2^-$ (generated by the HX/XO reaction) in the presence of NADH. A time-dependent decrease in the EPR signal intensity was observed. After completion of the reaction, addition of the one-electron oxidant ferricyanide restored the EPR signal to its original level. All other nitroxides tested also underwent reduction in the presence of NADH and $\cdot O_2^-$. Control reactions in which HX was omitted or to which SOD was added showed negligible loss of EPR signal (Fig. 2 *Upper*). Likewise, no direct reaction of nitroxides with NADH was detected. The rate of nitroxide reduction was dependent on NADH concentration, as shown in Fig. 2 *Lower*. The reduction was supported by either NADH or NADPH but not by NAD^+ or $NADP^+$. Concomitant oxidation of NADH to NAD^+ was verified spectrophotometrically. Addition of SOD inhibited the loss of nitroxide EPR signal (as shown in Fig. 2 *Upper*) and NADH oxidation. These results suggest a two-electron reduction of an oxidized form of the nitroxide produced initially during $\cdot O_2^-$ dismutation.

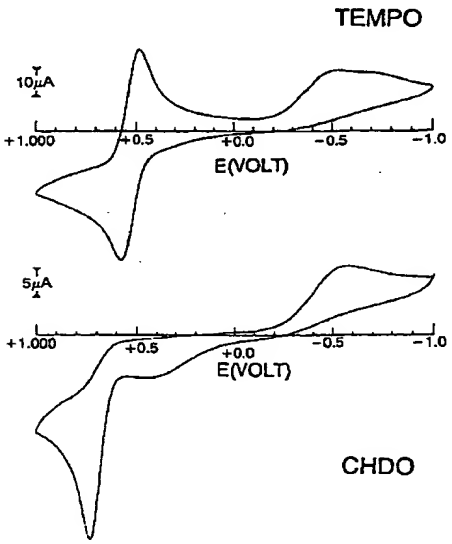

FIG. 3. CV of nitroxides in aqueous solution. CV was carried out on anaerobic 2.0 mM nitroxide solutions in phosphate buffer (pH 7.4) containing 0.154 M NaCl, at 0.200 V/s (see text). CHDO, 2-spirocyclohexane-5,5-dimethyl-3-oxazolidine-1-oxyl.

CV. For catalytic dismutation of $\cdot O_2^-$ by a nitroxide/oxoammonium cation couple, a redox potential in the range of −0.33 V ($O_2/\cdot O_2^-$) to +0.89 V ($\cdot O_2^-/H_2O_2$) would be required (30). Therefore, the redox properties of various five- and six-membered nitroxides were investigated by CV and square wave voltammetry. Voltammogramic data from analysis of Tempo are presented in Fig. 3 *Upper*. The results show a reversible one-electron redox reaction in the region of positive potential attributed to the nitroxide/oxoammonium couple (31). In the region of negative potential, an irreversible reduction wave was detected, which possibly represents the generation of the hydroxylamine. The pattern shown in Fig. 3 *Upper* was typical of results from the six-membered and five-membered carbocyclic nitroxide derivatives tested. In contrast, the five-membered ring heterocyclic oxazolidinyl derivatives underwent irreversible oxidation, as shown in Fig. 3 *Lower*. Redox midpoint potentials measured for the various nitroxide derivatives are listed in Table 1. As shown for Tempo, Tempol, and Tempamine, which are known to catalyze $\cdot O_2^-$ dismutation, the redox potentials of the nitroxide/oxoammonium couple are in the range +0.722 V to 0.872 V. Furthermore, the rates of EPR signal loss in the presence of $\cdot O_2^-$ and NADH generally correlated with the midpoint potentials, as shown in Table 1. This type of correlation

Table 1. Oxidation/reduction midpoint potentials of various nitroxide radicals in aqueous solution

Compound	Apparent midpoint potential,* mV	Method(s)†	Reduction rate‡
Tempo	722	CV, OSWV	1.00
Tempol	810 (720)	CV, OSWV	0.88
Tempamine	826 (872)	CV	—
Tempone§	913 (912)	CV, OSWV	0.33
3-Carboxyproxyl	792 (772)	CV, OSWV	0.45
3-Aminomethyl-proxyl	853	CV	—
3-Carbamoylproxyl	861 (872)	CV, OSWV	0.17
3-Cyanoproxyl	976 (982)	CV, OSWV	0.02
3-Carbamoyl-3-pyrroline	966 (972)	CV	0.03
OXANO¶	960‖	OSWV	—
CHDO¶	900‖	CV, OSWV	—
Ferri/ferrocyanide	410, 408**, 430††	CV	

Potentials are reported versus NHE.

*Values in parentheses were obtained from ref. 32 and were adjusted by +242 mV for comparison based on NHE.

†OSWV, Osteryoung square wave voltammetry. Where indicated, both methods were used, and in all cases results from both methods agreed to within 4 mV for compounds where oxidation was freely reversible.

‡Reduction rates of nitroxides (100 μM) by $\cdot O_2^-$ generated by XO (0.02 unit/ml) in air-saturated phosphate buffer (50 mM, pH 7.8) containing 50 μM DTPA and CAT (100 units/ml) in the presence of 250 μM NADH. The rates are normalized with respect to the rate for Tempo.

§Irreversible oxidation at low sweep rates.

¶Irreversible oxidation under all conditions tested up to 50 V/s.

‖Pseudo midpoint estimation from oxidation wave peaks (after subtraction of 30 mV) in CV carried out at scan rates of 2–20 V/s. Peak potentials of scans at 0.020 V/s were roughly 80 mV less than values at 20 V/s. For CHDO square wave voltammetry peaks were found at +895 mV in scans done from positive to negative direction. The peak currents were much weaker than in scans done in the oxidative direction (which show a +875 mV peak). However, it is reasonable in cases where rapid chemical reaction of the oxidized species removes it from the electrode reaction that the pseudo midpoint is provided by the peak potential from the negative scan, rather than by scans in the oxidative reaction.

**Data from ref. 33.

††Data from ref. 34.

would be expected if an initial one-electron oxidation was required prior to reductive loss of the EPR signal.

Bulk Electrolysis. To extend the results obtained from CV, controlled-potential bulk electrolysis was carried out on the nitroxides Tempo and Tempol. Electrochemical oxidation of 0.2 mM aqueous solutions of these nitroxides at 0.810 V (NHE) resulted in extensive (88–94%) loss of the EPR signal. In the case of Tempol, the residual EPR signal resulted in part from formation of a second nitroxide, with a nitrogen hyperfine coupling of a_N = 16.0 G (1 G = 0.1 mT), tentatively identified as Tempone. In contrast, when the unsubstituted Tempo was electrolyzed, there was no evidence for the formation of a second nitroxide. When the oxidized solutions were immediately (<5 min) subjected to reduction at +0.64 V, recovery of the nitroxide signal was substantial (>75% in the case of Tempo). Therefore, an EPR silent, metastable oxidized form of the nitroxide was generated at potentials predicted from the CV experiments.

DISCUSSION

The widespread use of stable nitroxides and persistent spin adduct nitroxides in biology suggests a need to understand better the factors influencing the stability of these compounds in the cellular milieu. The present study strongly suggests that stable nitroxides (piperidinyl and pyrrolidine derivatives) catalyze the dismutation of $\cdot O_2^-$ by utilizing the oxoammonium cation/nitroxide redox couple. The $\cdot O_2^-/H_2O_2$ couple has a redox potential of +0.89 V, and the catalytic dismutation rate was found to be directly related to the midpoint redox potential of the corresponding nitroxide. Tempo (0.722 V), Tempol (0.810 V), and Tempamine (0.826 V) have catalytic rates of $\cdot O_2^-$ dismutation of 1.2×10^5 $M^{-1}s^{-1}$, 6.5×10^4 $M^{-1}s^{-1}$, and 6.5×10^4 $M^{-1}s^{-1}$, respectively (25). The doxyl (oxazolidine-1-oxyl) derivatives dismutate $\cdot O_2^-$ by utilizing the hydroxylamine/nitroxide pair (18) and consequently catalyze the reaction at 1/100th the rate of the piperidinyl and proxyl (pyrrolidine-1-oxyl) nitroxides. All nitroxides studied with the exception of the doxyl derivatives exhibited reversible electrochemical behavior when oxidized. The doxyl derivatives, OXANO and CHDO, were not reversible in either direction (Fig. 3 *Lower*). The reactions of nitroxides with $\cdot O_2^-$ reveal that the piperidinyl and the proxyl derivatives are reduced in an $\cdot O_2^-$-dependent manner only in the presence of two-electron donors such as NADH and NADPH. The reduction products of these nitroxides are the corresponding hydroxylamines. These results suggest that the initial reaction with $\cdot O_2^-$ is a one-electron oxidation to the oxoammonium cation. This transient species either may be reduced back to the nitroxide by $\cdot O_2^-$ or may react with NADH or NADPH to form the corresponding hydroxylamine. Additional support for the proposed oxoammonium intermediate was obtained by bulk electrolysis experiments, wherein the nitroxide EPR signal was found to decrease at potentials predicted from CV.

During dismutation of $\cdot O_2^-$, high steady-state levels of piperidinyl and proxyl derivative nitroxides remain. This suggests that the reduction of the oxoammonium cation by $\cdot O_2^-$ is relatively fast. The doxyl derivatives, on the other hand, are directly reduced by $\cdot O_2^-$ to their hydroxylamines (18, 25). The irreversible electrochemical oxidation of the doxyl derivatives suggests a mechanism for dismutation of $\cdot O_2^-$ that would not involve catalysis by an oxidized nitroxide intermediate. Based on the observations, the following reactions are proposed for the nitroxide-mediated dismutation of $\cdot O_2^-$.

$$RR'NO\cdot + \cdot O_2^- + 2H^+ \xrightarrow{k_1} [RR'NO^+] + H_2O_2. \quad [1]$$

$$[RR'NO^+] + \cdot O_2^- \xrightarrow{k_2} RR'NO\cdot + O_2. \quad [2]$$

Reaction 1 involves the oxidation of nitroxide (RR'NO·) to form the oxoammonium cation intermediate [RR'NO$^+$]. This intermediate is subsequently reduced by $\cdot O_2^-$ (reaction 2) to reform nitroxide, resulting in the overall dismutation of $\cdot O_2^-$, as shown in reaction 3.

$$2 \cdot O_2^- + 2H^+ \xrightarrow{k_{cat}} O_2 + H_2O_2. \quad [3]$$

Although direct evidence for reaction of the oxoammonium cation with $\cdot O_2^-$ (reaction 2) was not obtained, in biological systems this intermediate may be expected to react with many endogenous one- and two-electron reducing agents. Thus the pathway for $\cdot O_2^-$ dismutation *in vivo* would not necessarily involve direct reduction of $\cdot O_2^-$ (reaction 2) as the major route for regeneration of the cyclic nitroxide. In view of the instability of the oxoammonium cation (ref. 35; also noted in our bulk electrolysis experiments) it would appear that regeneration of the nitroxide would occur predominantly by reaction of the oxoammonium with endogenous substrates other than $\cdot O_2^-$. This raises the possibility of deleterious reactions with critical biomolecules if repair (rereduction) mechanisms are too slow to prevent subsequent irreversible processes.

In the absence of two-electron reductants, reactions 1 and 2 do not contribute to hydroxylamine formation. In the presence of two-electron donors such as NADH (under conditions of [NADH] >> [$\cdot O_2^-$]), competition for the oxoammonium cation may occur and decrease the product from reaction 2. The competitive reaction would involve direct two-electron reduction of the oxoammonium cation as follows:

$$NADH + [RR'NO^+] \rightarrow NAD^+ + RR'NOH. \quad [4]$$

Since complete reduction of the nitroxide was observed with excess [NADH], any reoxidation of the hydroxylamine would be slow, consistent with the results shown in Fig. 1.

Metabolic processes result in the reduction of nitroxides to their hydroxylamines. The efficiency of reduction was found to be faster in hypoxic cells (11). More detailed analyses of the cellular components responsible for reduction showed that the cytosolic fractions of cells reduce nitroxides by utilizing ascorbic acid (15), whereas the microsomal fractions mediate the reaction through enzymatic processes (14). It has been suggested that the primary organelle responsible for intracellular reduction of nitroxides is the mitochondrion (14). At the cellular level it has been found that reduction is faster for six-membered piperidinyl nitroxides than for five-membered nitroxides (32). The hydroxylamines, on the other hand, are oxidized by cellular processes only under aerobic conditions at the level of cytochrome *c* oxidase (11). In a recent report (32), midpoint potentials for the one-electron oxidation of various nitroxide derivatives have been correlated to the substituent constants for inductive effects on the ring. It was suggested that midpoint reduction potential, in addition to the lipophilicity, might influence the intracellular stability of nitroxides. Fig. 4 demonstrates that, subsequent to oxidation, the two-electron reduction of the six-membered nitroxides (Tempo, Tempol, and Tempone) correlates with the midpoint oxidation potential, whereas, when Table 1 is examined, the influence of ring size on reduction rate can be seen when different ring sizes with similar midpoint oxidation potentials are compared. The trends shown in Table 1 have also been observed for microsomal and mitochondrial reduction of nitroxides (10, 32, 36). Increases in endogenous cellular reducing equivalents would be expected to facilitate the reaction product through reaction 4. When considering

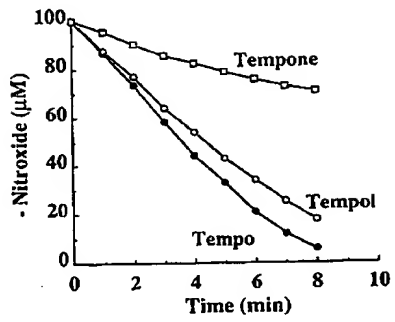

FIG. 4. Plot of the $\cdot O_2^-$-induced reduction rates of various piperidine nitroxides (100 mM) in the presence of NADH (250 μM). A reaction containing HX (2.5 mM) and XO (0.02 unit/ml) in air-saturated phosphate buffer (50 mM, pH 7.8) containing 50 μM DTPA and CAT (100 units/ml) was used to generate $\cdot O_2^-$. The rates of reduction were measured following the addition of XO by continually monitoring the EPR signal intensities of the nitroxides. Closed circles, Tempo; open circles, Tempol; and open squares, Tempone.

the special case of cellular hypoxia, reaction 4 may become predominant because molecular oxygen is no longer the primary electron sink and, therefore, the oxidized nitroxide no longer competes with molecular oxygen for reducing equivalents (32). For the case of persistent spin adducts in cellular environments, the metabolism is apparently more complex (9). It is known that nitroxides, formed from the addition of unstable radicals to a variety of spin traps, are destroyed by recombination with other radical species (17). In cells, the spin adduct nitroxides have short lifetimes and are rapidly metabolized to species other than the hydroxylamines (16).

The present study demonstrates a pathway for $\cdot O_2^-$ dismutation that is distinct from the pathway involving one-electron reduction of nitroxides. It is proposed that during reaction of $\cdot O_2^-$ with piperidinyl and proxyl nitroxides in the presence of reducing agents the generation of the hydroxylamine results from a two-electron reduction of the corresponding oxoammonium cation intermediate. Moreover, the results suggest the possibility that cellular destruction of persistent spin adduct nitroxides may be facilitated by primary univalent oxidation. Factors that influence either the redox state of cells or concentrations of oxygen and $\cdot O_2^-$ may well determine which nitroxides are chosen as probes of cellular metabolism or as NMR contrast agents. Ultimately, such factors should also aid in the choice of the appropriate nitroxide to be used for *in vivo* EPR imaging.

M.C.K. and D.A.G. contributed equally to this investigation. We thank Frank S. Harrington for fabrication of the bulk electrochemical reactor and Dr. T. E. Goffman for synthesis of OXANO. This research is partially supported by Grant 89-00124 from the United States–Israel Binational Science Foundation (BSF), Jerusalem, Israel.

1. Swartz, H. M. (1987) *J. Chem. Soc. Faraday Trans. 1* **83**, 191–202.
2. Lai, C. S., Hopwood, L. E., Hyde, J. S. & Lukiewicz, S. (1982) *Proc. Natl. Acad. Sci. USA* **79**, 1166–1170.
3. Mehlhorn, R. & Probst, I. (1982) *Methods Enzymol.* **88**, 334–344.
4. Dobrucki, J. W., Demsar, F., Walczak, T., Woods, R. K., Bacic, G. & Swartz, H. M. (1990) *Br. J. Cancer* **61**, 221–224.
5. Swartz, H. M. (1983) *Bull. Magn. Reson.* **8**, 172–175.
6. Berliner, L. J. & Fuji, H. (1985) *Science* **227**, 517–519.
7. Towell, J. & Kalyanaraman, B. (1991) *Anal. Biochem.* **196**, 111–119.
8. Iannone, A., Bini, A., Swartz, H. M., Tomasi, A. & Vannini, V. (1989) *Biochem. Pharmacol.* **38**, 2581–2586.
9. Swartz, H. M. (1990) *Free Radical Res. Commun.* **9**, 399–405.
10. Belkin, S., Mehlhorn, R. J., Hideg, K., Hankovsky, O. & Packer, L. (1987) *Arch. Biochem. Biophys.* **256**, 232–243.
11. Chen, K., Glockner, J. F., Morse, P. D. & Swartz, H. M. (1989) *Biochemistry* **28**, 2496–2501.
12. Sentjurc, M., Pecar, S., Chen, K., Wu, M. & Swartz, H. M. (1989) *Biochim. Biophys. Acta* **1073**, 329–335.
13. Chen, K. & Swartz, H. M. (1991) *Biochim. Biophys. Acta* **1073**, 329–335.
14. Iannone, A., Tomasi, A., Vannini, V. & Swartz, H. M. (1990) *Biochim. Biophys. Acta* **1034**, 285–289.
15. Iannone, A., Tomasi, A., Vannini, V. & Swartz, H. M. (1990) *Biochim. Biophys. Acta* **1034**, 290–293.
16. Samuni, A., Carmichael, A. J., Russo, A., Mitchell, J. B. & Riesz, P. (1986) *Proc. Natl. Acad. Sci. USA* **83**, 7593–7597.
17. Samuni, A., Krishna, C. M., Riesz, P., Finkelstein, E. & Russo, A. (1989) *Free Radical Biol. Med.* **6**, 141–148.
18. Samuni, A., Krishna, C. M., Riesz, P., Finkelstein, E. & Russo, A. (1988) *J. Biol. Chem.* **263**, 17921–17924.
19. Mitchell, J. B., Samuni, A., Krishna, C. M., Degraff, W. G., Min, S. A., Samuni, U. & Russo, A. (1989) *Biochemistry* **29**, 2802–2807.
20. Mitchell, J. B., Degraff, W. G., Kaufman, D., Krishna, C. M., Samuni, A., Finkelstein, E., Ahn, M. S., Hahn, S. M., Gamson, J. & Russo, A. (1991) *Arch. Biochem. Biophys.* **289**, 62–70.
21. Samuni, A., Ahn, M. S., Krishna, C. M., Mitchell, J. B. & Russo, A. (1990) *Adv. Exp. Med. Biol.* **264**, 85–92.
22. Gelvan, D., Saultman, P. & Powell, S. (1991) *Proc. Natl. Acad. Sci. USA* **88**, 4680–4684.
23. Nilsson, U. A., Olsson, L. I., Carlin, G. & Bylund-Fellenius, A. C. (1989) *J. Biol. Chem.* **264**, 11131–11135.
24. Chateauneuf, J., Lusztyk, J. & Ingold, K. U. (1988) *J. Org. Chem.* **53**, 1629–1632.
25. Samuni, A., Krishna, C. M., Mitchell, J. B., Collins, C. R. & Russo, A. (1990) *Free Radical Res. Commun.* **9**, 241–249.
26. Osteryoung, J. G. & Osteryoung, R. A. (1985) *Anal. Chem.* **57**, 101A–109A.
27. Miner, D. J. & Kissinger, P. T. (1979) *Biochem. Pharmacol.* **28**, 3285–3290.
28. Rosen, G. M., Finkelstein, E. & Rauckman, E. J. (1982) *Arch. Biochem. Biophys.* **215**, 367–378.
29. Finkelstein, E., Rosen, G. M. & Rauckman, E. J. (1984) *Biochim. Biophys. Acta* **802**, 90–98.
30. Sawyer, D. T. & Valentine, J. S. (1981) *Acc. Chem. Res.* **14**, 393–400.
31. Fish, J. R., Swarts, S. G., Sevilla, M. D. & Malinski, T. (1988) *J. Phys. Chem.* **92**, 3745–3751.
32. Morris, S., Sosnovsky, G., Hui, B., Huber, C. O., Rao, N. U. M. & Swartz, H. M. (1991) *J. Pharm. Sci.* **80**, 149–152.
33. Wilson, G. S. (1978) *Methods Enzymol.* **54**, 396–410.
34. Dutton, L. P. (1978) *Methods Enzymol.* **54**, 411–435.
35. Rozantsev, E. G. (1970) *Free Nitroxyl Radicals* (Plenum, New York), pp. 99–101.
36. Chen, K. & Swartz, H. M. (1988) *Biochim. Biophys. Acta* **970**, 270–277.

THE JOURNAL OF BIOLOGICAL CHEMISTRY Vol. 271, No. 42, Issue of October 18, pp. 26026–26031, 1996
Printed in U.S.A.

Do Nitroxide Antioxidants Act as Scavengers of $O_2^{\cdot-}$ or as SOD Mimics?*

(Received for publication, April 3, 1996, and in revised form, July 30, 1996)

Murali C. Krishna‡§, Angelo Russo‡, James B. Mitchell‡, Sara Goldstein¶, Hagit Dafni, and Amram Samuni

From the Molecular Biology and ¶Physical Chemistry Departments at the Hebrew University, Jerusalem, 91120, Israel and the ‡Radiation Biology Branch, NCI, National Institutes of Health, Bethesda, Maryland 20892

Stable nitroxide radicals were reported to act as SOD mimics and catalyze the dismutation of $O_2^{\cdot-}$ through two different catalytic pathways including reductive and oxidative reaction mechanisms (Samuni, A., Krishna, C. M., Riesz, P., Finkelstein, E. & Russo, A. (1988) *J. Biol Chem.* 263, 17921–17924). Recent studies directly monitoring $O_2^{\cdot-}$ and employing kinetics analysis did not reveal SOD activity of nitroxides (Weiss, R. H., Flickinger, A. G., Rivers, W. J., Hardy, M. M., Aston, K. W., Ryan, U. S. & Riley, D. P. (1993) *J. Biol. Chem.* 268, 23049–23054). Such discrepancy may result in cases where distinction of stoichiometric scavengers from catalytic detoxifiers of $O_2^{\cdot-}$ is not readily feasible. Nitroxides are effective antioxidants that protect against oxidative injury in various pathological processes. The distinction of their SOD mimic activity from $O_2^{\cdot-}$ scavenging was established by examining the validity of direct and indirect methods employed to assay SOD-like catalytic activity. Kinetics analysis along with direct EPR monitoring were used to study the mechanism underlying nitroxide reactions with $O_2^{\cdot-}$. The nitroxide EPR signal decayed in the presence of NADH but otherwise did not decrease with time, thus substantiating its catalytic role in $O_2^{\cdot-}$ dismutation. The catalytic rate constants for $O_2^{\cdot-}$ dismutation, determined for the nitroxides tested, were found to increase with $[H^+]$, indicating that $^{\cdot}OOH$ rather than $O_2^{\cdot-}$ is oxidizing the nitroxide. The results demonstrate the limitations associated with direct kinetics analysis in evaluating SOD mimic activity, underscoring the need for independent assays for valid discrimination of SOD mimics from stoichiometric scavengers of $O_2^{\cdot-}$.

The toxic effects of oxygen-derived reactive species along with the physiological role of superoxide dismutase (SOD)[1] in catalyzing the dismutation of $O_2^{\cdot-}$ are well documented (1, 2). Various strategies such as elevating the level of SOD inside and/or outside the cells have been employed for protection against oxidative injury. Exogenously added SOD may be immunogenic, does not penetrate readily into the cells, and unless bound to a protein or polyethylene glycol has a metabolic half-life of only several minutes (3, 4).

To circumvent such limitations, cell-permeable, low molecular weight compounds that mimic the activity of SOD were used (5–14). Usually SOD mimics are chelates of transition metals such as copper, iron, or manganese (denoted L-M^{n+}), which like the metal center in native SOD can undergo alternate reduction and oxidation of the metal (Mechanism I) to yield O_2 and H_2O_2.

$$\text{L-M}^{n+} + O_2^{\cdot-} \underset{k_{-1}}{\overset{k_1}{\rightleftharpoons}} \text{L-M}^{(n-1)+} + O_2 \qquad \text{(Eq. 1)}$$

$$\text{L-M}^{(n-1)+} + O_2^{\cdot-} + 2H^+ \xrightarrow{k_2} \text{L-M}_{n+} + H_2O_2 \qquad \text{(Eq. 2)}$$

There are, however, cases where alternate oxidation and reduction take place (Mechanism II).

$$\text{L-M}^{n+} + O_2^{\cdot-} + 2H^+ \underset{k_{-3}}{\overset{k_3}{\rightleftharpoons}} \text{L-M}^{(n+1)+} + H_2O_2 \qquad \text{(Eq. 3)}$$

$$\text{L-M}^{(n+1)+} + O_2^{\cdot-} \xrightarrow{k_4} \text{L-M}^{n+} + O_2 \qquad \text{(Eq. 4)}$$

In both cases the net reaction is the same as that of the spontaneous dismutation of superoxide.

$$2O_2^{\cdot-} + 2H^+ \xrightarrow{k_5} O_2 + H_2O_2 \qquad \text{(Eq. 5)}$$

Cell-permeable SOD mimics can facilitate the reaction shown in Equation 5 and diminish $O_2^{\cdot-}$ concentration both extra- and intracellularly. On the other hand, metal-containing SOD mimics are prone to dissociation in the presence of cellular proteins, thus not only causing loss of SOD mimic activity but also mobilization of potentially toxic redox-active metals (15). The catalytic activity of certain metal-based SOD mimics has been previously questioned (15), and the methods for assaying SOD activity have been critically evaluated (16–18). More recently, metal-free reagents have been reported to act as mimics of SOD (27), yet a controversy still exists regarding their mode of action (29).

Nitroxide stable radicals demonstrate effective antioxidative activity (19) in various biological systems ranging from molecular (20), cellular (21–24), and laboratory animal level (25, 26). Nitroxides have been reported to catalyze $O_2^{\cdot-}$ dismutation through two different catalytic pathways including reductive (27) and oxidative (28) reaction mechanisms. Conversely, kinetics analysis of rapid mixing stopped flow experiments designed to measure the effect of nitroxides on superoxide decay did not reveal any SOD activity (29), leading to the conclusion

* This work was supported by research Grant 309/931 from the Israel Science Foundation of the Israel Academy of Science, Jerusalem, Israel. The costs of publication of this article were defrayed in part by the payment of page charges. This article must therefore be hereby marked "*advertisement*" in accordance with 18 U.S.C. Section 1734 solely to indicate this fact.

§ To whom correspondence correspondence should be addressed: Radiation Biology Branch, Bldg. 10, Rm. B3 B69, NCI, NIH, Bethesda, MD 20892-1002. Tel.: 301-496-7511; Fax: 301-480-2238.

[1] The abbreviations used are: SOD, superoxide dismutase; cyt-c^{III}, ferricytochrome c; cyt-c^{II}, ferrocytochrome c; DTPA, diethylenetriamine pentaacetic acid; EPR, electron paramagnetic resonance; HX, hypoxanthine; TPO, 2,2,6,6-tetramethyl-piperidinoxyl; TPO^+, oxo-ammonium cation of TPO; TPL, 4-OH-2,2,6,6-tetramethyl-piperidinoxyl; TPL^+, oxo-ammonium cation of TPL; XO, xanthine oxidase.

that nitroxides act as scavengers of $O_2^{\cdot-}$.

Detoxification of $O_2^{\cdot-}$ is also achievable by scavengers that stoichiometrically react with it. Yet, $O_2^{\cdot-}$ removal by any scavenger differs from that exerted by SOD mimics by the mechanisms underlying the reactions and also by the respective products. Although catalytic reactions are generally readily identifiable, the distinction of a scavenger of $O_2^{\cdot-}$ from an authentic SOD mimic is not always straightforward. An inadequate distinction might derive from the ambiguous definition of an SOD mimic along with the unique nature of SOD, which distinguishes it from most enzymes. In view of the present results, previous approaches adopted for the evaluation of SOD mimics are analyzed and critically examined.

EXPERIMENTAL PROCEDURES

Materials—Catalase (H_2O_2 oxidoreductase, EC 1.11.1.6), xanthine oxidase (EC 1.2.3.2, xanthine:oxygen oxidoreductase) (XO) and Cu-Zn SOD were purchased from Boehringer-Mannheim Co.; 2,2,6,6-tetramethylpiperidine-1-oxyl (TPO) and 4-hydroxy-2,2,6,6-tetramethylpiperidine-1-oxyl (TPL) were purchased from Aldrich; hypoxanthine (HX) and ferricytochrome c (cyt-c^{III}) were obtained from Sigma. Distilled deionized water was used throughout all experiments.

Superoxide Radical Flux—All experiments involved a continuous flux of superoxide radicals generated enzymatically. Unless otherwise stated, the reaction mixture contained 50 mM phosphate buffer at pH 7, 1–5 mM HX, 50 μM diethylenetriamine pentaacetic acid (DTPA) to minimize the effect of adventitious redox-active metal ions, and 130–260 units/ml catalase to avoid undesired effects of H_2O_2. The reaction was generally started by adding about 0.01–0.08 units/ml XO, providing a steady flux of ~2–16 μM $O_2^{\cdot-}$/min. Throughout the text superoxide radicals are denoted as $O_2^{\cdot-}$ rather than $O_2^{\cdot-}$/·OOH, although it is the protonated form that is oxidizing the nitroxide.

Electron Paramagnetic Resonance Assay—Samples of 100 μl for EPR experiments were drawn into a gas-permeable teflon capillary (Zeus Industries, Raritran, NJ) of 0.8-mm inner diameter, 0.38-mm wall thickness, and 15-cm length. Each capillary was folded twice, inserted into a narrow quartz tube that was open at both ends (2.5-mm inner diameter), and then placed into the EPR cavity. To maintain constant level of O_2 during the experiments, air was blown around the sample without having to disturb the alignment of the tube within the spectrometer cavity. EPR spectra were recorded on a Varian E9 X-band spectrometer, with field set at 3357 G, modulation frequency of 100 KHz, modulation amplitude of 1 G, and a nonsaturating incident microwave power of 10 mW.

Analysis of the Kinetic Data—The kinetic experiments were conducted by following (*a*) the rate of cyt-c^{II} formation using absorption spectroscopy ($OD_{550\ nm}$, $\Delta\epsilon = 21\ mM^{-1}\ cm^{-1}$) and (*b*) the rate of decay of nitroxide signal using EPR spectrometry, induced by a constant flux of superoxide. Competition kinetics were studied by introducing various concentrations of nitroxide or SOD, which compete for superoxide radicals and consequently lower the rate of $O_2^{\cdot-}$-induced cyt-c^{III} reduction (spectrophotometric assays) or spin loss of the nitroxide (EPR assays). To analyze the data, the rate of reaction in the absence of scavenger/catalyst, denoted *V* and equal to the flux of $O_2^{\cdot-}$, was divided by the rate of reaction observed in the presence of scavenger/catalyst, denoted *v*. The values of *V*/*v* were plotted *versus* the concentration of the competitive additive (scavenger/catalyst). Upon the addition of SOD in the optical experiments, the values of *V*/*v* for the rates of cyt-c^{III} reduction depended linearly on [SOD] according to:

$$V/v_{(optical)} = 1 + [SOD] \cdot k_{SOD+superoxide}/[cyt\text{-}c^{III}] \cdot k_{cyt\text{-}c^{III}+superoxide}$$

EXPRESSION I

where $k_{SOD+superoxide}$ is the catalytic rate constant of $O_2^{\cdot-}$ dismutation by SOD. For competition against nitroxide, *V*/*v* values depended linearly on [nitroxide] according to:

$$V/v_{(optical)} = 1 + [nitroxide] \cdot k_{app}/[cyt\text{-}c^{III}] \cdot k_{cyt\text{-}c^{III}+superoxide}$$

EXPRESSION II

where k_{app} denotes the rate constant of $O_2^{\cdot-}$ reaction with the nitroxide (be it a scavenger or a catalyst). For the EPR experiments SOD was used to compete for $O_2^{\cdot-}$ against the nitroxide. There the *V*/*v* values of spin loss rates of nitroxide depended linearly on [SOD] according to:

$$V/v_{(EPR)} = 1 + [SOD] \cdot k_{SOD+superoxide}/[TPO] \cdot k_{app(EPR)}$$

EXPRESSION III

To evaluate $k_{app(EPR)}$, the values of the slopes obtained from expressions II (optical experiment) and III (EPR experiment) were divided yielding expression IV, which is independent of SOD concentration,

$$slope_{(optical)}/slope_{(EPR)} = [TPO] \cdot k_{app(EPR)}/[cyt\text{-}c^{III}] \cdot k_{cyt\text{-}c^{III}+superoxide}$$

EXPRESSION IV

from which $k_{app(EPR)}$ was evaluated using the known value for $k_{cyt\text{-}cIII+superoxide}$ (30, 31). It should be noted that k_{app} evaluated from expression II is not the same as $k_{app(EPR)}$ evaluated from expression IV.

RESULTS

The reaction of $O_2^{\cdot-}$ with two nitroxides TPO and TPL was studied using both direct (EPR) and indirect (optical) techniques. Previous studies showed that nitroxides shuttle among three oxidation states as depicted in Scheme 1 of Ref. 41. Oxazolidine nitroxide derivatives react with superoxide via a reductive mode in which $O_2^{\cdot-}$ reduces the nitroxide directly to its corresponding hydroxylamine, which in turn is oxidized to the parent nitroxide by an additional superoxide (27, 32, 33). In contrast, piperidine derivatives such as TPO and TPL are readily oxidized by protonated superoxide, ·OOH, to yield oxoammonium cation (28),

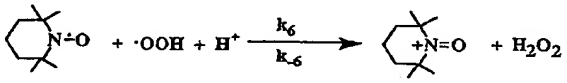

(Eq. 6)

which in turn oxidizes another superoxide to molecular oxygen:

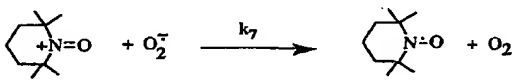

(Eq. 7)

The net process (Equation 5) is anticipated to remove $O_2^{\cdot-}$ without affecting nitroxide concentration.

Spectrophotometric Assay of Nitroxide Reaction with $O_2^{\cdot-}$ by Competition versus Ferricytochrome c—A constant flux of superoxide was generated enzymatically, and the competition between nitroxide (catalyst/scavenger) and cyt-c^{III} for $O_2^{\cdot-}$ was used for studying the reaction kinetics. The use of SOD-inhibitable reduction of cyt-c^{III} by $O_2^{\cdot-}$ radicals to study SOD activity of nitroxides is limited because the cyt-c^{II} formed is oxidizable by H_2O_2 (34–36) and also by nitroxide (29). Therefore, catalase was always included, nitroxide concentrations were kept low to minimize any reverse reaction (29), and only the initial rates of reaction were used for the evaluation of the activity. Control experiments showed that the rate of cyt-c^{II} oxidation by 10–20 μM nitroxide was negligible as compared with the rate of cyt-c^{III} reduction by $O_2^{\cdot-}$ (data not shown).

To study the reaction of nitroxides with superoxide, the rate of formation of cyt-c^{II} was spectrophotometrically monitored at pH 7 in the absence (*V*) and in the presence (*v*) of various nitroxide concentrations. TPO and TPL inhibited the reduction of 22 μM cyt-c^{III} by competing for the superoxide in a concentration-dependent manner, the data were analyzed by plotting *V*/*v* as a function of [nitroxide] according to Expression II, and the results of a typical experiment are displayed in Fig. 1. From the slope of the lines as in Fig. 1 and knowing $k_{superoxide+cyt\text{-}cIII}$ (30, 31) at pH 7, k_{app} was calculated to be $1.8 \times 10^6\ M^{-1}\ s^{-1}$ and $6.5 \times 10^5\ M^{-1}\ s^{-1}$ for TPO and TPL, respectively. These results alone, however, cannot

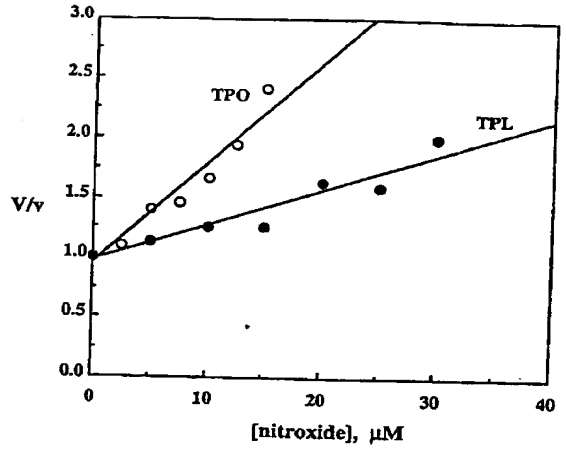

FIG. 1. **Determination of the catalytic rate constant k_{cat}(superoxide+nitroxide) for superoxide dismutation by nitroxide.** Competition against cytochrome *c*. A constant flux of $O_2^{\cdot-}$ was generated at 23 ± 2 °C by 1 mM HX and 0.01 unit/ml XO in 50 mM phosphate buffer, pH 7, containing 50 μM DTPA, 22 μM cyt-c^{III}, and 260 units/ml catalase, where cyt-c^{II} formation was followed spectrophotometrically at 550 nm. The initial rates of reaction were measured in the absence (*V*) and the presence (*v*) of various concentrations of TPO (○) or TPL (●), and *V/v* values were plotted *versus* [nitroxide]. The catalytic rate constant of superoxide dismutation by each SOD mimic was calculated from the slope of each respective plot, knowing the concentration of cyt-c^{III} and its reaction rate constant $k_{superoxide+cyt\text{-}c^{III}}$ (30).

distinguish whether nitroxides react with $O_2^{\cdot-}$ as catalysts or scavengers.

The pH Dependence of Nitroxide Reaction with Superoxide—The competition of nitroxide against cyt-c^{III} for $O_2^{\cdot-}$ was repeated at 30 °C while varying the pH using 50 mM phosphate buffer. The rate constants were calculated taking into account the rate constants of cyt-c^{III} with $O_2^{\cdot-}$ previously measured at the respective pH (30) and corrected for 30 °C (31). The results are displayed in Fig. 2 and show that k_{app} increases with $[H^+]$, indicating, as anticipated, that $^{\cdot}OOH$ rather than $O_2^{\cdot-}$ (pK_a = 4.8) oxidizes the nitroxide.

Time Dependence of Nitroxide Concentration during Exposure to Superoxide—EPR was used to investigate the fate of the nitroxide upon its reaction with superoxide generated by HX/XO. To examine the catalytic activity of nitroxides, the effect of a constant flux of $O_2^{\cdot-}$ on 10–50 μM TPO or TPL was investigated by directly monitoring their EPR signal. The reaction mixture, placed in a gas-permeable teflon capillary inserted inside the cavity of an EPR spectrometer, was continuously flushed with air at room temperature. The reaction was started by adding 0.08 units/ml XO, and the intensity of the EPR signal of the nitroxide was continuously monitored. The rate of $O_2^{\cdot-}$ generation was independently determined by following at 550 nm the SOD-inhibitable reduction of cyt-c^{III} in the absence of nitroxide. Fig. 3 shows that under a steady $O_2^{\cdot-}$ flux of ~16 μM·min^{-1}, which was maintained for over 1 h, no change of nitroxide EPR signal intensity was detectable. It shows that the restoration of nitroxide *via* Equation 7 is so fast that no accumulation of the oxo-ammonium cation is detectable. These results provide direct evidence for the catalytic role played by nitroxides where superoxide is removed by both Equations 6 and 7. Furthermore, because

$$k_{cat} = 2k_6k_7/(k_6 + k_7)$$

EXPRESSION V

and $k_7 \gg k_6$, the value of k_{app}, determined from expression II, actually reflects $k_{cat} = 2k_6$ and not k_6.

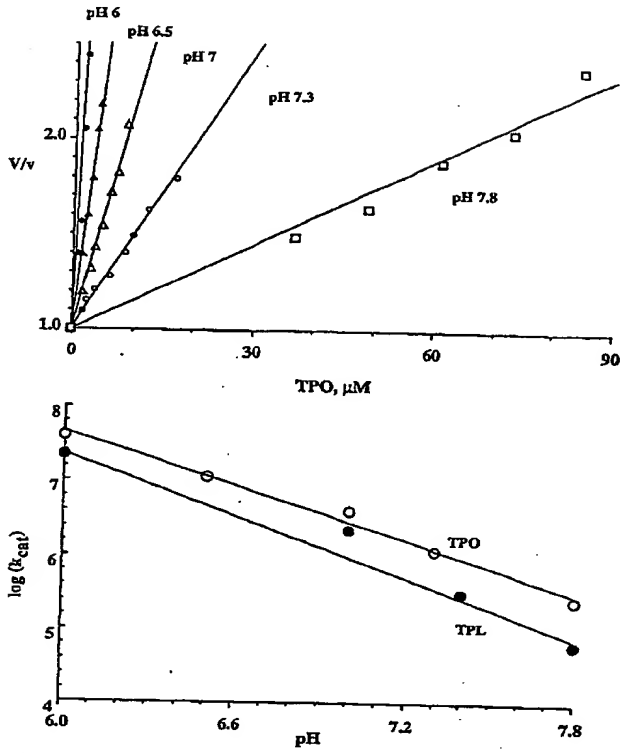

FIG. 2. **The pH dependence of nitroxide reaction with superoxide ($k_{app} = k_{cat}$).** *Top*, a constant flux of $O_2^{\cdot-}$ was generated at 30 °C by 1 mM HX and 0.01 unit/ml XO in 50 mM phosphate buffer containing 50 μM DTPA, 260 units/ml catalase, and 23.1 μM cyt-c^{III} at various pH values: ●, pH 6; ▲, pH 6.5; △, pH 7; ○, pH 7.3; □, pH 7.8. The initial rates of cyt-c^{III} reduction were measured in the absence (*V*) and the presence (*v*) of various TPO concentrations, and the values of *V/v* were plotted *versus* [TPO]. The catalytic rate constant (k_{cat}) of superoxide dismutation by TPO (TPL) was calculated from the slope of each $k_{superoxide+cyt\text{-}c^{III}}$ at each pH previously measured (30) and corrected for 30 °C (31). *Bottom*, the calculated values of $k_{app} = k_{cat}$ for nitroxides are presented as log(k_{cat}) *versus* pH. *Open symbols*, TPO; *closed symbols*, TPL.

The addition of 1 mM NADH, however, caused a rapid and complete loss of the EPR signal of TPO (Fig. 3) because of a two-electron reduction of the oxo-ammonium transient (TPO^+), formed in Reaction 6, to its respective cyclic hydroxylamine (28):

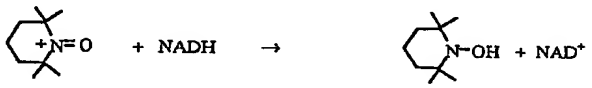

(Eq. 8)

The loss of EPR signal was preventable by 100 units/ml SOD (data not shown), demonstrating that a simultaneous presence of $^{\cdot}HO_2/O_2^{\cdot-}$ and the two-electron reductant is required to convert TPO to its respective cyclic hydroxylamine (*via* TPO^+), further substantiating the role played by Equations 6 and 8.

Competition between SOD and SOD Mimic—The competition between SOD and TPO (or TPL) for $O_2^{\cdot-}$ and the direct detection in real time of the nitroxides by EPR were also used to determine their reactivity toward superoxide. To determine the rate constant (k_6) for nitroxide oxidation by $^{\cdot}OOH$/

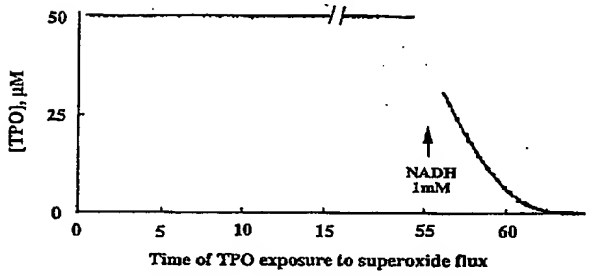

FIG. 3. **Time invariance of the SOD mimic TPO subjected to superoxide flux.** A constant flux of ~16 μM/min $O_2^{\cdot-}$ was generated at 23 ± 2 °C by 5 mM HX and 0.08 unit/ml XO in 50 mM phosphate buffer, pH 7, containing 50 μM TPO, 50 μM DTPA, and 260 units/ml catalase. The reaction mixture was inserted in a gas-permeable capillary, placed inside the EPR cavity, and flushed with air, whereas the intensity of TPO EPR signal was continuously monitored. Upon the addition of 1 mM NADH to the reaction mixture (*arrow*), the EPR signal of TPO decayed.

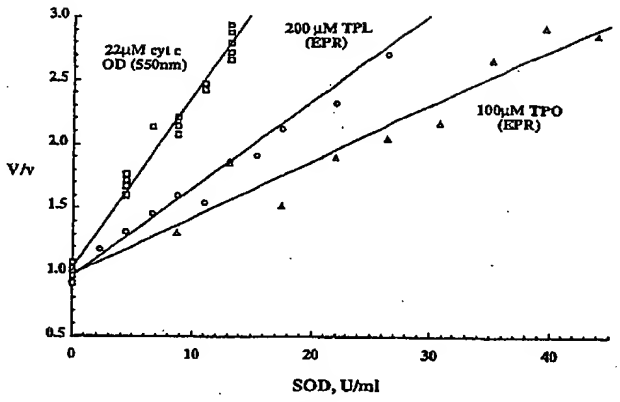

FIG. 4. **Determination of the rate constant $k_{6(superoxide+nitroxide)}$ for nitroxide oxidation by $^{\cdot}OOH$.** A constant flux of $O_2^{\cdot-}$ was generated at 23 ± 2 °C by 1 mM HX and 0.02 unit/ml XO in 50 mM phosphate buffer, pH 7, containing 50 μM DTPA, 260 units/ml catalase, and various concentrations of SOD. The reaction mixture included either 22 μM cyt-c^{III}, where cyt-c^{II} formation was followed spectrophotometrically at 550 nm (r), or 0.5 mM NADH and 100 μM TPO (Δ) or 0.5 mM NADH and 200 μM TPL (O), where the loss of nitroxide EPR signal was monitored as shown in Fig. 3 after NADH (see *arrow*) addition. The initial rates of reaction were measured in the absence (V) and the presence (v) of various SOD concentrations, and values of V/v were plotted *versus* [SOD].

$O_2^{\cdot-}$, NADH was added to eliminate the contribution of Equation 7 toward $O_2^{\cdot-}$ decay. In this assay TPO is exposed to $O_2^{\cdot-}$ flux in the presence of an excess of NADH. Increasing the TPO concentration did not enhance the rate of spin loss, indicating that all $O_2^{\cdot-}$ formed react with TPO to yield TPO^+ (Equation 6), which in turn is reduced by NADH to cyclic hydroxylamine (Equation 8). Under these conditions the initial rate of spin loss validly reflects the flux of superoxide (denoted V). Upon repeating the experiment in the presence of increasing concentration of SOD, the rate of spin loss (denoted v) decreases as a result of a competition between SOD and nitroxide for $O_2^{\cdot-}/^{\cdot}OOH$.

The results of a typical experiment done with 100 μM TPO (or 200 μM TPL) and 1 mM NADH are displayed in Fig. 4. The values of V/v were plotted *versus* [SOD] according to Expression III. The inhibition by SOD of $O_2^{\cdot-}$-induced reduction of cyt-c^{III} is also included in Fig. 4 in order to simplify calculation of the rate constants, as detailed under "Experimental Procedures." The reaction rate constants $k_{app(EPR)} = k_6$ evaluated from Expression IV were 7.4×10^5 M^{-1} s^{-1} and 2.5×10^5 M^{-1} s^{-1} for TPO and TPL, respectively.

DISCUSSION

Catalysts and Scavenger—Because a catalyst is defined as a substance that accelerates a chemical reaction in which it itself is not consumed in the overall process, its amount bears no stoichiometric relationship to the quantity of the substrate altered. This is not the case with a stoichiometric scavenger, which is consumed in the reaction. Generally, for an enzyme-substrate (or any catalyst-substrate) interaction, the concentration of the catalyst is far below that of its substrate. Generally, this perception is true for any homogeneous reaction system. In contrast, SOD whose substrate is a free radical, is unique because its physiological concentration exceeds that of its substrate by several orders of magnitude. The concentration of cellular SOD can achieve 10 μM (37), whereas that of its substrate is about 10^6-fold lower, ranging around 10 pM (37). Unlike enzymes, which obey the Michaelis-Menten model, SOD flip-flops between its two oxidation states, is never saturated even with super-physiologic $O_2^{\cdot-}$ concentrations, and exhibits first order reaction kinetics with respect to $[O_2^{\cdot-}]$.

The Kinetics Analysis of the Direct Assay—It was previously attempted to distinguish a catalytic process from a stoichiometric reaction by analyzing the reaction kinetics (29). To do that, a reaction system in which $O_2^{\cdot-}$ radicals spontaneously dismutate was supplemented with a tested compound (scavenger/catalyst), which is capable of reacting with the radicals:

$$\text{scavenger/catalyst} + O_2^{\cdot-} \xrightarrow{k_9} \text{reaction products} \qquad \text{(Eq. 9)}$$

Whenever the test compound modifies the decay kinetics of $O_2^{\cdot-}$, the new kinetic order should reflect the mechanism underlying the perturbing reaction. Using this method, an initial super-physiologic concentration of $O_2^{\cdot-}$ is employed in both pulse radiolysis (17) and rapid mixing stopped flow (29) techniques. The decay of $O_2^{\cdot-}$ is then followed spectrophotometrically, and the reaction kinetics are studied. The method requires that the reagent under investigation (scavenger or putative SOD mimic) significantly perturbs the spontaneous decay of $O_2^{\cdot-}$ under the condition where $[\text{tested compound}]_o < [O_2^{\cdot-}]_o$. This implies that the rate of reaction with any scavenger/catalyst should be at least comparable with that of the spontaneous dismutation of superoxide in order to see an effect when $O_2^{\cdot-}$ is directly monitored. In other words, unless the conditions of Expression VI

$$k_5[O_2^{\cdot-}]^2 << k_9[O_2^{\cdot-}][\text{tested compound}]$$

EXPRESSION VI

are met, the direct kinetics analysis cannot provide conclusive information of the mechanism underlying the activity of the reagent under investigation. This limitation cannot be circumvented by increasing the concentration of the reagent under investigation because the reaction would exhibit pseudo-first order kinetics and pre-empt any discrimination between stoichiometric and catalytic processes.

The direct kinetics analysis suffers from another serious limitation when the reduced form of the SOD mimic under study is rapidly oxidizable by molecular oxygen (38). With physiological concentrations of $O_2^{\cdot-}$, where $k_{-1}[O_2] > k_2[O_2^{\cdot-}]$, the actual catalytic rate constant, k_{actual}, is much lower than the limiting value of k_{cat} (38).

$$k_{actual} = 2k_1k_2/\{k_1 + k_2 + k_{-1}\cdot([O_2]/[O_2^-])\}$$

EXPRESSION VII

Therefore, direct assay methods can overestimate the catalytic activity and erroneously assess the physiological efficiency of SOD mimics (17).

The Distinction of Catalysts from Scavengers—When $[O_2^-] \ll$ [scavenger/catalyst], as is the case under physiological concentrations, the reaction shown in Equation 9 would exhibit a pseudo-zero order kinetics even with respect to a scavenger as long as its concentration remains practically unchanged. Consequently, a stoichiometric scavenger would erroneously appear to act as a catalyst. The opposite error might exist upon the assessment of reagents that remove O_2^- catalytically but have a lower value of k_{cat} compared with spontaneous dismutation. Such genuine, although less reactive, SOD mimics would be inadvertently evaluated by the direct method of kinetics analysis as being inactive (29).

Comparison of the nitroxide k_{cat} with the rate constant of the spontaneous decay of superoxide at pH 7.8 or 8.1 readily explains the previous failure to detect SOD mimic activity of nitroxides (29). With the relatively high initial $[O_2^-]$ used in the rapid mixing stopped flow technique, the conditions for Expression VI was not met, and there was no possibility to detect any effect of nitroxide on superoxide decay (29). Had this assay been conducted at lower pH, such as pH7, the nitroxide catalytic activity would have been detected.

Although the steady state concentration of O_2^- in biological systems is indeed low, cellular SOD or any scavenger has to cope with a continuous flux of the radical. A valid discrimination of a catalyst from a stoichiometric scavenger requires that the concentration of the scavenger/catalyst, exposed to O_2^- flux, would remain time-invariant upon exposure to O_2^- flux for a period of Δt such that

$$[\text{scavenger}]_0 < \text{flux} \cdot \Delta t$$

EXPRESSION VIII

the conditions for Expression VIII is met for nitroxides where 10 μM TPO (or TPL) persisted over 50 min under O_2^- flux of ~16 $\mu M \cdot min^{-1}$ (Fig. 3), thus substantiating the identification of TPL and TPO as genuine catalysts. Because $^{\cdot}OOH/H_2O_2$ redox couple has a midpoint potential of 1.06 V *versus* normal hydrogen electrode (39), SOD mimics capable of catalytic dismutation of superoxide by utilizing a primary oxidation step should have a reversible electrochemical behavior in the same potential region. Electrochemical studies of stable nitroxides show that both TPO and TPL exhibit a reversible one-electron oxidation corresponding to the nitroxide/oxo-ammonium cation redox couple (28). The midpoint potentials for TPO (722 mV *versus* normal hydrogen electrode) and TPL (810 mV *versus* normal hydrogen electrode) indicate that they can be oxidized by $^{\cdot}HO_2$. The oxo-ammonium cation, on the other hand, has been shown to be reduced to the nitroxide by O_2^- at diffusion controlled rates (40). These considerations substantiate the mechanism depicted by Equations 6 and 7.

The Catalytic Rate Constants of Superoxide Dismutation by Nitroxides—In the EPR experiment and in the presence of NADH (Fig. 3), the intermediate TPO^+ reacts with the two-electron reductant rather than oxidizing another O_2^- radical. The rate constant, $k_{app(EPR)}$, determined under such conditions (using Expression IV) represents only the first half of the catalytic cycle (Equation 6) rather than the full cycle, *i.e.* $k_{app(EPR)}$ equals k_6 rather than k_{cat}. Equation 6 is the rate-limiting step in the catalytic dismutation of O_2^- by nitroxide, because the second step (Equation 7) is much faster having $k_7 = 1.5 \times 10^{10}\ M^{-1}\ s^{-1}$, as previously reported (40). Because TPO^- does not react with oxygen and because $k_7 \gg k_6$, $k_{cat} = 2k_6$, Expression VII approaches Expression V.

The situation is different in the spectroscopic experiments. Because in the competition reaction of nitroxide with cyt-c^{III} for superoxide (Fig. 1) both the nitroxide and its oxidized form TPO^+ (or TPL^+) react with and remove superoxide, the kinetics analysis enables the determination (from Expression II) of k_{app}, which in fact represents k_{cat}.

The values of k_{cat} thus calculated from $k_{app(EPR)} = k_6$ obtained by EPR through competition *versus* SOD (Fig. 3) did not exactly match but were comparable with those independently evaluated from the competition against cyt-c^{III} (Fig. 1), where both the nitroxide and its oxidized form TPO^+ (or TPL^+) react with and remove superoxide. The final values of k_{cat} at pH 7, determined by averaging the results independently obtained by the optical and EPR assays, are $(1.8 \pm 0.4) \times 10^6\ M^{-1}\ s^{-1}$ and $(6.9 \pm 2.9) \times 10^5\ M^{-1}\ s^{-1}$ for TPO and TPL, respectively.

In conclusion, the present results define the limitations of the direct kinetics analysis in evaluating SOD mimics and demonstrate how appropriate application of various assays can validly discriminate between a catalyst and a stoichiometric scavenger. They also show that stable nitroxide radicals are genuine SOD mimics having k_{cat} values that exceed $10^7\ M^{-1}\ s^{-1}$ at pH 6, evidently capable of greatly affecting the O_2^- level in cells and tissues, thus providing effective detoxification measure.

REFERENCES

1. McCord, J. & Fridovich, I. (1969) *J. Biol. Chem.* **244**, 6049–6055
2. Fridovich, I. (1989) *J. Biol. Chem.* **264**, 7761–7764
3. Boccu, E., Velo, G. P. & Veronese, F. M. (1982) *Pharmacol. Res. Commun.* **14**, 113–120
4. Veronese, F. M., Boccu, E., Schiavon, O., Velo, G. P., Conforti, A., Franco, L. & Milanino, R. (1983) *J. Pharm. Pharmacol.* **35**, 757–758
5. Brigelius, R., Hartmann, H. J., Bors, W., Saran, M., Lengfelder, E. & Weser, U. (1975) *Hoppe-Seyler's Z. Physiol. Chem.* **356**, 739–745
6. Lengfelder, E. & Elstner, E. F. (1978) *Hoppe-Seyler's Z. Physiol. Chem.* **359**, 751–757
7. Weser, U., Sellinger, K. H., Lengfelder, E., Werner, W. & Strahle, J. (1980) *Biochim. Biophys. Acta* **631**, 232–245
8. Koppenol, W. H., Levine, F., Hatmaker, T. L., Epp, J. & Rush, J. D. (1986) *Arch. Biochem. Biophys.* **251**, 594–599
9. Darr, D., Zarilla, K. A. & Fridovich, I. (1987) *Arch. Biochem. Biophys.* **258**, 351–355
10. Huber, K. R., Sridhar, R., Griffith, E. H., Amma, E. L. & Roberts, J. (1987) *Biochim. Biophys. Acta* **915**, 267–276
11. Nagano, T., Hirano, T. & Hirobe, M. (1989) *J. Biol Chem.* **264**, 9243–9249
12. Beyer, W. J. & Fridovich, I. (1989) *Arch. Biochem. Biophys.* **271**, 149–156
13. Robertson, P. J. & Fridovich, I. (1980) *Arch. Biochem. Biophys.* **203**, 830–831
14. Rabinowitch, H. D., Rosen, G. M. & Fridovich, I. (1989) *Free Radical Biol. & Med.* **6**, 45–48
15. Hahn, S. M., Krishna, C. M., Samuni, A., Mitchell, J. B. & Russo, A. (1991) *Arch. Biochem. Biophys.* **288**, 215–219
16. Goldstein, S. & Czapski, G. (1986) *J. Free Radicals Biol. Med.* **2**, 3–11
17. Goldstein, S., Michel, C., Bors, W., Saran, M. & Czapski, G. (1988) *Free Radical Biol. & Med.* **4**, 295–303
18. Goldstein, S. & Czapski, G. (1991) *Free Radical Res. Commun.* **1**, 5–10
19. Krishna, M. C. & Samuni, A. (1994) *Methods Enzymol.* **234**, 580–589
20. Miura, Y., Utsumi, H. & Hamada, A. (1993) *Arch. Biochem. Biophys.* **300**, 148–156
21. Mitchell, J. B., Samuni, A., Krishna, M. C., DeGraff, W. G., Ahn, M. S., Samuni, U. & Russo, A. (1990) *Biochemistry* **29**, 2802–2807
22. Samuni, A., Winkelsberg, D., Pinson, A., Hahn, S. M., Mitchell, J. B. & Russo, A. (1991) *J. Clin. Invest.* **87**, 1526–1530
23. Samuni, A., Godinger, D., Aronovitch, J., Russo, A. & Mitchell, J. B. (1991) *Biochemistry* **30**, 555–561
24. Mohsen, M., Pinson, A., Zhang, R. & Samuni, A. (1995) *Mol. Cell. Biochem.* **145**, 103–110
25. Rachmilewitz, D., Karmeli, F., Okon, E. & Samuni, A. (1994) *Gut* **35**, 1181–1188
26. Beit-Yannai, E., Zhang, R., Trembovler, V., Samuni, A. & Shohami, E. (1996) *Brain Res.* **717**, 22–28
27. Samuni, A., Krishna, C. M., Riesz, P., Finkelstein, E. & Russo, A. (1988) *J. Biol Chem.* **263**, 17921–17924
28. Krishna, M. C., Graham, D. A., Samuni, A., Mitchell, J. B. & Russo, A. (1992) *Proc. Natl. Acad. Sci. U. S. A.* **89**, 5537–5541
29. Weiss, R. H., Flickinger, A. G., Rivers, W. J., Hardy, M. M., Aston, K. W., Ryan, U. S. & Riley, D. P. (1993) *J. Biol. Chem.* **268**, 23049–23054
30. Butler, J., Jayson, G. G. & Swallow, A. J. (1975) *Biochim. Biophys. Acta* **408**, 215–222

31. Butler, J., Koppenol, W. H. & Margoliash, E. (1982) *J. Biol. Chem.* **257**, 10747–10750
32. Samuni, A., Min, A., Krishna, C. M., Mitchell, J. B. & Russo, A. (1990) *Adv. Exp. Med. Biol.* **264**, 85–92
33. Samuni, A., Krishna, C. M., Mitchell, J. B., Collins, C. R. & Russo, A. (1990) *Free Radical Res. Commun.* **9**, 241–249
34. Turrens, J. F. & McCord, J. M. (1988) *FEBS Lett.* **227**, 43–46
35. Radi, R., Thomson, L., Rubbo, H. & Prodanov, E. (1991) *Arch. Biochem. Biophys.* **288**, 112–117
36. Barr, D. P. & Mason, R. P. (1995) *J. Biol. Chem.* **270**, 12709–12716
37. Brawn, K. & Fridovich, I. (1980) *Acta Physiol. Scand. Suppl.* **492**, 9–18
38. Czapski, G., Goldstein, S. & Meyerstein, D. (1988) *Free Radical Res. Commun.* **4**, 231–236
39. Sawyer, D. T. & Valentine, J. S. (1981) *Acc. Chem. Res.* **14**, 393–400
40. Korcherginski, N. & Swartz, H. M. (1995) *Nitroxide Spin Labels* (Korcherginski, N., and Swartz H. M., eds) pp. 27–66, CRC Press, Inc., Boca Raton, FL
41. Krishna, M. C., Samuni, A., Taira, J., Goldstein, S., Mitchell, J. B., and Russo, A. (1996) *J. Biol. Chem.* **271**, 26018–26025

Studies of Structure–Activity Relationship of Nitroxide Free Radicals and Their Precursors as Modifiers Against Oxidative Damage

Murali C. Krishna,† William DeGraff,† Olga H. Hankovszky,‡ Cecília P. Sár,‡ Tamás Kálai,‡ József Jekő,§ Angelo Russo,† James B. Mitchell,† and Kálmán Hideg*,‡

Radiation Biology Branch, National Cancer Institute, Bethesda, Maryland 20892, Institute of Organic and Medicinal Chemistry, University of Pécs, H-7643 Pécs, P.O. Box 99, Hungary, and ICN Alkaloida Company Ltd., H-4440 Tiszavasvári, P.O. Box 1, Hungary

Received April 8, 1998

The protective effects of stable nitroxides, as well as their hydroxylamine and amine precursors, have been tested in Chinese hamster V79 cells subjected to H_2O_2 exposure at fixed concentration or exposure to ionizing radiation. Cytotoxicity was evaluated by monitoring the viability of the cells assessed by the clonogenic assay. The compounds tested at fixed concentration varied in terms of ring size, oxidation state, and ring substituents. Electrochemical studies were carried out to measure the redox midpoint potentials. The studies show that in the case of protection against H_2O_2 exposure, the protection was determined by the ring size, oxidation state, and redox midpoint potentials. In general the protection factors followed the order nitroxides > hydroxylamines > amines. Both the six-membered ring nitroxides and substituted five-membered ring nitroxides were efficient protectors. For six-membered ring nitroxides, the compounds exhibiting the lowest midpoint potentials exhibited maximal protection. In the case of X-radiation, nitroxides were the most protective though some hydroxylamines were also efficient. The amines were in some cases found to sensitize the toxicity of aerobic radiation exposure. The protection observed by the nitroxides was not dependent on the ring size. However, the ring substituents had significant influence on the protection. Compounds containing a basic side chain were found to provide enhanced protection. The results in this study suggest that these compounds are novel antioxidants which can provide cytoprotection in mammalian cells against diverse types of oxidative insult and identify structural determinants optimal for protection against individual types of damage.

Introduction

Reactive oxygen species (ROS) are byproducts of normal metabolic processes in aerobic environments.[1] These species can exert cytotoxicity by damaging critical cellular components necessary for viability.[2] Examples of the ROS are superoxide, hydrogen peroxide, and hydroxyl radicals produced by sources such as bioreductively activated xenobiotics and ultraviolet and ionizing radiation. Low-molecular-weight complexes of transition metals such as iron and copper can also catalyze the formation of some of these oxidizing species. In addition to exerting toxicity by oxidation, ROS have been also implicated in the activation of factors such as NF-κB via mechanisms involving redox reactions. Detoxification of these oxidants is provided by enzymatic and nonenzymatic mechanisms. Enzymatic antioxidants include superoxide dismutase (SOD), catalase (Cat), and glutathione peroxidase (GPX) which catalytically detoxify oxidants, while nonenzymatic antioxidants are primarily reducing agents such as vitamin C and vitamin E which can scavenge oxidants by H atom donation in a stoichiometric manner.[3] Imbalances in the detoxification of ROS relative to their production lead to what is a widely accepted phenomenon called "oxidative stress". In most cases the defense provided by the enzymatic and nonenzymatic antioxidants is adequate. However, in acute situations, such as radiation-induced normal tissue toxicity, anthracycline-induced cardiomyopathy, and iron overload, supplementation with exogenous antioxidants may be necessary to minimize tissue damage. However, the targets and sites of free radical damage vary depending on the kind of stress. For example, organic peroxides exert cytotoxicity by damaging cell membranes, whereas ionizing radiation induces cytotoxicity by causing DNA double-strand breaks. Therefore, the sites of damage need to be identified, and appropriate antioxidant strategies need to be devised to effectively limit tissue injury depending on the type of insult. This has prompted a search for efficient antioxidants which can augment the normal antioxidant defense and provide defense against a stress imposed by a wide range of modalities in chronic as well as acute pathological conditions. Desired features in an effective antioxidant would include (a) ability to localize in subcellular compartments, (b) ability to react and scavenge with a wide range of reactive species, and (c) ability to be regenerated to the active form efficiently.

Stable nitroxide free radicals, which have been used as biophysical probes, have been identified as novel antioxidants. By undergoing one-electron-transfer reactions, nitroxides are readily reduced to the hydroxylamines[4,5] or oxidized to the oxoammonium cation.[6,7] Consequently, all three forms of the oxidation states

* Address correspondence to Kálmán Hideg at University of Pécs. Phone/Fax: (36) (72) 325-731. E-mail: KHIDEG@main.pote.hu.
† National Cancer Institute.
‡ University of Pécs.
§ ICN Alkaloida Co. Ltd.

S0022-2623(98)00216-7 CCC: $15.00
Published on Web 08/12/1998

might exist in a biological system. The nitroxide/oxoammonium pair behaves as an efficient and electrochemically reversible redox pair and is involved in the catalytic decomposition of superoxide[6,8] as well as inducing catalase-like activity in heme proteins.[9] Though not directly oxidizing, piperidin-1-oxyl nitroxides are often used as cooxidants in organic chemistry.[10] The hydroxylamine, on the other hand, can function as a typical reducing agent like vitamins C and E to scavenge oxidants,[11] while the nitroxide participates in radical–radical recombination reactions.[12] The metabolism of nitroxides in biological systems has been investigated in detail and found to be reduced to the corresponding hydroxylamines through enzyme-related mechanisms.[4] The oxidation of the hydroxylamines can also occur efficiently. Consequently, a distribution of nitroxide/hydroxylamine is achieved regardless of which form is administered in vivo. Sterically hindered five- and six-membered cyclic amines without H atoms at α-positions have the ability of undergoing oxidation to paramagnetic *N*-oxyl compounds.[13] The influence of the ring structure on the nitroxide/hydroxylamine distribution in cells and tissues has been studied. Nitroxides belonging to the six-membered piperidine ring structure have been shown to be rapidly converted to the hydroxylamine, unlike the five-membered pyrrolidine or pyrroline nitroxides.[4]

It was found that compared to nitrones, which trap short-lived radicals to form stable nitroxide adducts, several nitroxide free radicals possess better antioxidant properties and decrease the oxidative damage caused by reactive oxygen-centered free radicals ($HO^{\bullet}$, $O_2^{\bullet-}$, $HO_2^{\bullet}$).[8] Studies conducted in this laboratory have identified protective effects of nitroxides in several cellular and in vivo studies.[14] For example, nitroxides and hydroxylamines have been shown to protect mammalian cells exposed to superoxide, hydrogen peroxide (H_2O_2), organic hydroperoxides, and redox cycling anticancer agents.[15–18] A variety of sterically hindered pyrrolinecarboxamides were prepared and tested for antiarrhythmic effects.[19] It was recently demonstrated that one of these compounds, *N*-[(2,2,5,5-tetramethyl-3-pyrroline-3-carboxamido)propyl]phthalimide which is currently under clinical trial, was oxidized in vivo to stable nontoxic nitroxide free radical as detected by in vivo EPR spectroscopy in living animals.[20] Mechanisms explaining the protective effects include (a) SOD-mimic activity, (b) oxidizing redox active transition metals, (c) reducing hypervalent heme states, (d) radical–radical recombination, and (e) chain-breaking antioxidants. However, in the case of exposure to ionizing radiation, nitroxides were effective in inhibiting the aerobic cytotoxicity, whereas the hydroxylamines, which are reducing agents, were ineffective similar to other reducing agents such as vitamin C and vitamin E.[21] The thiol-based radioprotectors, where the sulfhydryl agent provides radioprotection either by radical scavenging or by chemical repair, inhibit radiation-induced DNA lesions.[22] The most effective thiol-based radioprotectors require the presence of basic functions (amino, amidino, or guanidino).[23,24] The enhanced protection afforded by thiols with basic functional groups has been attributed to the better affinity of the positively charged substituents on the thiol to the DNA thus allowing the scavenging of short-lived radicals generated in close proximity to DNA.

To study the structural requirements of nitroxide for general antioxidant effects as well as radioprotection, a systematic screening of these agents was performed using an in vitro assay. The effect of ring size, substituents, and oxidation state of the test compounds at a fixed concentration, in providing protection to mammalian cells exposed to oxidative damage induced by exposure to H_2O_2 or ionizing radiation, was evaluated using the clonogenic viability of Chinese hamster lung fibroblasts. The results indicate that the requirements of an agent to be effective in providing protection against H_2O_2-induced toxicity are predominantly influenced by the ring size, redox potential, and oxidation state. In the case of protection against ionizing radiation, the ring substituents and the oxidation state were the main determinants of the radiation modification.

Chemistry

Generally speaking the structure of nitroxides can be modified by three methods: first, five- or six-membered ring can be constructed as it is required; second, the nitroxide function can be reduced partially, totally removed, or restored; third, the functional group on the ring can be altered as well. Nitroxides (**14c**, **16c**, **22c**, **23c**, **25c**, **36c**, **37c**, **40c**, **55c**) were reduced to secondary amines with Fe/AcOH[24] without alteration of other functional groups attached to the nitroxide ring. In a reverse process sterically hindered amine **55a** could be oxidized to nitroxide with H_2O_2 in the presence of Na_2WO_4.[13] The *N*-hydroxylamines (**1b**, **2b**, **5b**, **6b**, **9b**, **11b–17b**, **19b**, **22b**, **23b**, **25b–27b**, **29b**, **36b–38b**, **40b**, **42b**, **48b**, **52b**, **53b**, **55b**) could be obtained by refluxing nitroxides with EtOH saturated with HCl gas.[13] The *N*-hydroxylamines in basic or buffered media were oxidized to nitroxides with PbO_2 or MnO_2 accompanied by bubbling oxygen through the solution.

The synthesis of all pyrroline or piperidine nitroxides utilized 4-oxo-2,2,6,6-tetramethylpiperidine[13] as starting material. Favorskii rearrangement of 3,5-dibromo-4-oxo-2,2,6,6-tetramethylpiperidine (**59**) with sodium methoxide afforded the pyrroline methyl ester (**42a**), which could be reduced to allylic alcohol (**14a**) by SMEAH. This compound was readily oxidized to α,β-unsaturated aldehyde[26] **36a** which was methylated at its amino function to tertiary amine **36d** (Scheme 1).

Secondary amines (**18c–20c**, **25c**, **28c**) were obtained by sodium borohydride reduction of nonisolated Schiff's bases synthesized from aldehydes[26,27] (**36c**, **37c**). The secondary amine could be alkylated with methyl iodide in the presence of NaH to yield tertiary amines (**26c**, **29c**). Tertiary amine **10c** in which the nitrogen atom is attached to a secondary carbon atom could be achieved by reductive alkylation with sodium cyanoborohydride[28,29] starting from TEMPON (**39c**) and dibutylamine. Assessing the fact that paramagnetic ethers exhibited excellent NMR relaxitivity,[30] several of them, such as **15c**, were synthesized by alkylating the corresponding alcohol **14c** (Scheme 2).

The most convenient method for obtaining paramagnetic tertiary amines (**17c**, **21c**, **22c**) was the alkylating of secondary amines with allylic bromide **60**.[31] This paramagnetic alkylating agent was used to get am-

Scheme 1[a]

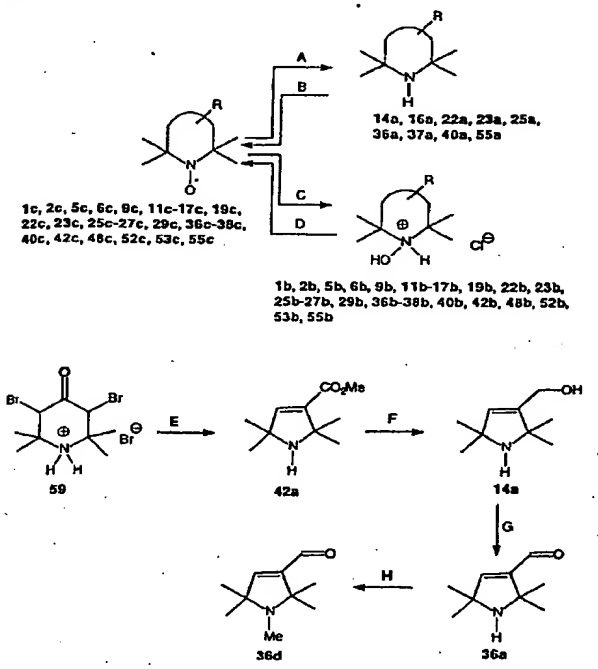

[a] Reagents: (A) Fe powder, AcOH, 3 h, 40–50 °C; (B) 30% H_2O_2, MeOH, 3 days; (C) HCl/EtOH, 30 min; (D) K_2CO_3, $CHCl_3$, then MnO_2, 30 min; (E) MeONa, MeOH, 1 h; (F) SMEAH, toluene, 40 °C, 1 h; (G) MnO_2, $CHCl_3$, 30 min; (H) MeI, acetone, reflux, 4 h.

Scheme 2[a]

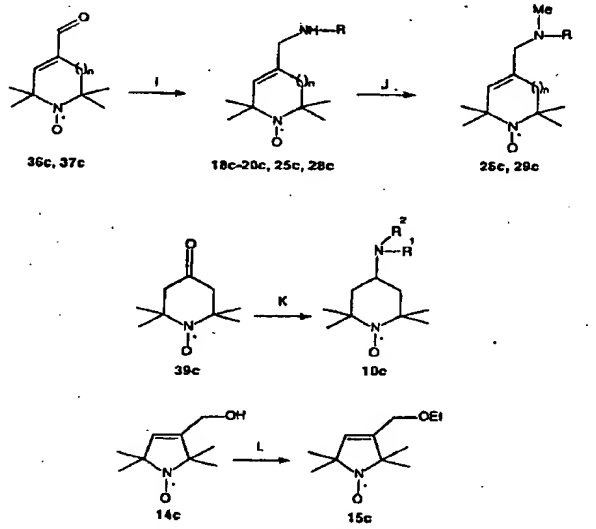

[a] Reagents: (I) (i) 1-aminoadamantane, cat. *p*-toluenesulfonic acid, toluene, reflux, 12 h, (ii) $NaBH_4$, EtOH, 0 °C then reflux for 1 h; (J) NaH, THF, reflux, 1 h then MeI, reflux 6 h; (K) dibutylamine hydrochloride, $NaCNBH_3$, MeOH, reflux, 48 h; (L) NaH, THF, rt, 1 h then EtBr, DMF, reflux, 2 h.

monium (**30d**, **31d**) and phosphonium (**32e**) salts from tertiary amines and triphenylphosphines.[32] The isoindolyl derivative **24c** was obtained most conveniently by alkylating allylic amine **61**[33] with α,α′-dibromo-*o*-xylene. Attractive challenging target was to achieve spin-labeled guanidine **33c** and urea **43c** from amine **61** and S-methylisothiouronium salt and from isocyanate **62**[33]

Scheme 3[a]

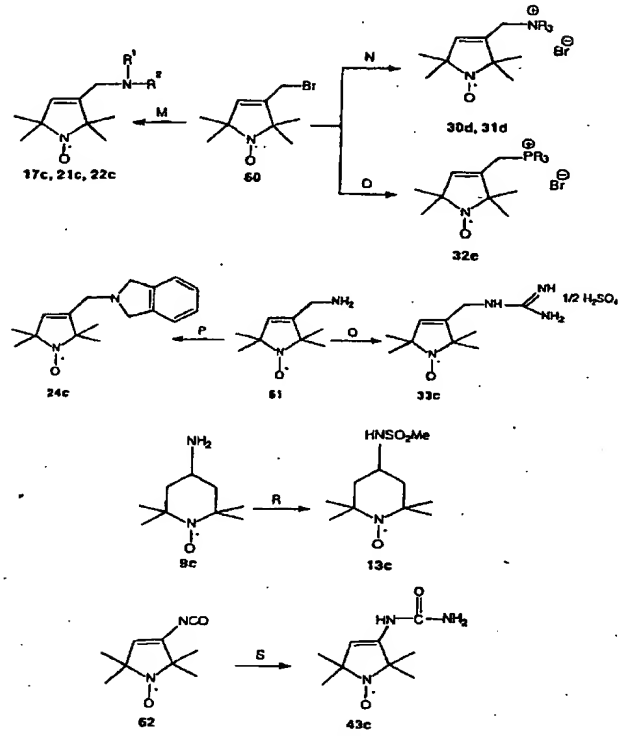

[a] Reagents: (M) pyrrolidine, $CHCl_3$, reflux, 3 h; (N) *n*-tributylamine, acetone, reflux, 6 days; (O) triphenylphosphine, acetone, reflux, 3 h; (P) *o*-dibromoxilol, K_2CO_3, $CHCl_3$, reflux, 3 h; (Q) *S*-methylisothiouronium sulfate, EtOH, reflux, 3 h; (R) Et_3N, $MeSO_2Cl$, CH_2Cl_2, rt, 3 h; (S) NH_3, cyclohexane.

and ammonia. The investigation of these compounds is well-supported so that parent compounds, i.e., guanidine and urea, often appear in bioactive molecules and drugs. Besides the amines which proved the most efficient agents, we synthesized their sulfonylated **13c** derivative. Compound **13c** was obtained with standard procedure, e.g., reacting amine **9c** with methanesulfonyl chloride in the presence of triethylamine (Scheme 3).

Paramagnetic amides (**45c**, **46c**, **48c**, **49c**) were achieved by acylating the corresponding amines with paramagnetic mixed anhydride ester **63**[34] or 1-acylimidazole **64**. To avoid catalytic hydrogenation of double bond in pyrrolines, pyrrolidine derivative **66** was obtained by reaction of 1-oxyl-3-bromo-4-oxo-2,2,6,6-tetramethylpiperidine[35] (**65**) with 1,3-diaminopropane. Fusing compound **66** with phthalimide without solvent at 120 °C yielded compound **52c** while ammonia gas was released.[36] This method had to be used in synthesis of **55c** from **9c**, since in this case the alkylation did not give the desired product, while alkylation of phthalimide with allylic bromide **60** furnished **53c** in good yield (Scheme 4).

Results and Discussion

The compounds evaluated in this study as potential modifiers of cytotoxicity of both ionizing radiation and H_2O_2 are listed in Tables 1–10. Figure 1 shows the general structure of the compounds tested. For each ring type, three possible oxidation states may exist:

Scheme 4[a]

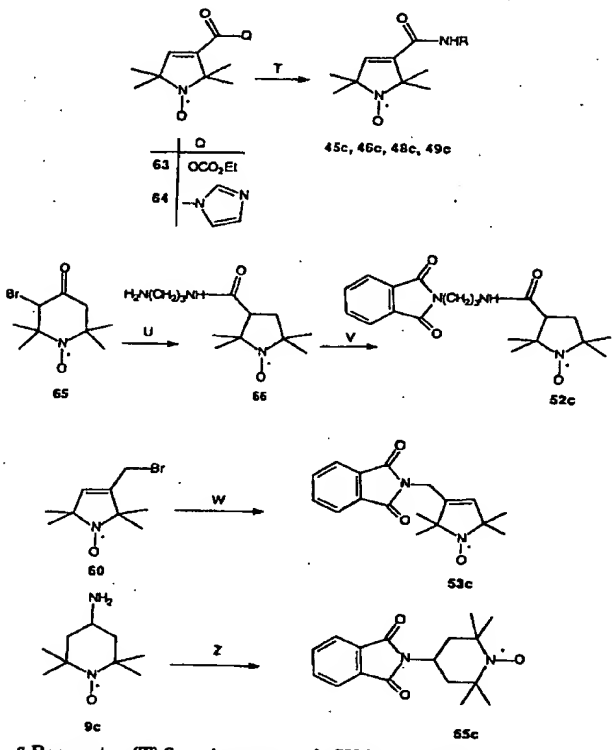

[a] Reagents: (T) 3-aminopropanol, $CHCl_3$, reflux, 30 min; or 1,3-diaminopropane, THF, 0 °C → rt, 1 h; (U) 1,3-diaminopropane, H_2O/THF, rt, 2 h; (V) phthalimide, 120 °C, 1 h; (W) phthalimide K_2CO_3, KOH, 18-K-6, dioxane, reflux, 4 h; (Z) phthalimide, 120 °C, 50 min.

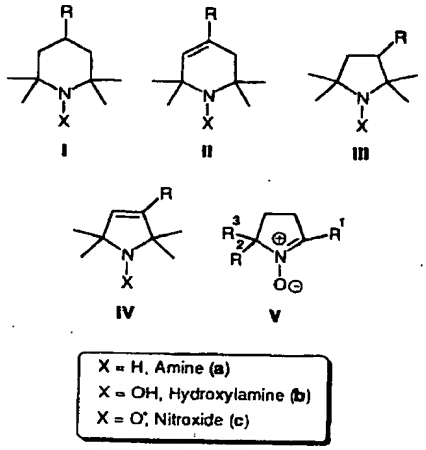

Figure 1. General chemical structures of the nitroxides studied.

namely, the fully reduced secondary amine (type **a**), the hydroxylamine (type **b**), and the nitroxide (type **c**). In some cases the redox midpoint potential of the nitroxide/oxoammonium cation redox pair was estimated.

Hydrogen Peroxide Treatment. The mean surviving fraction of V79 cells following a 1-h exposure to H_2O_2 alone (500 μM) was 0.14 ± 0.016. Possible modulation of H_2O_2-mediated cytotoxicity by the test compounds was evaluated using a fixed final concentration of 100 μM, present during the 1-h H_2O_2 exposure. This concentration was selected for several reasons. First, based on our experience with Tempol (**5c**), a final concentration of 100 μM provides partial protection against H_2O_2 cytotoxicity, whereas higher concentrations (1000 μM) completely protect.[15] A final concentration of 100 μM of each compound would, therefore, afford comparison to our lead compound and allow identification of agents with greater protective properties than Tempol (**5c**). Second, because numerous compounds were evaluated, only small quantities were synthesized making the use of higher concentrations prohibitive. The protection afforded by the compounds against H_2O_2-induced cytotoxicity is shown in Tables 1–10 and Figure 2 (Supporting Information). The results shown in Figure 2 indicate that the test compounds exhibited a broad range in modifying the cytotoxic effects of H_2O_2. Most agents tested were effective in providing protective effects against exposure. In comparison to Tempol (**5c**) which gave a PF of 2.5, 12 compounds yielded greater PFs. The most efficient protector identified by the screen was Tempo (**2c**) which provided a PF of 3.5. With respect to structure and the protective effects against H_2O_2 exposure, the following observations can be made.

The efficacy of stable nitroxides as well as the corresponding hydroxylamines in reversing the free radical-mediated damage induced by oxidative stress prompted this study to identify structural requirements of this class of compounds for optimal antioxidant effects. The model chosen to screen for the efficacy of the antioxidant effects of the test compounds was by exposing Chinese hamster V79 cells to hydrogen peroxide for a fixed duration of time and assessing the clonogenic viability in the absence and presence of a fixed concentration of the compound to be tested. Hydrogen peroxide is produced cellularly as a result of incomplete reduction of oxygen to water or also produced by phagocytic cells as well as by redox cycling xenobiotic drugs. The damage associated with exposure to hydrogen peroxide is understood to be mediated by free radical generation presumably by the generation of $^{\bullet}OH$ radical or an equally strong oxidant catalyzed by redox active transition-metal complexes (eq 1).

$$H_2O_2 + Fe^{2+}\text{–chelate} \rightarrow {}^{\bullet}OH + {}^{-}OH + Fe^{3+}\text{–chelate} \quad (1)$$

$$^{\bullet}OH + LH \rightarrow L^{\bullet} + H_2O \text{ (initiation)} \quad (2)$$

$$L^{\bullet} + O_2 \rightarrow LOO^{\bullet} \text{ (propagation)} \quad (3)$$

$$LOO^{\bullet} + LH \rightarrow LOOH + L^{\bullet} \text{ (propagation)} \quad (4)$$

$$LOOH \rightarrow LO^{\bullet} + {}^{\bullet}OH \text{ (propagation)} \quad (5)$$

$$LOO^{\bullet} + LOO^{\bullet} \rightarrow \text{products (termination)} \quad (6)$$

Earlier studies have shown that both free radical scavengers as well as metal chelators such as desferal can significantly inhibit both the cytotoxicity as well as the oxidation of cellular components. Thus cellular incubation of H_2O_2 represents a valid modality of oxidant stress and has been widely used to screen for agents to reverse this damage. The damage is associ-

Table 1. Alcohols, Amines, and Amides

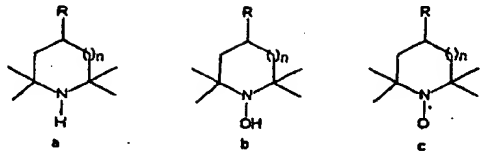

compd	*n*	R	method	yield, %	mp, °C	formula[a]	mol wt	ref	H_2O_2 prot	radiat prot
1b	0	H	C	78	170	$C_8H_{17}NO\cdot HCl$	179.69	43	2.3 (0.52)	0.70 (0.10)
1c	0	H				$C_8H_{16}NO$	142.22	50	0.9 (0.06)	4.60 (0.40)
2b	1	H	C	67	180 dec	$C_9H_{19}NO\cdot HCl$	193.72	43	1.5 (0.20)	0.68 (0.10)
2c	1	H				$C_9H_{18}NO$	156.25	44	3.5 (0.28)	4.20 (0.00)
3c	0	OH				$C_8H_{16}NO_2$	158.22	13	1.4 (0.14)	2.90 (1.40)
4c	0	CH_2OH				$C_9H_{18}NO_2$	172.25	26	1.1 (0.00)	4.7 (0.20)
5a	1	OH				$C_9H_{19}NO$	157.26	44	0.4 (0.00)	0.90 (0.08)
5b	1	OH	C	65	>240	$C_9H_{19}NO_2\cdot HCl$	209.72	43	NT[b]	1.05 (0.04)
5c	1	OH				$C_9H_{18}NO_2$	172.25	13	2.5 (0.23)	5.10 (0.08)
6b	1	OCH_2CH_3	C	63	120	$C_{11}H_{23}NO_2\cdot HCl$	237.77	43	1.6 (0.30)	NT
6c	1	OCH_2CH_3				$C_{11}H_{23}NO_2$	200.30	30	1.9 (0.50)	NT
7c	0	NH_2				$C_8H_{17}N_2O$	157.24	44	1.1 (0.00)	12.9 (0.02)
8c	0	CH_2NH_2				$C_9H_{19}N_2O$	171.26	44	0.7 (0.00)	13.7 (0.00)
9b	1	NH_2	C	74	>230	$C_9H_{20}N_2O\cdot 2HCl$	245.19	43	1.0 (0.00)	1.10 (0.04)
9c	1	NH_2				$C_9H_{19}N_2O$	171.26	44, 13	2.8 (0.14)	18.5 (0.31)
10c	1	$N(n\text{-}Bu)_2$	K	35	oil	$C_{17}H_{35}N_2O$	283.48	43	2.9 (0.64)	NT
11b	1	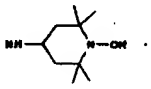	C	61	>230	$C_{18}H_{37}N_3O_2.3HCl$	436.89	43	1.9 (0.30)	1.40 (0.13)
12b	1	$NHCOCH_3$	C	73	128–130	$C_{11}H_{22}N_2O_2\cdot HCl$	250.77	43	1.8 (0.00)	0.85 (0.20)
13b	1	$NHSO_2CH_3$	C	78	182–184	$C_{10}H_{22}N_2O_3S\cdot HCl$	286.82	43	NT	0.77 (0.05)

[a] Analyses for C, H, N, S, Br, and Cl are within ±0.4% of the expected value for the formula. [b] NT, not tested.

ated with DNA single- and double-strand breaks (in the presence of specific chelators) as well as damage to other cellular organelles.

In this study nitroxides of four different ring classes were evaluated such as the six-membered piperidine class (**I**), the six-membered 1,2,5,6-tetrahydropyridine class (**II**), the saturated five-membered pyrrolidine class (**III**), the unsaturated five-membered pyrroline class (**IV**), and nitrones (**V**) (Figure 1). Electrochemical studies on these agents show that while the hydroxylamines undergo an irreversible oxidation around 200 mV vs NHE, at higher potentials, a reversible redox couple consistent with the nitroxide and the corresponding one-electron oxidation product, the oxoammonium cation, exists around in the range 700–1100 mV for the compounds tested. The nitroxide/oxoammonium redox couple has been shown in earlier studies to mediate enzyme mimetic reactions catalytically, such as SOD-mimicking activity.[6]

$$RRNO^{\bullet} + H^{+} + HO_2^{\bullet} \rightarrow RRNO^{+} + H_2O_2 \quad (7)$$

$$RRNO^{+} + O_2^{-\bullet} \rightarrow RRNO^{\bullet} + O_2 \quad (8)$$

The catalytic efficiencies of superoxide dismutation were found to depend on the ease of oxidation of the nitroxide to the corresponding oxoammonium cation, which represents the rate-limiting step. The catalytic rate constants were found to be inversely correlated to the redox midpoint potential of the nitroxide/oxoammonium couple.[8] The nitroxide/oxoammonium couple has also been postulated to induce catalase-like activity in heme proteins.[9] Either of these roles can confer antioxidant activity in the nitroxides. In addition, nitroxides have been shown to prevent the generation of oxidants via Fenton reactions (eq 1) by maintaining the metals in the oxidized state.[15]

Table 2. Alcohols and Amines

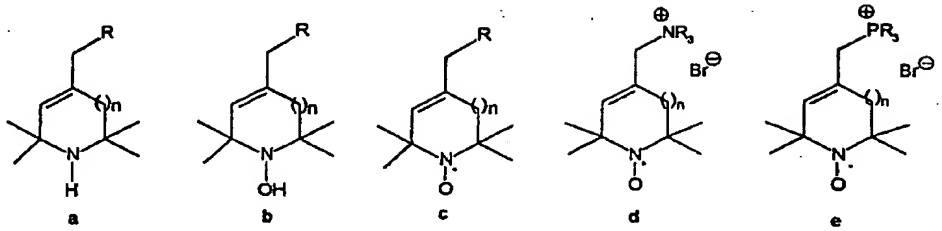

a b c d e

compd	*n*	R	method	yield, %	mp, °C	formula[a]	mol wt	ref	H_2O_2 prot	radist prot
14a	0	OH	A, F	64, 78	66-69	$C_9H_{17}NO$	155.24	43	0.9 (0.06)	1.50 (0.30)
14b	0	OH	C	69	157-159	$C_9H_{17}NO_2$·HCl	207.70	43	3.1 (0.34)	0.92 (0.07)
14c	0	OH				$C_9H_{16}NO_2$	170.23	25	1.8 (0.00)	2.6 (0.07)
15b	0	OCH_2CH_3	C	62	89-92	$C_{11}H_{21}NO_2$·HCl	235.75	43	3.2 (0.61)	NT[b]
15c	0	OCH_2CH_3	L	57	oil	$C_{11}H_{20}NO_2$	198.29	43	1.3 (0.20)	NT
16a	0	NMe_2	A	58	oil	$C_{11}H_{22}N_2$	182.31	43	NT	0.95 (0.18)
16b	0	NMe_2	C	71	hygrosc.	$C_{11}H_{22}N_2O$·2HCl	271.23	43	NT	16.0 (1.02)
16c	0	NMe_2				$C_{11}H_{21}N_2O$	197.30	32	2.1 (0.43)	13.9 (0.70)
17b	0	NEt_2	C	74	189-191	$C_{13}H_{26}N_2O$·2HCl	299.28	43	NT	0.96 (0.03)
17c	0	NEt_2	M	82	oil	$C_{13}H_{25}N_2O$	225.35	43	NT	17.2 (1.20)
18c	0	NH-*n*-Bu	I	64	oil	$C_{13}H_{25}N_2O$	225.35	43	2.5 (0.21)	3.96 (1.75)
19b	0	NH-*t*-Bu	C	68	> 250	$C_{13}H_{26}N_2O$·2HCl	299.28	43	2.1 (0.12)	1.20 (0.00)
19c	0	NH-*t*-Bu	I	67	56-60	$C_{13}H_{25}N_2O$	225.35	43	2.0 (0.35)	19.3 (3.15)
20c/Ts	0	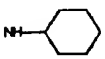	I	60	186 dec	$C_{15}H_{27}N_2O$·$C_7H_8O_3S$	423.59	43	NT	4.40 (0.40)
21c	0	$N(n\text{-}Bu)_2$	M	72	oil	$C_{17}H_{33}N_2O$	281.46	43	3.2 (0.14)	NT
22a	0		A	47	> 240	$C_{13}H_{24}N_2$·2HCl	281.27	43	1.0 (0.00)	0.34 (0.00)

Table 2 (Continued)

compd	*n*	R	method	yield, %	mp, °C	formula[a]	mol wt	ref	H_2O_2 prot	radist prot
22b	0	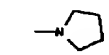	C	67	219-221	$C_{13}H_{24}N_2O\cdot 2HCl$	297.27	43	NT	28.3 (0.20)
22c/Ts	0	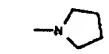	M	78	129-132	$C_{13}H_{23}N_2O\cdot C_7H_8O_3S$	395.54	43	NT	21.4 (1.15)
23a	0	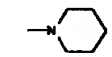	A	45	oil	$C_{14}H_{26}N_2$	222.37	43	NT	0.95 (0.00)
23b	0	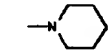	C	70	210-212	$C_{14}H_{26}N_2O\cdot 2HCl$	311.30	43	NT	30.0 (5.40)
23c	0	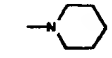				$C_{14}H_{25}N_2O\cdot C_7H_8O_3S$	409.56	32	NT	19.1 (3.50)
24c	0	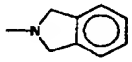	P	68	89-90	$C_{17}H_{23}N_2O$	271.38	43	NT	3.90 (0.00)
25a	0	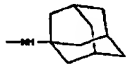	A	62	116-118	$C_{19}H_{32}N_2$	288.48	43	1.9 (0.60)	1.40 (0.13)
25b	0	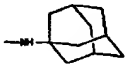	C	70	215-216	$C_{19}H_{32}N_2O\cdot 2HCl$	377.40	43	2.5 (0.43)	1.80 (0.07)
25c	0	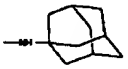	I	72	109-111	$C_{19}H_{31}N_2O$	303.47	43	3.3 (0.63)	NT
26b	0	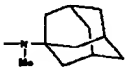	C	67	210-212	$C_{20}H_{34}N_2O\cdot 2HCl$	391.42	43	2.6 (0.92)	NT
26c	0		J	62	110-112	$C_{20}H_{33}N_2O$	317.49	43	3.3 (0.50)	NT
27b	1	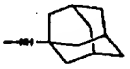	C	66	>200	$C_{20}H_{34}N_2O.2HCl$	391.42	43	2.1 (0.07)	NT
28c	0	$NHCH_2Ph$	I	59	oil	$C_{16}H_{23}N_2O$	259.39	43	2.0 (0.07)	5.20 (1.10)
29c	0	$N(Me)CH_2Ph$	J	56	oil	$C_{17}H_{25}N_2O$	273.42	43	2.0 (0.35)	NT
30d	0	$^{\oplus}N(Et)_3\ Br^{\ominus}$	N	66	238-240 dec	$C_{15}H_{30}BrN_2O$	334.32	43	NT	1.20 (0.00)
31d	0	$^{\oplus}N(n\text{-}Bu)_3\ Br^{\ominus}$	N	63	180-181	$C_{21}H_{42}BrN_2O$	418.48	43	1.1 (0.35)	0.69 (0.02)
32e	0	$^{\oplus}P(Ph)_3\ Br^{\ominus}$	O	71	224-226	$C_{27}H_{30}BrNOP$	495.42	32, 43	NT	0.72 (0.07)
33c	0	$-CH_2NHCONHNH_2$	Q	55	180 dec	$C_{10}H_{19}N_4O$ 1/2 H_2SO_4	260.34	43	NT	1.00 (0.00)

Table 2 (Continued)

compd	n	R	method	yield, %	mp, °C	formula[a]	mol wt	ref	H_2O_2 prot	radiat prot
34c	0	—$CH_2SC(NH)NH_2$				$C_{11}H_{20}N_3OS$	338.46	31	2.2	7.50
						CH_4O_3S			(0.29)	(1.10)
35c	0	—$CH_2SeC(NH)NH_2$				$C_{11}H_{20}N_3OSe$	370.17	46	1.3	NT
						HBr			(0.12)	

[a] Analyses for C, H, N, S, Br, and Cl are within ±0.4% of the expected value for the formula. [b] NT, not tested.

$$RRNO^{\bullet} + H^{+} + Fe^{2+}\text{–chelate} \rightarrow RRNOH + Fe^{3+}\text{–chelate} \quad (9)$$

The hydroxylamines, on the other hand, were found to behave like classic reducing agents such as ascorbate and tocopherol by being oxidized to the corresponding nitroxide by the oxidant in the detoxifying reaction.

$$RRNOH + {}^{\bullet}OH \rightarrow RRNO^{\bullet} + H_2O \quad (10)$$

However, unlike ascorbate, tocopherol, and other phenolic antioxidants, the product (nitroxide) is also capable of further detoxification modalities such radical–radical recombination reactions and interrupting chain propagation of lipid peroxidation reactions.[37]

$$RRNO^{\bullet} + L^{\bullet} \rightarrow RRNOL \quad (11)$$

For a given ring size, the effect of the midpoint redox potential of the nitroxide/oxoammonium catalytic couple has also been examined for its influence on the protective effects. On the basis of the results obtained in this study, some observations can be made.

Structure–Activity Relationships. The compounds of type a (amines) were in general ineffective in providing protection or in some cases actually enhanced the cytotoxicity of H_2O_2 exposure. The nitroxides and hydroxylamines were in general protective.

The well-known six-membered nitroxides (**2c**, **5c**, **9c**, **39c**) were investigated earlier and showed better protecting activity then the corresponding five-membered nitroxides (**1c**, **3c**, **7c**, **38c**). Redox behavior alone might not be able to account for this behavior since no significant differences in their midpoint potentials were found. However, on the basis of several earlier reports which found six-membered nitroxides more reactive with radicals and are more likely to be converted to the corresponding hydroxylamine than the corresponding five-membered counterparts,[4] the enhanced ability of the pideridine class of nitroxides can be attributed to their reactivities. This has been explained in terms of the access to the nitroxide moiety in the ring to reactants. In the case of six-membered ring nitroxides, the "boat" or "chair" conformations of the piperidine ring provide easy access to the nitroxide moiety to participate in electron-transfer reactions involved in antioxidant effects.

The protecting activity is also influenced by ring saturation and functional groups; for instance, the protecting activity of substituted pyrroline nitroxides (**21c**, **25c**, **26c**) approaches the efficiency of six-membered nitroxides. This is a remarkable fact because of the lower toxicity of five-membered ring maintaining the similar H_2O_2 protecting activity.[38,39] Saturated five-membered alcohol **4c** exhibited a smaller protecting activity than its unsaturated derivative **14c**. Among saturated (**50c**, **51c**) and unsaturated (**41c**, **44c**) acid derivatives, there is no significant difference in H_2O_2 protecting activity. In the range of well-available unsaturated acid derivatives, we observed that ester **42c** has better protecting activity than the corresponding acid **41c**. Among all the compounds which exhibit the best protecting activity are amines **9c**, **10c**, **21c**, **25c**, and **26c**; however, quaternary salts **30d**, **31d**, **33c**, **34c**, and **35c** show small protecting activity. The amine-substituted five-membered and six-membered nitroxides (**9c**, **10c**, **25c** **26c**) show good protecting activity. The order of amines was not found to have significant influence on protecting activity as was observed in the case of **25c** and **26c**.

Among the six-membered piperidines, where the nitroxide and the hydroxylamines were compared at similar concentrations, nitroxides were found to be better protectors. However, the protection was inversely proportional to the midpoint potentials of the nitroxide/oxoammonium couple for the piperidines (Figure 3A). The nitroxides which were easily oxidizable provided better protection. However, in the case of five-membered nitroxides such as the pyrrolidines and the pyrrolines such a correlation was absent (Figure 3B). However, in this case, several hydroxylamines exhibited better protection than the corresponding nitroxides suggesting that a H atom donation might be the predominant operating factor in these cases, similar to antioxidants such as ascorbate, thiols, etc.

Ionizing Radiation Treatment. The mean surviving fraction of V79 cells following a 12-Gy dose of radiation alone was 0.02 ± 0.002. Possible modulation of radiation-mediated cytotoxicity by the test compounds was evaluated using a fixed final concentration of 10 mM, present during the 10 min prior to radiation exposure. This concentration was selected for several reasons. From prior results obtained with Tempol, a final concentration of 10 mM provides partial protection against radiation-induced cytotoxicity. A final concentration of 10 mM of each compound would therefore afford comparison to our lead compound and allow identification of agents with greater protective properties than Tempol. As stated above, because numerous compounds were evaluated, only small quantities were synthesized making the use of higher concentrations prohibitive. Additionally, our earlier studies showed

Table 3. Aldehydes

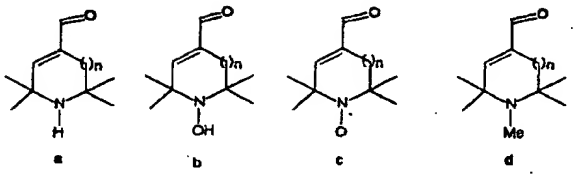

compd	*n*	method	yield, %	mp, °C	formula[a]	mol wt	ref	H_2O_2 prot	radiat prot
36a	0	A, G	62, 89	oil	$C_9H_{15}NO$	153.22	43	0.9 (0.06)	0.07 (0.02)
36b	0	C	69	153–158	$C_9H_{15}NO_2$·HCl	205.68	43	2.7 (0.29)	0.13 (0.30)
36c	0	D	91	77–79	$C_9H_{14}NO_2$	168.22	26, 43	1.3 (0.00)	2.70 (0.23)
36d	0	H	85	oil	$C_{10}H_{17}NO$	167.25	43	NT[b]	0.60 (0.10)
37a	1	A	45	oil	$C_{10}H_{17}NO$	167.25	43	NT	0.40 (0.00)
37b	1	C	77	194–197	$C_{10}H_{17}NO_2$·HCl	219.71	43	NT	1.50 (0.15)
37c	1				$C_{10}H_{16}NO_2$	182.24	27	0.8 (0.00)	6.10 (0.25)

[a] Analyses for C, H, N, S, Br, and Cl are within ±0.4% of the expected value for the formula. [b] NT, not tested.

Table 4. Ketones

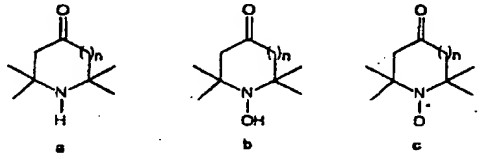

compd	*n*	method	yield, %	mp, °C	formula[a]	mol wt	ref	H_2O_2 prot	radiat prot
38b	0	C	68	151–153	$C_8H_{15}NO_2$·HCl	193.67	43	1.1 (0.00)	1.0 (0.20)
38c	0				$C_8H_{14}NO_2$	156.20	13	0.9 (0.00)	10.2 (0.45)
39a	1				$C_9H_{17}NO$	155.24	47	0.5 (0.00)	1.10 (0.10)
39b	1				$C_9H_{17}NO_2$·HCl	207.70	35	NT[b]	0.68 (0.15)
39c	1				$C_9H_{16}NO_2$	170.23	13, 47	1.1 (0.00)	7.10 (0.85)

[a] Analyses for C, H, N, S, Br, and Cl are within ±0.4% of the expected value for the formula. [b] NT, not tested.

Table 5. Ketones

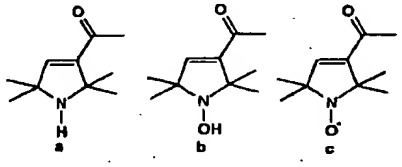

compd	method	yield, %	mp, °C	formula[a]	mol wt	ref	H_2O_2 prot	radiat prot
40a	A	57	oil	$C_{10}H_{17}NO$	167.25	43	NT[b]	0.63 (0.13)
40b	C	80	181–183	$C_{10}H_{17}NO_2$·HCl	219.71	43	NT	0.15 (0.02)
40c				$C_{10}H_{16}NO_2$	182.24	48, 49	NT	4.80 (0.20)

[a] Analyses for C, H, N, S, Br, and Cl are within ±0.4% of the expected value for the formula. [b] NT, not tested.

that nitroxides, but not the hydroxylamines, were radioprotective under aerobic conditions.[21] The protection afforded by the compounds against radiation-induced cytotoxicity is shown in Tables 1–10 and Figure 3. The studies show that the protective effects of the test compounds varied from protection factors of 1 to

Table 6. Acids, Esters, and Amides

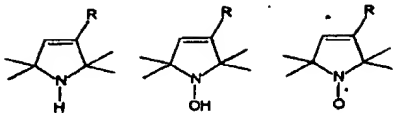

a b c

compd	R	method	yield, %	mp, °C	formula[a]	mol wt	ref	H_2O_2 prot	radiat prot
41c	CO_2H				$C_9H_{14}NO_3$	184.24	13	1.0 (0.00)	NT[b]
42a	CO_2Me	E	82	oil	$C_{10}H_{17}NO_2$	183.25	43	1.3 (0.35)	NT
42b	CO_2Me	C	64	143–145	$C_{10}H_{17}NO_3$·HCl	235.71	43	2.7 (0.46)	NT
42c	CO_2Me				$C_{10}H_{16}NO_3$	198.24	13	1.5 (0.29)	0.94 (0.08)
43c	$NHCONH_2$	S	70	189–190	$C_9H_{16}N_3O_2$	198.24	43	1.2 (0.00)	NT
44c	$CONH_2$				$C_9H_{15}N_2O_2$	183.23	13	1.0 (0.00)	10.7 (3.80)
45c	$CONH(CH_2)_2OH$	T1	62	99–100	$C_{11}H_{19}N_2O_3$	227.28	43	1.2 (0.04)	NT
46c	$CONH(CH_2)_3OH$	T1	84	95–96	$C_{12}H_{21}N_2O_3$	241.31	43	1.1 (0.14)	NT
47c	$CONHCH_2CO_2H$				$C_{11}H_{17}N_2O_4$	241.26	33	0.9 (0.20)	0.98 (0.02)
48a	$CONH(CH_2)_3NH_2$				$C_{12}H_{23}N_3O$	225.33	19	NT	0.52 (0.07)
48b	$CONH(CH_2)_3NH_2$	C	66	hygrosc	$C_{12}H_{23}N_3O_2$·2HCl	314.26	43	1.0 (0.12)	NT
48c	$CONH(CH_2)_3NH_2$	T1, T2	73, 55	104–108	$C_{12}H_{22}N_3O_2$	240.33	43	1.1 (0.17)	NT
49c	$CONH(CH_2)_3NMe_2$	T1	59	94–96	$C_{14}H_{26}N_3O_2$·$C_2H_2O_4$	358.41	43	NT	15.0 (4.20)

[a] Analyses for C, H, N, S, Br, and Cl are within ±0.4% of the expected value for the formula. [b] NT, not tested.

Table 7. Acids, Amides, and Imides

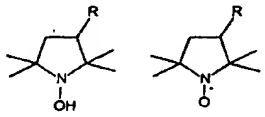

b c

compd	R	method	yield, %	mp, °C	formula[a]	mol wt	ref	H_2O_2 prot	radiat prot
50c	CO_2H				$C_9H_{16}NO_3$	186.23	13	1.0 (0.00)	NT[b]
51c	$CONH_2$				$C_9H_{17}N_2O_2$	185.25	13	1.7 (0.00)	11.2 (1.80)
52b	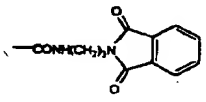	C	68	dec	$C_{20}H_{27}N_3O_4$·HCl	409.91	43	NT	1.26 (0.00)

[a] Analyses for C, H, N, S, Br, and Cl are within ±0.4% of the expected value for the formula. [b] NT, not tested.

30 (Figure 4 in Supporting Information). In comparison to Tempol (**5c**) which gave a PF of 2.2, 19 compounds yielded greater PFs. In some cases the agents provided sensitization of radiation effects with sensitization factors ranging between 1 and 0.1. A correlation between the protective effects and the structure and oxidation state was made to evaluate the determinant factors governing the radiation-modifying effects.

Among the compounds studied, the nitroxides were found to be the most effective in providing the protection followed by the hydroxylamines under identical concentrations. Though the nitroxides and hydroxylamines were both effective in reversing the toxicity mediated by H_2O_2, the results obtained from radiation studies differ presumably as a result of kinetic reasons as well as differences in the sites of damage.

The possible chemical reactions involved in the protective reactions for nitroxides are as follows. If TH is a target molecule which is a critical biomolecule such as DNA, abstraction of the H atom by the radiation-induced species ($X^{\bullet}$) causes the initial lesion.

$$TH + X^{\bullet} \rightarrow T^{\bullet} + XH \text{ (radical formation)} \quad (12)$$

Table 8. Imides

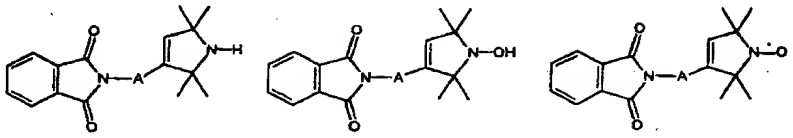

a b c

compd	A	method	yield, %	mp, °C	formula[a]	mol wt	ref	H_2O_2 prot	radiat prot
53b	CH_2	C	78	118–120	$C_{17}H_{20}N_2O_3$·HCl	336.82	43	3.3 (0.52)	0.49 (0.03)
54a	$(CH_2)_3NHCO$				$C_{20}H_{25}N_3O_3$·HCl	391.90	19	1.1 (0.23)	1.90 (0.23)
54b	$(CH_2)_3NHCO$				$C_{20}H_{25}N_3O_4$·HCl	407.90	19	2.2 (0.23)	1.30 (0.17)

[a] Analyses for C, H, N, S, Br, and Cl are within ±0.4% of the expected value for the formula.

Table 9. Imides

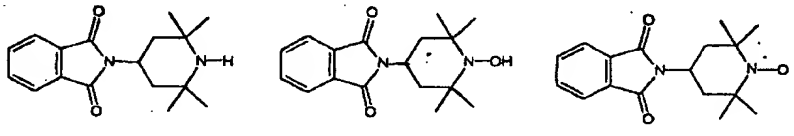

a b c

compd	method	yield, %	mp, °C	formula[a]	mol wt	ref	H_2O_2 prot	radiat prot
55a	A	54	128–129	$C_{17}H_{22}N_2O_2$	286.37	43	0.8 (0.00)	1.70 (0.29)
55b	C	72	>235	$C_{17}H_{22}N_2O_3$·HCl	338.83	43	1.5 (0.14)	NT[b]

[a] Analyses for C, H, N, S, Br, and Cl are within ±0.4% of the expected value for the formula. [b] NT, not tested.

Table 10. Nitrones

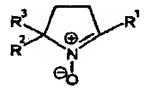

compd	R^1	R^2	R^3	formula[a]	mol wt	ref	H_2O_2 prot	radiat prot
56	H	CH_3	CH_3	$C_6H_{11}NO$	113.15	44	0.9 (0.17)	0.93
57	CH_3	H	CH_3	$C_6H_{11}NO$	113.15	51	1.1 (0.09)	0.91
58	CH_3	CH_3	CH_3	$C_7H_{13}NO$	127.18	52	0.8 (0.12)	1.10

In the presence of oxygen or other hypoxic cell radiation sensitizers such as nitric oxide, the damage on the molecule is fixed by radical–radical recombination reactions.

$$T^{\bullet} + O_2 \rightarrow TOO^{\bullet} \quad (13)$$

These intermediates lead to further breakdown products leading to single- and double-strand breaks in DNA. However, thiol-based radioprotectors have been shown to be effective H atom donors and compete with O_2 and restore the damage.

$$T^{\bullet} + RSH \rightarrow TH + RS^{\bullet} \quad (14)$$

The thiyl radical, being a weak oxidant, is presumed to be minimally involved in mediating further biologic damage.

If $X^{\bullet}$ represents the species generated by ionizing radiation which mediate biological damage, then protection by radical scavenging can proceed by:

$$H^+ + X^{\bullet} + RRNO^{\bullet} \rightarrow XH + RRNO^+ \text{ (electron transfer)} \quad (15)$$

$$X^{\bullet} + RRNO^{\bullet} \rightarrow RRNOX \text{ (radical–radical recombination)} \quad (16)$$

Protection by chemical repair is also feasible with nitroxides:

$$H^+ + T^{\bullet} + RRNO^{\bullet} \rightarrow TH + RRNO^+ \quad (17)$$

Thus, nitroxides can afford radioprotection by radical scavenging as well as by chemical repair.

The hydroxylamines can mediate both electron-transfer and chemical repair reactions and provide

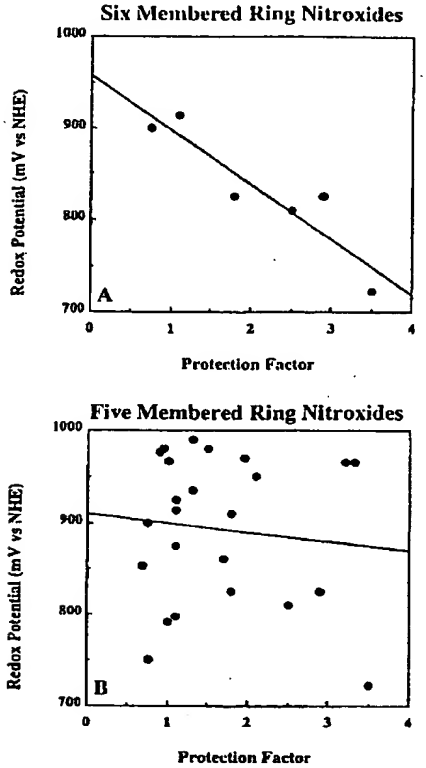

Figure 3. Protection factors of hydrogen peroxide-induced cytotoxicity as a function of redox potential of selected compounds: (A) six-membered ring nitroxides and (B) five-membered ring nitroxides.

protective effects.

$$X^{\bullet} + RRNOH \rightarrow HX + RRNO^{\bullet}\ \text{(electron-transfer)} \quad (18)$$

$$T^{\bullet} + RRNOH \rightarrow TH + RRNO^{\bullet}\ \text{(chemical repair)} \quad (19)$$

The fully reduced amines were found to provide radiosensitization in some cases. These effects are consistent with the reactions listed below:

$$X^{\bullet} + RRNH \rightarrow XH + RRN^{\bullet} \quad (20)$$

$$X^{\bullet} + TH \rightarrow T^{\bullet} + XH \quad (21)$$

$$RRN^{\bullet} + TH \rightarrow T^{\bullet} + RRNH\ \text{(damage)} \quad (22)$$

$$T^{\bullet} + RRN^{\bullet} \rightarrow RRN\text{-}T\ \text{(damage fixation)} \quad (23)$$

The ring size was not found to be of significant effect in determining the radiation response. DNA binding characteristics of the nitroxide-based radioprotectors have been evaluated by nonequilibrium dialysis of DNA with individual nitroxides. These studies show that the positively charged nitroxides had higher degrees of association with DNA as compared to the negatively charged nitroxides. However, since the binding to DNA should be significantly similar for a given ring substituent, nitroxide and hydroxylamine should accumulate at the DNA to similar extent. In a recent study, Milligan et al.[40] show that a diradical intermediate with lifetime of 1 μs is involved in the formation of dsbs. Hence agents which can scavenge such intermediates should effectively inhibit the radiation-induced cytotoxicity. While both hydroxylamine and nitroxides are effective radical scavengers, the mechanisms and the kinetics are expected to be different.

Structure–Activity Relationships. The unsubstituted base compounds (**1c**, **2c**) afforded modest radioprotective activity similar to that found for Tempol (**5c**). Effective radioprotection from nitroxides was observed when the substituent contained an amino group in the side chain. The protection however, was not found to dependent on the order of the amine; primary amines (**7c**–**9c**), secondary amines (**19c**), or tertiary amines (**16c**, **17c**, **22c**, **23c**, **49c**) were all found to have significant radioprotecting activity. The positively charged isothiouronium salt (**34c**) also exhibited remarkable radioprotective activity.

Only **c** type nitroxide compounds or in some cases **b** type hydroxylamines showed X-ray protecting activity. The latter compounds, which are *N*-hydroxy derivatives, could be active because of the possible propensity to undergo spontaneous oxidation back to nitroxide. In addition it was found that upon reducing the nitroxide free radical function to amine, the protecting activity disappeared. This effect was independent of the type of side chain or other functional group.

In addition to the amino substituents, five- and six-membered nitroxide compounds (**c** type) containing a formyl function (**36c**, **37c**) were found to have protecting activity, but in their amine oxidation state (**a** type), they exhibited significant radiosensitization effects (**36a**, **37a**).

Oxidation state of the ring appears to be a critical factor in influencing the protective effects of the compounds. The fully reduced amines (compounds type **a**) predominantly exhibited sensitizing effects, whereas the nitroxides and hydroxylamines exhibited protective effects. Among the nitroxides tested, a comparison of the protective effects with the corresponding redox midpoint potentials shows that there is no significant correlation between the observed protection and the redox potentials. This indicates that even for an amine-based ring oxidation state to be an efficient sensitizer, DNA seems to be the likely target, and therefore, accumulation at DNA to sufficient concentrations confers effective radiosensitizing properties.

Conclusions

The results from the present study show that the nitroxide-based antioxidants represent a novel class of recycling antioxidants which have both catalytic as well as stoichiometric scavenging effects. A general screen of their effectiveness against two types of damage such as H_2O_2 exposure and ionizing radiation shows that while they are effective in both cases, the structural requirements are distinctly different. For protection against H_2O_2 exposure, the kinetic effects predominate, and both six-membered ring and substituted five-membered ring nitroxides were found to be effective. In the case of ionizing radiation, accumulation of the agent at the site of damage was critical. In this case, nitrox-

)des with basic side groups were most effective. With respect to toxicity, none of the agents evaluated in the present study exhibited cytotoxicity. The toxicity of only a few selected nitroxides has been evaluated in mice where sufficient concentrations of the nitroxides for antioxidant and radioprotective purposes were achieved without untoward toxicity.[41,42] The results from this screen will hopefully provide optimal candidates for more intensive evaluation as agents with respect to toxicity and for chemical modification of damaging agents such as H_2O_2 and ionizing radiation.

Experimental Section

The syntheses of the compounds are described by way of typical examples: the methods are denoted in the same way as in Schemes 1–4. The structural and molecular formulas and physical properties of the compounds are summarized in Tables 1–10.

Melting points (uncorrected) were determined on a Boetius micromelting point apparatus. Elemental analyses (C, H, N, S) were obtained on a Carlo-Erba EA 1110 apparatus or (Hal) determined titrimetrically by Schöniger's method. Mass spectra were recorded on a VG TRIO-2 instrument in the EI mode (70 eV, direct inlet) or with thermospray technique. Samples were analyzed in the bypass mode; 10 μL of the sample solution in CH_3OH was introduced via the thermospray interface. The mobile phase was CH_3OH/H_2O, 1:1, solution containing 0.1 M NH_4OAc. The capillary tip temperature was 230 °C, the electrode voltage was 180 V, and the source temperature was 210 °C. The ESR spectra were obtained from 10^{-5} M solution, using a BRUKER 300-E spectrometer. All the monoradicals exhibited three equidistant lines with a_N = 14.7–15.5 G. Flash column chromatography was performed with silica gel 60 (230–400 mesh) (Merck).

Method A. 3-[*N*-(1-Adamantyl)aminomethyl]-2,2,5,5-tetramethyl-3-pyrroline (25a). The nitroxide **25c** (3.04 g, 10 mmol) was dissolved in AcOH (10 mL); then Fe powder (2 g, 36 mmol) was added. The reaction mixture was stirred at 40–50 °C for 3 h, diluted with water (10 mL), and filtered from unreacted Fe. The filtrate was basified by adding solid K_2CO_3, then extracted with $CHCl_3$ (3 × 20 mL), dried ($MgSO_4$), and filtered again, and the solvent was evaporated. The residue was flash-chromatographed on silica gel (Merck 60) with $CHCl_3$–Et_2O and evaporated to dryness. The product was crystallized from Et_2O–hexane, to give the base **25a** (1.78 g, 62%) as off-white crystals: mp 116–118 °C; EI (*m/z*, %) 288 (M^+, 2), 273 (65), 135 (100), 122 (81). Anal. ($C_{19}H_{32}N_2$) C, H, N.

Preparation of hydrochloride salt: The base (0.86 g, 3 mmol) was acidified with HCl in EtOH to pH 3 and then diluted with Et_2O to start crystallization (0.92 g, 85%). The analytical sample of the salt of **25a/HCl** was recrystallized from EtOH–Et_2O (mp 226 °C dec). Anal. ($C_{19}H_{34}N_2Cl_2$) C, H, N, Cl.

Compounds **14a**, **16a**, **22a**, **23a**, **36a**, **37a**, **40a**, and **55a** were prepared following a procedure similar to method A.

Method B. 1-Oxyl-4-(*N*-phthalimid-1-yl)-2,2,6,6-tetramethylpiperidine (55c). To a solution of amine **55a** (2.86 g, 10 mmol) in methanol (10 mL) was added 30% H_2O_2 solution (5 mL, 50 mmol), and the solution was allowed to stand for 3 days. Then the reaction mixture was evaporated to one-half volume and extracted with $CHCl_3$. The organic phase was dried ($MgSO_4$) and evaporated. The product was crystallized from $CHCl_3$–hexane to give nitroxide **55c** (2.17 g, 72%) as pale-yellow crystals: mp 134–136 °C; EI (*m/z*, %) 301 (M^+, 2), 287 (20), 147 (85), 76 (100). Anal. ($C_{17}H_{21}N_2O_3$) C, H, N.

Method C. 1-Hydroxy-3-[*N*-(1-adamantyl)aminomethyl]-2,2,5,5-tetramethyl-3-pyrroline (25b). The paramagnetic compound **25c** (0.61 g, 2 mmol) was dissolved in EtOH saturated with HCl gas (10 mL), then refluxed until the color of nitroxide disappeared (about 30 min), and diluted with Et_2O to start crystallization. The crystalline hydrochloride **25b** that separated on refrigeration was filtered off, washed with Et_2O, and dried (0.53 g, 70%) as off-white crystals: mp 215–216 °C; TSP $[M + H]^+$ 304. Anal. ($C_{18}H_{32}N_2O{\cdot}2HCl$) C, H, N, Cl.

Compounds **1b**, **2b**, **5b**, **6b**, **9b**, **11b–17b**, **19b**, **22b**, **23b**, **26b**, **27b**, **29b**, **36b-38b**, **40b**, **42b**, **48b**, **52b**, **53b**, and **55b** were prepared following a procedure similar to method C.

Method D. 1-Oxyl-3-formyl-2,2,5,5-tetramethyl-3-pyrroline (36c). *N*-Hydroxylamine hydrochloride salt **36b** (2.06 g, 10 mmol) was dissolved in saturated K_2CO_3 solution (15 mL) and extracted with $CHCl_3$. To the organic phase were added drying agent ($MgSO_4$) and catalytic amount of MnO_2 (50 mg), and this mixture was aerated for 30 min. Then the reaction mixture was filtered and evaporated. The crystalline product **36c** was filtered off and evaporated with hexane (1.53 g, 91%) as yellow crystals: mp 77–79 °C; EI (*m/z*, %) 168 (M^+, 35), 138 (41), 123 (100), 95 (88). Anal. ($C_9H_{14}NO_2$) C, H, N.

Method E. Methyl (2,2,5,5-Tetramethyl-3-pyrrolin-3-yl)carboxylate (42a). 2,2,6,6-Tetramethyl-3,5-dibromo-4-piperidone hydrobromide[13] (**59**) (39.39 g, 0.1 mol) was added during about 1 h to a stirred methanol solution of sodium methoxide (30%) (57 mL, 0.3 mol) at room temperature; then the formed NaBr was filtered off, the filtrate evaporated to dryness, and the residual pale oil distilled under reduced pressure (1.3 mmHg, 56–58 °C) to yield the pure product **42a** (15.0 g, 82%) as an oil: EI (*m/z*, %) 183 (M^+, 1), 168 (100), 136 (49), 108 (64). Anal. ($C_{10}H_{17}NO_2$) C, H, N.

Method F. 3-(Hydroxymethyl)-2,2,5,5-tetramethyl-3-pyrroline (14a). To a solution of ester **42a** (1.83 g, 10 mmol) in toluene (10 mL) was added SMEAH (70% solution in toluene, 6.4 mL, 23 mmol) dropwise in argon atmosphere. The reaction mixture was kept at 40 °C for 1 h and then added to a NaOH solution (20%, 20 mL). THF (10 mL) was also added, and the organic phase was separated, dried ($MgSO_4$), and evaporated. The crystalline product **14a** was filtered and washed with hexane (1.21 g, 78%) as pale-yellow crystals: mp 66–69 °C; EI (*m/z*, %) 155 (M^+, 1), 140 (40), 122 (18), 110 (100). Anal. ($C_9H_{17}NO$) C, H, N.

Method G. 3-Formyl-2,2,5,5-tetramethyl-3-pyrroline (36a). A stirred solution of **14a** (1.55 g, 10 mmol) in $CHCl_3$ (30 mL) was refluxed with active MnO_2 (5 g, 56 mmol) until oxidation of alcohol **14a** was completed and then filtered, the filtrate evaporated to dryness, and the residual solidified when cooled to give the aldehyde **36a** (1.36 g, 89%) as a pale-yellow oil: EI (*m/z*, %) 153 (M^+, 1), 138 (48), 110 (100), 95 (44). Anal. ($C_9H_{15}NO$) C, H, N.

Method H. 3-Formyl-1,2,2,5,5-pentamethyl-3-pyrroline (36d). A solution of aldehyde **36a**[25] (0.77 g, 5 mmol) and MeI (1.42 g, 10 mmol) in acetone (10 mL) was refluxed for 4 h and then evaporated to dryness. The residual solid was dissolved in water, basified with solid K_2CO_3, extracted with $CHCl_3$ (3 × 20 mL), dried ($MgSO_4$), and evaporated to dryness. The oily residue was flash-chromatographed on silica gel (Merck 60) to get the pure compound **36d** (0.71 g, 85%): EI (*m/z*, %) 167 (M^+, 11), 152 (41), 124 (100), 109 (42). Anal. ($C_{10}H_{17}NO$) C, H, N.

Method I. 1-Oxyl-3-[*N*-(1-adamantyl)aminomethyl]-2,2,5,5-tetramethyl-3-pyrroline (25c). A solution of aldehyde **36c**[26] (1.68 g, 10 mmol) and 1-aminoadamantane (1.66 g, 11 mmol) in toluene was refluxed in the presence of catalytic amount of *p*-toluenesulfonic acid, in a flask equipped with a Dean–Stark water separator. After the separation of the calculated amount of water (about 12 h), the mixture was concentrated under reduced pressure (water pump). The remaining Schiff base was dissolved in EtOH (20 mL) and added slowly to a stirred suspension of $NaBH_4$ (0.57 g, 15 mmol) in EtOH (30 mL) at 0 °C; then the mixture refluxed for 1 h. It was diluted with water (50 mL) and evaporated in a vacuum to about one-half volume, and the oily aqueous residue was extracted with $CHCl_3$ (3 × 50 mL). The extract was dried ($MgSO_4$), filtered, and concentrated. The crude base **25c** was recrystallized from a mixture of Et_2O and hexanes (2.18 g, 72%) as yellow crystals: mp 109–111 °C; EI (*m/z*, %) 303 (M^+, 10), 273 (34), 164 (48), 135 (100). Anal. ($C_{19}H_{31}N_2O$) C, H, N.

The base was converted into its tosylate salt. To the base in acetone was added an equivalent amount of *p*-toluene-

sulfonic acid in acetone (10 mL), and the mixture was cooled. The precipitated salt **25c/Ts** was filtered off, washed with Et_2O, and dried to give **25c/Ts** (3.76 g, 79%) as yellow crystals: mp 250−251 °C. Anal. ($C_{19}H_{31}N_2O \cdot C_7H_8O_3S$) C, H, N, S.

Compounds **18c**−**20c**, and **28c** were prepared following a procedure similar to method I.

Method J. 1-Oxyl-3-[*N*-methyl-*N*-(1-adamantyl)aminomethyl]-2,2,5,5-tetramethyl-3-pyrroline (26c). To a stirred solution of **25c** (608 mg, 2 mmol) in dry tetrahydrofuran (THF) (20 mL) in argon atmosphere was added NaH (60 mg, 2.5 mmol), and the mixture refluxed for 1 h. After MeI (284 mg, 2.0 mmol) was added to the reaction mixture and refluxed for 6 h, the cooled reaction mixture was washed with saturated NaCl solution (10 mL), and the organic phase was dried ($MgSO_4$), filtered, and evaporated. The residue was chromatographed (hexanes−Et_2O) to separate the nonmethylated starting compound. The pure compound **26c** was recrystallized from $CHCl_3$−hexanes (394 mg, 62%) as yellow crystals: mp 110−112 °C; EI (*m/z*, %) 317 (M^+, 2), 287 (5), 165 (55), 135 (100). Anal. ($C_{20}H_{33}N_2O$) C, H, N.

Compound **29c** was prepared following a procedure similar to method J.

Method K. 1-Oxyl-4-(*N,N*-*n*-dibutylamino)-2,2,6,6-tetramethylpiperidine (10c). To solution of ketone **39c** (TEMPONE)[41] (1.70 g, 10 mmol) and di-*n*-butylamine hydrochloride (6.63 g, 40 mmol) in dry methanol (100 mL) was added $NaCNBH_3$ (3.77 g, 60 mmol), and the reaction mixture was refluxed for 48 h and finally evaporated to dryness. The residue was taken up in water (30 mL), acidified by adding diluted H_2SO_4 (5%), and extracted with $CHCl_3$ (3 × 20 mL) to remove the unreacted ketone. The aqueous phase was basified by adding solid K_2CO_3, extracted again with $CHCl_3$ (3 × 20 mL), then dried, evaporated, and purified by flash chromatography to give the product **10c** (0.99 g, 35%) as a deep-red thick oil: TSP 284 ($M + H)^+$. Anal. ($C_{17}H_{35}N_2O$) C, H, N.

Method L. 1-Oxyl-3-(ethoxymethyl)-2,2,5,5-tetramethyl-3-pyrroline (15c). To a suspension of NaH (0.24 g, 10 mmol) in dry THF (15 mL) was added alcohol **14c**[26] (1.70 g, 10 mmol) dropwise in dry THF (10 mL), and the mixture was stirred at room temperature for 1 h. After that EtBr (1.09 g, 10 mmol) in dry DMF (10 mL) was added dropwise, and the reaction mixture was refluxed for 2 h. Then the cooled reaction mixture was extracted with brine (20 mL), and the organic phase was dried ($MgSO_4$), filtered, and evaporated. The residue was flash-chromatographed (hexanes−Et_2O) to give the pure product **15c** (1.13 g, 57%) as a yellow oil: EI (*m/z*, %) 198 (M^-, 10), 138 (9), 122 (26), 107 (100). Anal. ($C_{11}H_{20}NO_2$) C, H, N.

Method M. 1-Oxyl-3-(*N*-pyrrolidinylmethyl)-2,2,5,5-tetramethyl-3-pyrroline (22c). A solution of 1-oxyl-3-(bromomethyl)-2,2,5,5-tetramethyl-3-pyrroline[31] (**60**) (2.33 g, 10 mmol) and pyrrolidine (2.13 g, 30 mmol) in $CHCl_3$ (30 mL) was refluxed for 3 h and then evaporated, and the residue was diluted with water (20 mL) and extracted with Et_2O (3 × 20 mL). The extract was dried ($MgSO_4$), filtered, and concentrated. The residue was purified by chromatography (hexanes−Et_2O) to give the base **22c** (1.74 g, 78%) as a red oil. Anal. ($C_{13}H_{23}N_2O$) C, H, N.

The pure base **22c** was converted to its tosylate salt (3.08 g, quantitatively) in the same way as described in method I: yellow crystals; mp 129−132 °C; TSP 224 $[M + H]^+$. Anal. ($C_{13}H_{23}N_2O \cdot C_7H_8O_3S$) C, H, N, S.

Compounds **17c** and **21c** were prepared following a procedure similar to method M.

Method N. 1-Oxyl-3-(tributylammoniumylmethyl)-2,2,5,5-tetramethyl-3-pyrroline Bromide (31d). A solution of 1-oxyl-3-(bromomethyl)-2,2,5,5-tetramethyl-3-pyrroline[31] (**60**) (2.33 g, 10 mmol) and the excess of *n*-tributylamine (3.71 g, 20 mmol) was heated in acetone (10 mL) for 6 days and then diluted with Et_2O to start crystallization. The solid residue was recrystallized from acetone−Et_2O to give the pure compound **31d** (2.64 g, 63%) as yellow crystals: mp 180−181 °C; EI (*m/z*, %) 338 (M^+, 1), 281 (2), 202 (8), 142 (100). Anal. ($C_{21}H_{42}BrN_2O$) C, H, N, Br.

Compound **30d** was prepared following a procedure similar to method N.

Method O. 1-Oxyl-3-(triphenylphosphoniumylmethyl)-2,2,5,5-tetramethyl-3-pyrroline Bromide (32e). A solution of 1-oxyl-3-(bromomethyl)-2,2,5,5-tetramethyl-3-pyrroline[31] (**60**) (2.33 g, 10 mmol) and triphenylphosphine (2.62 g, 10 mmol) was heated in acetone (10 mL) for 3 h and then diluted with Et_2O to start crystallization. The solid residue was recrystallized from $CHCl_3$−Et_2O to give the pure compound **32e** (3.51 g, 71%) as pale-brown crystals: mp 224−226 °C; TSP 416 $(M + H)^+$. Anal. ($C_{27}H_{30}BrNOP$) C, H, N, Br.

Method P. 1-Oxyl-*N*-(2-isoindolinylmethyl)-2,2,5,5-tetramethyl-3-pyrroline (24c). A solution of 1-oxyl-3-(aminomethyl)-2,2,5,5-tetramethyl-3-pyrroline[33] (**61**) (1.69 g, 10 mmol), and *o*-dibromoxilol (2.64 g, 10 mmol), and K_2CO_3 (2.76 g, 20 mmol) in $CHCl_3$ (50 mL) was stirred and refluxed for 3 h and then evaporated, and the residue was diluted with water (20 mL) and extracted with Et_2O (3 × 20 mL). The extract was dried ($MgSO_4$), filtered, and concentrated. The residue was purified by chromatography ($CHCl_3$−Et_2O) to give the base **24c** (1.85 g, 68%) as pale-yellow crystals: mp 89−90 °C; TSP 272 $(M + H)^+$. Anal. ($C_{17}H_{23}N_2O$) C, H, N.

Method Q. 1-Oxyl-3-(guanidinomethyl)-2,2,5,5-tetramethyl-3-pyrroline Hydrogen Sulfate Salt (33c). A suspension of 1-oxyl-3-(aminomethyl)-2,2,5,5-tetramethyl-3-pyrroline[33] (**61**) (340 mg, 2 mmol) and *S*-methylisothiouronium sulfate (278 mg, 1 mmol) in EtOH (10 mL) was refluxed for 3 h, then the hot reaction mixture was filtered, and the filtrate was diluted with Et_2O to precipitate off-white crystalline product **33c** (287 mg, 55%) as yellow crystals: mp >180 °C dec; TSP 212 $(M + H)^+$. Anal. ($C_{10}H_{19}N_4O \cdot {}^1/_2H_2SO_4$) C, H, N, S.

Method R. 1-Oxyl-4-(methylsulfonylamino)-2,2,6,6-tetramethylpiperidine (13c). To a stirred solution of amino compound **9c**[28] (342 mg, 2 mmol) and triethylamine (TEA) (303 mg, 3 mmol) in dry CH_2Cl_2 (20 mL) was added methanesulfonyl chloride (252 mg, 2.2 mmol) at 0 °C, and the reaction mixture was stirred at room temperature for 3 h, then washed with saturated aqueous NaCl solution (10 mL), dried ($MgSO_4$), and evaporated to dryness. The solid residue was recrystallized from $CHCl_3$−hexane to give the pure orange compound **13c** (409 mg, 82%) as yellow crystals: mp 141−143 °C; EI (*m/z*, %) 249 (M^+, 3), 235 (23), 124 (61), 84 (100). Anal. ($C_{10}H_{21}N_2O_3S$) C, H, N, S.

Method S. 1-Oxyl-3-ureido-2,2,5,5-tetramethyl-3-pyrroline (43c). To a cyclohexane solution of the freshly prepared isocyanate **62**[33] (0.91 g, 5 mmol) was introduced ammonia gas. The precipitated solid urea **43c** was filtered off and recrystallized from $CHCl_3$−Et_2O to give a pure compound (0.69 g, 70%) as yellow crystals: mp 189−190 °C; EI (*m/z*, %) 198 (M^+, 7), 168 (41), 110 (58), 41 (100). Anal. ($C_9H_{16}N_3O_2$) C, H, N.

Method T1. 1-Oxyl-*N*-(3-hydroxypropyl)-3-carboxamido-2,2,5,5-tetramethyl-3-pyrroline (46c). To a solution of 1-oxyl-3-[(ethoxycarbonyl)oxycarbonyl]-2,2,5,5-tetramethyl-3-pyrroline[34] (**63**) (2.56 g, 10 mmol) in dry $CHCl_3$ (20 mL) was added 3-aminopropanole (0.75 g, 10 mmol), and the mixture refluxed for 30 min. Then evaporation to dryness and recrystallization from Et_2O−hexane gave **46c** (2.03 g, 84%) as yellow crystals: mp 95−96 °C; EI (*m/z*, %) 241 (M^-, 2), 211 (32), 136 (32), 110 (100). Anal. ($C_{12}H_{21}N_2O_3$) C, H, N.

Compounds **45c**, **48c**, and **49c** were prepared following a procedure similar to method T1.

Method T2. 1-Oxyl-*N*-(3-aminopropyl)-3-carboxamido-2,2,5,5-tetramethyl-3-pyrroline (48c). To a stirred solution of 1,3-diaminopropane (2.22 g, 30 mmol) in dry THF (50 mL) was added 1-oxyl-3-(*N*-imidazolylcarbonyl)-2,2,5,5-tetramethyl-3-pyrroline[26] (**64**) (2.56 g, 10 mmol) at 0 °C. Then the reaction mixture was warmed to room temperature, 1 h later evaporated, and flash-chromatographed with $CHCl_3$−Et_2O. The first band was the birradical (0.43 g; mp 177−178 °C), and the second yellow band was the monoradical **48c** (1.32 g, 55%) as yellow crystals: mp 104−108 °C; EI (*m/z*, %) 240 (M^+, 8), 226 (18), 136 (65), 41 (100). Anal. ($C_{12}H_{22}N_3O_2$) C, H, N.

Method U. 1-Oxyl-3-[*N*-(3-aminopropyl)-3-carboxamido]-2,2,5,5-tetramethylpyrrolidine (66). To a stirred solution of 1,3-diaminopropane (2.22 g, 30 mmol) in water–THF (2:1, 20 mL) was added 1-oxyl-3-bromo-4-oxo-2,2,6,6-tetramethylpiperidine[35] (**65**) (2.49 g, 10 mmol) in portions. The solution was extracted after stirring for 2 h with $CHCl_3$. The organic phase was dried, evaporated, and purified by flash chromatography to give the product **66** (1.50 g, 62%) as yellow crystals: mp 102–105 °C; EI (*m/z*, %) 242 (M^+, 18), 212 (11), 156 (54), 41 (100). Anal. ($C_{12}H_{24}N_3O_2$) C, H, N.

Method V. *N*-[(1-Oxyl-2,2,5,5-tetramethylpyrrolidine-3-carboxamido)propyl]phthalimide (52c). A mixture of equivalent amounts of 1-oxyl-3-[*N*-(3-aminopropyl)-3-carboxamido]-2,2,5,5-tetramethylpyrrolidine[19] (**66**) (2.42 g, 10 mmol) and phthalimide (1.47 g, 10 mmol) was heated at 120 °C without any solvent until the evolution of ammonia had ceased (about 60 min). After cooling the melt was dissolved in $CHCl_3$ (20 mL) and flash-chromatographed on silica gel (eluted with $CHCl_3$–Et_2O). The pure product was crystallized from $CHCl_3$–hexane to give **52c** (2.15 g, 58%) as yellow crystals: mp 118–120 °C; EI (*m/z*, %) 372 (M^+, 15), 358 (9), 342 (89), 41 (100). Anal. ($C_{20}H_{26}N_3O_4$) C, H, N.

Method W. 1-Oxyl-3-(*N*-phthalimid-1-ylmethyl)-2,2,5,5-tetramethyl-3-pyrroline (53c). A vigorously stirred solution of phthalimide (1.47 g, 10 mmol), 1-oxyl-3-(bromomethyl)-2,2,5,5-tetramethyl-3-pyrroline[31] (**60**) (2.33 g, 10 mmol), powdered K_2CO_3 (2 g), powdered KOH (100 mg), and 18-crown-6 (300 mg) in dioxane (30 mL) was refluxed for 4 h and filtered, and the filtrate was evaporated to dryness. Residue was flash-chromatographed with $CHCl_3$–Et_2O and then recrystallized from $CHCl_3$–hexane to give **53c** (2.18 g, 73%) as yellow crystals: mp 127–129 °C; EI (*m/z*, %) 299 (M^-, 13), 285 (27), 269 (100), 213 (42). Anal. ($C_{17}H_{18}N_2O_3$) C, H, N.

Method Z. 1-Oxyl-4-(*N*-phthalimid-1-yl)-2,2,6,6-tetramethylpiperidine (55c). A mixture of equivalent amounts of 1-oxyl-4-amino-2,2,6,6-tetramethylpiperidine[44] (**9c**) (1.71 g, 10 mmol) and phthalimide (1.47 g, 10 mmol) was heated at 120 °C without any solvent until the evolution of ammonia had ceased (about 50 min). After cooling the melt was dissolved in $CHCl_3$ (20 mL) and flash-chromatographed on silica gel (eluted with $CHCl_3$–Et_2O). The pure product was crystallized from $CHCl_3$–hexane to give **55c** (2.01 g, 67%) as yellow crystals: mp 134–136 °C; EI (*m/z*, %) 301 (M^-, 2), 287 (20), 147 (85), 76 (100). Anal. ($C_{17}H_{21}N_2O_3$) C, H, N.

Electrochemistry. Cyclic voltammetry was performed on the nitroxides in phosphate-buffered saline using a glassy carbon working electrode and a platinum auxiliary electrode. All other conditions are similar to that reported.[6]

Cell Culture. Chinese hamster V79 cells were grown in F12 medium supplemented with 10% fetal calf serum, penicillin, and streptomycin. Survival was assessed in all studies by the clonogenic assay. The plating efficiency ranged between 80% and 90%. Stock cultures of exponentially growing cells were trypsinized, rinsed, and plated (5×10^5 cells/dish) into a number of 100-mm Petri dishes and incubated for 16 h at 37 °C prior to experimental protocols. Nitroxides were added to exponentially growing cells in complete F12 medium (final concentration, 100 μM) at room temperature immediately prior to treatment with H_2O_2 (final concentration, 500 μM) for 1 h. For radiation studies, nitroxides were added to exponentially growing cells in complete F12 medium (final concentration, 10 mM) at room temperature 10 min prior to a single radiation dose of 12 Gy. Plates were irradiated at room temperature with a cobalt-60 irradiator at a dose rate of 5.0 Gy/min. Full electron equilibrium was ensured for all irradiations. The time required for irradiation (at room temperature) was approximately 10 min. Immediately after treatment, cells were rinsed, trypsinized, counted, and plated for macroscopic colony formation. Using these conditions, none of the nitroxides exerted cytotoxicity alone. Each nitroxide/H_2O_2 or nitroxide/radiation determination was plated in triplicate, and experiments were repeated a minimum of two times. Plates were incubated for 7 days; colonies were then fixed with methanol/acetic acid (3:1) and stained with crystal violet. Colonies containing >50 cells were scored.

The results for H_2O_2 treatment were formulated to express a protection factor (PF, derived by dividing the surviving fraction of nitroxide plus H_2O_2 treatment by the surviving fraction of H_2O_2 treatment alone). A PF > 1.0 means that the agent provided protection against H_2O_2 cytotoxicity. PF values were also derived for radiation studies (PF, derived by dividing the surviving fraction at 12 Gy of nitroxide treatment by the surviving fraction of 12 Gy of treatment alone). PFs > 1.0 mean that the agent provided radiation protection, and values < 1.0 mean that radiation sensitization occurred. The PFs from individual experiments were pooled to find the mean PF ± standard deviation. Each nitroxide was then compared to the untreated irradiated control (PF = 1.0) using a two-tailed paired Students *t*-test to determine statistical significance.[45]

Acknowledgment. This work was supported in part by grants from the Hungarian National Research Foundation (T 021277 and T 017842).

Supporting Information Available: Graphical presentation of protection factors against H_2O_2- and radiation-induced cytotoxicity (Figures 2 and 4) (2 pages). Ordering information is given on any current masthead page.

References

(1) Chance, B.; Sies, H.; Boveris, A. Hydroperoxide metabolism in mammalian organs. *Physiol. Rev.* **1979**, *59*, 527–605.
(2) Imlay, J. A.; Chin, S. M.; Linn, S. Toxic DNA damage by hydrogen peroxide through the Fenton reaction in vivo and in vitro. *Science* **1988**, *240*, 640–642.
(3) Halliwell, B.; Gutteridge, J. M. C. *Free Radicals in Biology and Medicine*; Clarendon Press: 1989; pp 210–211.
(4) Swartz, H. M. Principles of the metabolism of nitroxides and their implications for spin trapping. *Free Radical Res. Commun.* **1990**, *9*, 399–405.
(5) Paleos, C. M.; Pais, D. Ready Reduction of Some Nitroxide Radicals with Ascorbic Acid. *J. Chem. Soc., Chem. Commun.* **1977**, 428.
(6) Krishna, M. C.; Grahame, D. A.; Samuni, A.; Mitchell, J. B.; Russo, A. Oxoammonium cation intermediate in the nitroxide-catalyzed dismutation of superoxide. *Proc. Natl. Acad. Sci. U.S.A.* **1992**, *89*, 5537–5541.
(7) Rozantsev, E. G.; Kagan, E. S. H.; Sholle, V. D. Triacetonamine in the Chemistry of Nitroxyl Radicals. In *Bioactive Spin Labels*; Zhdanov, R. I., Ed.; Springer-Verlag: Berlin, 1992; pp 83–118.
(8) Krishna, M. C.; Russo, A.; Mitchell, J. B.; Goldstein, S.; Dafni, H.; Samuni, A. Do nitroxides antioxidants act as scavengers of superoxide or as SOD mimics? *J. Biol. Chem.* **1996**, *271*, 26026–26031.
(9) Krishna, M. C.; Samuni, A.; Taira, J.; Goldstein, S.; Mitchell, J. B.; Russo, A. Stimulation by nitroxides of catalase-like activity of hemeproteins. *J. Biol. Chem.* **1996**, *271*, 26018–26025.
(10) Nooy, A. E. J.; Besemer, A. C.; van Bekkum, H. On the Use of Stable Organic Nitroxyl Radicals for the Oxidation of Primary and Secondary Alcohols. *Synthesis* **1996**, 1153–1174.
(11) Zhdanov, R. I.; Komarov, P. G. Sterically hindered hydroxylamines as bioactive spin labels. *Free Radical Res. Commun.* **1990**, *9*, 367–377.
(12) Chateauneuf, J.; Lusztyk, J.; Ingold, K. U. Absolute rate constants for the reactions of some carbon-centered radicals with 2,2,6,6-tetramethylpiperidine-*N*-oxyl. *J. Org. Chem.* **1988**, *53*, 1629–1632.
(13) Rozantsev, E. G. *Free Nitroxyl Radicals*; Plenum Press: New York, 1970.
(14) Mitchell, J. B.; Krishna, M. C.; Samuni, A.; Russo, A.; Hahn, S. M. Nitroxides as Protectors Against Oxidative Stress. *Reactive Oxygen Species in Biological Systems: An Interdisciplinary Approach*; 1997, in press.
(15) Mitchell, J. B.; Samuni, A.; Krishna, M. C.; DeGraff, W. G.; Ahn, M. S.; Samuni, U.; Russo, A. Biologically active metal-independent superoxide dismutase mimics. *Biochemistry* **1990**, *29*, 2802–2807.
(16) Samuni, A.; Mitchell, J. B.; DeGraff, W.; Krishna, C. M.; Samuni, U.; Russo, A. Nitroxide SOD-mimics: Modes of action. *Free Radical Res. Commun.* **1991**, *12–13*, 187–194.
(17) Krishna, C. M.; DeGraff, W.; Tamura, S.; Gonzalez, F.; Samuni, A.; Russo, A.; Mitchell, J. B. Mechanisms of hypoxic and aerobic cytotoxicity of Mitomycin C in Chinese hamster V79 cells. *Cancer Res.* **1991**, *51*, 6622–6628.

(18) Sosnovsky, G.; Bell, P. In the search for new anticancer drugs. 29. A study on the correlation of lipophilicities, ionization constants and anticancer activities of aminoxyl labeled TEPA congeners. *Life Sci.* **1998**, *62*, 639−648.
(19) Hankovszky, H. O.; Hideg, K.; Bódi, I.; Frank, L. New Antiarrhythmic Agents. 2,2,5,5-Tetramethyl-3-pyrroline-3-carboxamides and 2,2,5,5-tetramethylpyrrolidine-3-carboxamides. *J. Med. Chem.* **1986**, *29*, 1138−1152.
(20) Twomey, P.; Taira, J.; DeGraff, W.; Mitchell, J. B.; Russo, A.; Krishna, M. C.; Hankovszky, H. O.; Frank, L.; Hideg, K. In Vivo Nitroxide Free Radical Production from the new Anti-arrhythmic Drug as Evidenced by EPR Spectroscopy. *Free Radical Biol. Med.* **1997**, *22*, 909−916.
(21) Mitchell, J. B.; DeGraff, W.; Kaufman, D.; Krishna, M. C.; Samuni, A.; Finkelstein, E.; Ahn, M. S.; Hahn, S. M.; Gamson, J.; Russo, A. Inhibition of oxygen-dependent radiation-induced damage by the nitroxide superoxide dismutase mimic, Tempol. *Arch. Biochem. Biophys.* **1991**, *289*, 62−70.
(22) Bacq, Z. M. *Chemical Protection Against Ionizing Radiation*; Thomas: Springfield, 1965.
(23) Aguilera, J. A.; Newton, G. L.; Fahey, R. C.; Ward, J. F. Thiol uptake by Chinese hamster V79 cells and aerobic radioprotection as a function of net charge on the thiol. *Radiat. Res.* **1992**, *130*, 194−204.
(24) Bump, E. A.; Foye, W. O. Radiosensitizers and Radioprotective Agents. In *Burger's Medicinal Chemistry and Drug Discovery*, 5th ed.; Wolff, M. E., Ed.; Wiley: New York, 1997; Vol. 4, pp 3−69.
(25) Sár, P. C.; Kálai, T.; Bárácz, M. N.; Jerkovich, Gy.; Hideg, K. Selective Reduction of Nitrones and Nitroxides to Functionalized Secondary Amines. *Synth. Commun.* **1995**, *25*, 2929−2940.
(26) Hideg, K.; Hankovszky, H. O.; Lex, L.; Kulcsár, Gy. Nitroxyls; VI. Synthesis and Reactions of 3-Hydroxymethyl-2,2,5,5-tetramethyl-2,5-dihydropyrrole-1-oxyl and 3-Formyl Derivatives. *Synthesis* **1980**, 911−914.
(27) Csekö, J.; Hankovszky, H. O.; Hideg, K. Synthesis of Novel, Highly Reactive 1-Oxyl- 2,2,6,6-tetramethyl-1,2,5,6-tetrahydropyridine Derivatives. *Can. J. Chem.* **1985**, *63*, 940- 943.
(28) Rauckman, E. W.; Rosen, G. M.; Hord, W. W. Use of Sodium Cyanoborohydride in the Synthesis of Biradical Nitroxides. *Org. Prep. Proc. Int.* **1977**, *9*, 53 -56.
(29) Rosen, M. G. Use of Sodium Cyanoborohydride in the Preparation of Biologically Active Nitroxides. *J. Med. Chem.* **1974**, *17*, 358−360.
(30) Vallet, P.; Haverbeke, Y.; Bonnet, A. P.; Subra, G.; Chapat, J.-P.; Muller, R. N. Relaxivity Enhancement of Low Molecular Weight Nitroxide Stable Free Radicals: Importance of Structure and Medium. *Magn. Reson. Med.* **1994**, *32*, 11−15.
(31) Hankovszky, H. O.; Hideg, K.; Lex, L. Nitroxyls; VII. Synthesis and Reactions of Highly Reactive 1-Oxyl-2,2,5,5-tetramethyl-2,5-dihydropyrrole-3-ylmethyl Sulfonates. *Synthesis* **1980**, 914−916.
(32) Belkin, S.; Mehlhorn, R. J.; Hideg, K.; Hankovszky, H. O.; Packer, L. Reduction and Destruction Rates of Nitroxide Spin Probes. *Arch. Biochem. Biophys.* **1987**, *256*, 232−243.
(33) Hankovszky, H. O.; Hideg, K.; Lex, L. Nitroxyls; VIII. Synthesis of Nitroxylphosphinimines: A Convenient Route to Amine, Isothiocyanate, Aminocarbonylaziridine, and Carbodiimide Nitroxyls. *Synthesis* **1981**, 147−149.
(34) Hankovszky, H. O.; Hideg, K.; Tigyi, J. Nitroxides, II. 1-Oxyl-2,2,5,5-tetramethylpyrroline-3-carboxylic acid derivatives. *Acta Chim. Acad. Sci. Hung.* **1978**, *98*, 339−348.
(35) Sosnovsky, G.; Cai, Z. A. Study of the Favorskii Rearrangement with 3-Bromo-4-oxo-2,2,6,6-tetramethylpiperidin-1-oxyl. *J. Org. Chem.* **1995**, *60*, 3414−3418.
(36) Hideg, K.; Hankovszky, H. O.; Frank, L.; Bódi, I.; Csák, J. 2-[(2,2,5,5-Tetramethyl-3-pyrrolin-3-carbonyl)]-amino Derivatives. U.S. Patent 4 731 376. 1988.
(37) Kieber, D. J.; Blough, N. V. Fluorescence detection of carbon-centered radicals in aqueous solution. *Free Radical Res. Commun.* **1990**, *10*, 109−117.
(38) Dikalov, S.; Skatchkov, M.; Fink, B.; Bassenge, E. Quantification of Superoxide Radicals and Peroxynitrite in Vascular Cells Using Oxidation of Sterically Hindered Hydroxylamines and Electron Spin Resonance. *Nitric Oxide* **1997**, *1*, 423−431.
(39) Afzal, V.; Brasch, R. C.; Niteczki, D. E.; Wolff, S. Nitroxyl spin labels contrast enhancers for magnetic resonance imaging. Studies of acute toxicity and mutagenesis. *Invest. Radiol.* **1984**, *19*, 549−552.
(40) Milligan, J. R.; Ng, J. Y.; Wu, C. C.; Aguilera, J. A.; Fahey, R. C.; Ward, J. F. DNA repair by thiols in air shows two radicals make a double strand break. *Radiat. Res.* **1995**, *143*, 273−280.
(41) Hahn, S. M.; Tochner, Z.; Krishna, C. M.; Glass, J.; Wilson, L.; Samuni, A.; Sprague, M.; Venzon, D.; Glatstein, E.; Mitchell, J. B. Tempol, a stable free raidcal, is a novel murine radiation protector. *Cancer Res.* **1992**, *52*, 1750−1753.
(42) Hahn, S. M.; Wilson, L.; Krishna, M. C.; Liebmann, J.; DeGraff, W.; Gamson, J.; Samuni, A.; Venzon, D.; Mitchell, J. B. Identification of nitroxide radioprotectors. *Radiat. Res.* **1992**, *132*, 87−93.
(43) This article.
(44) *Aldrich Catalogue Handbook of Fine Chemicals*; Aldrich: Milwaukee, WI, 1996−1997.
(45) Snedecor, G. W.; Cochran, W. G. *Statistical Methods;* Iowa State University: Ames, 1980; pp 83−106.
(46) Hideg, K.; Sár, C. P.; Hankovszky, O. H.; Jerkovich, Gy. Allylic nitroxyl spin label reagents. *Synthesis* **1991**, 616−620.
(47) *Reanal Catalogue of Fine Chemicals*, no. 20813-0-21.
(48) Hankovszky, H. O.; Hideg, K.; Lex, L.; Kulcsár, Gy.; Halász, H. A. Methods for preparation of heterobifunctional nitroxides: α,β-unsaturated ketones, β-ketoesters, cyano-nitro-derivatives. *Can. J. Chem.* **1982**, *60*, 1432−1438.
(49) Keana, J. F. W.; Hideg, K.; Birrell, G. B.; Hankovszky, H. O.; Ferguson, G.; Parvez, M. New mono- and difunctionalized 2,2,5,5-tetramethylpyrrolidine- and Δ^3-pyrroline-1-oxyl nitroxide spin label reagents. *Can. J. Chem.* **1982**, *60*, 1439−1447.
(50) Keana, J. F. W.; Lee, T. D.; Bernard, E. M. Side-Chain Substituted 2,2,5,5-Tetramethylpyrrolidine-*N*-oxyl (Proxyl) Nitroxides. A New Series of Lipid Spin Labels Showing Improved Properties for the Study of Biological Membranes. *J. Am. Chem. Soc.* **1976** *98*, 3052−3053.
(51) Keana, J. F. W. New aspects of nitroxide chemistry. In *Spin Labeling II, Theory and Applications*; Berliner, L. J., Ed.; Academic Press: New York, 1979; pp 115−172.
(52) Delpierre, G. R.; Lamchen, M. Nitrones. Part I. Cycloaddition of Unsymmetrical Olefins to the 1-Pyrroline 1-Oxides. *J. Chem. Soc.* **1963**, 4693−4701.

JM9802160